Université du Québec
Institut national de la recherche scientifique
Eau, Terre et Environnement

ÉTUDE DU COMPORTEMENT DE LA GOMME DE XANTHANE LORS DE SON INJECTION EN MILIEU POREUX

Par

Michaël Haberman

Mémoire présenté
Pour l'obtention
Du grade de Maître ès sciences (M.Sc.)

Jury d'évaluation

Examinateur externe	Daniel Cassidy, Ph.D. Université Laval
Examinateur interne	Guy Mercier, Ph.D. INRS-ETE
Directeur de recherche	Richard Martel, Ph.D. INRS-ETE
Codirecteur de recherche	René Lefebvre, Ph.D. INRS-ETE
Codirecteur de recherche	René Therrien, Ph.D. Université Laval

Août 2006

RÉSUMÉ

$\mathcal{L}$a réhabilitation des aquifères contaminés aux *"liquides immiscibles"* par des méthodes de traitement *in situ* par injection de solutions de lavage peut être optimisée par l'utilisation de polymères. Ces solutions de polymères ajoutées aux solutions de lavage ou injectées en pré ou post traitement de la solution nettoyante, contribuent à un meilleur balayage de la formation géologique par la formation de fronts stables entre les différents fluides présents dans le milieu poreux.

Le présent projet de recherche consiste à étudier le comportement rhéologique de la gomme de xanthane lors de son injection en milieu poreux. Des essais en colonne de sable ont été effectués afin de caractériser ce polymère et évaluer son comportement rhéofluidifiant. Des mesures de viscosité en fonction du taux de cisaillement ont confirmé le comportement rhéofluidifiant de la gomme de xanthane: la viscosité diminue avec le taux de cisaillement. Néanmoins, avec une solution à 250 mg/L pour des taux de cisaillement supérieurs à 6 s^{-1}, la viscosité augmente, due à un colmatage du milieu poreux. Ce colmatage est principalement causé par une accumulation de polymère dans la colonne. Les essais ont également montré qu'une solution de polymère préalablement cisaillée perd ses propriétés rhéologiques, dû probablement à une modification de la structure chimique de la gomme de xanthane, notamment par une rupture des chaînes. Une adsorption de polymère à la surface des grains de sable, un piégeage mécanique dans le sable ou une dilution par l'eau préalablement présente au niveau des pores avant son injection peuvent également en être les causes. Un autre essai en colonne de sable a permis de mettre en évidence l'effet d'hystérésis ou de "mémoire" de la gomme de xanthane pendant trois cycles d'injection à débits variables.

Des essais en bac de sable rectangulaire ont permis d'évaluer l'efficacité de balayage de la gomme de xanthane et la stabilité du front de déplacement dans un système d'injection/pompage par un doublet de puits à travers un milieu poreux. Deux tests ont été

réalisés: i) un premier essai en bac rempli d'une couche de sable fin et; ii) un second essai dans un bac composé de trois couches (une couche de sable grossier entre deux couches de sable fin). Les résultats ont confirmé un meilleur balayage de la formation géologique avec la solution de xanthane comparé à l'eau, tant pour le bac à une couche que pour le bac à trois couches, dû à la formation de fronts stables lors de l'injection.

_____
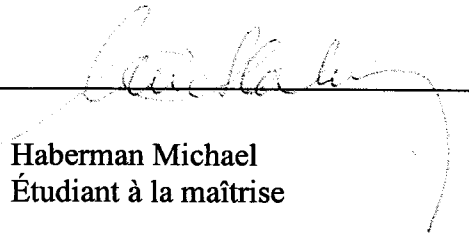
Haberman Michael
Étudiant à la maîtrise

_____

Martel Richard
Directeur de recherche

Remerciements

TABLE DES MATIÈRES

Liste des figures

LISTE DES TABLEAUX

LISTE DES ANNEXES

CHAPITRE 1
INTRODUCTION

1.1. Cadre du projet

$\mathscr{C}$e mémoire est consacré à l'étude du comportement d'un polymère rhéofluidifiant (la gomme de xanthane) lors de son injection en milieux poreux pour la réhabilitation de sites contaminés par des liquides immiscibles (communément appelés les *NAPL*: "Non Aqueous Phase Liquids"). Ces travaux de recherche visent à développer une méthode de restauration *in situ* des aquifères contaminés pour une utilisation sur le terrain. Ce projet est subventionné par le Conseil de Recherches en Sciences Naturelles et en Génie du Canada (CRSNG). Les essais en bac de sable ont été réalisés au laboratoire INRS/RDDC (Recherche et Développement pour la Défense Canada) à Valcartier.

1.2. Mise en contexte

1.2.1. Origine de la contamination des sols et des eaux souterraines

Depuis de nombreuses années, les activités humaines, notamment dans les secteurs industriels et agricoles, ont joué un rôle néfaste sur l'environnement et de ce fait, sur la qualité de vie de notre société. Ces larges activités sont d'ailleurs une des causes majeures de la grande contamination des sols et par la même occasion, des eaux souterraines par infiltration des eaux de précipitation. Les nombreuses pratiques inadéquates de gestion des déchets liquides ou solides y ont fortement contribué, telles que l'enfouissement,

les rejets des eaux usées ou encore les déversements accidentels de produits chimiques lors de leurs transports.

1.2.2. Problématique de la contamination

Selon le rapport publié par l'USEPA en 1998, près de 450 000 sites contaminés ont été recensés aux États-Unis dans les années quatre-vingt-dix. De ce nombre, près de la moitié exige encore à l'heure actuelle une intervention afin d'en extraire les substances toxiques (composés organiques ou inorganiques, etc.). L'Europe est tout aussi concernée par ces problèmes de contamination car elle compte entre ses frontières près de 600 000 sites potentiellement non conformes aux normes gouvernementales (NATO/CCMS, 1998; Tuin *et al.*, 1991). Au Québec, selon le Ministère du Développement Durable, de l'Environnement et des Parcs (MDDEP), plus de 1 870 sites contaminés ont été répertoriés depuis 1994 et quelques 800 sites uniquement dans la seule ville de Montréal (url.sciencepresse, 2001).

Cette contamination représente donc un souci majeur aux yeux des scientifiques dans la mesure où les substances considérées "dangereuses" et "toxiques" peuvent très facilement se retrouver dans les secteurs habités et se disperser tant par voie aérienne (volatilisation des composés toxiques ou entraînement de poussières contaminées) que par voie souterraine (migration des eaux contaminées issues du contact avec les déchets ou via l'infiltration des eaux de surface). Elle peut survenir directement par le biais de sols contaminés (ingestion de terre par les enfants, inhalation de poussières, contact cutané, etc.), par les eaux souterraines (contamination des eaux de consommation) ou encore par les produits potagers via la chaîne alimentaire.

L'application de mesures immédiates s'avère donc nécessaire et indispensable afin de minimiser les possibilités d'exposition directe des populations avec les contaminants. Les gouvernements de nombreux pays devront débourser des sommes considérables pour la restauration des sites pollués et limiter ainsi les risques de migration de la contamination.

1.3. Réhabilitation *in situ* des sites contaminés

La contamination des sols par les liquides immiscibles pose à l'heure actuelle des défis considérables de réhabilitation en hydrogéologie. Étant donné leur faible solubilité dans l'eau, ces liquides entraînent une contamination importante des eaux souterraines qui perdure pendant des années. Parmi eux, les composés plus denses que l'eau (*DNAPL*) posent davantage de problèmes quant à leur récupération, par opposition aux substances plus légères (*LNAPL*). Les *DNAPL* ont tendance à migrer par gravité vers la base de l'aquifère jusqu'à ce qu'ils atteignent une limite imperméable. De plus, une saturation variable (résiduelle ou complète) de ces contaminants peut également survenir tout au long de son cheminement vers le bas (par gravité) en se logeant à la surface des grains de la formation géologique ou au niveau des pores. Ils s'accumulent progressivement pour y former une lentille contaminée. Les *LNAPL*, plus légers que l'eau, ont tendance à flotter et se retrouver à la surface de l'aquifère. Dès lors, ils sont plus faciles à récupérer.

La réhabilitation d'un site contaminé peut se faire par différents procédés de traitements (url.ecoroute, 2002): i) l'**excavation** est la méthode la plus simple à mettre en œuvre et permet d'extraire rapidement une source de pollution locale de faible profondeur. Elle est souvent utilisée pour les sols contaminés aux *LNAPL*. Par la suite, il est possible de réhabiliter ces sols excavés par des traitements chimiques, thermiques ou physico-chimiques sur le site ou hors site; ii) le **confinement** ne constitue pas une solution définitive au problème et nécessite un suivi environnemental continu et; iii) les **traitements *in situ*** représentent un moyen direct pour décontaminer les sols, parmi lesquels les méthodes thermiques (utilisation de chaleur sous forme de vapeurs, de gaz ou de liquides pour la mobilisation, la dissolution ou la vaporisation des contaminants), physico-chimiques (modification de la structure chimique des contaminants par ajout d'un réactif) ou biologiques (dégradation des contaminants par l'action de micro-organismes). Les traitements biologiques sont par ailleurs les plus souvent appliqués au niveau commercial.

Malheureusement, dans chacun de ces procédés, le problème d'une décontamination efficace persiste et ce, pour plusieurs raisons : i) la présence d'une trop grande contamination ou d'une zone contaminée trop profonde et; ii) la faible température de l'eau souterraine, soit en moyenne 8 °C.

Parmi les solutions proposées, le processus le plus couramment discuté est la méthode par récupération assistée par injection d'eau ("waterflooding"). Cette technique, peu onéreuse, consiste à injecter un certain volume d'eau à travers la formation géologique et à pomper cette eau et les contaminants qu'elle déloge. Cette eau est ensuite traitée à la surface (Figure 1.1).
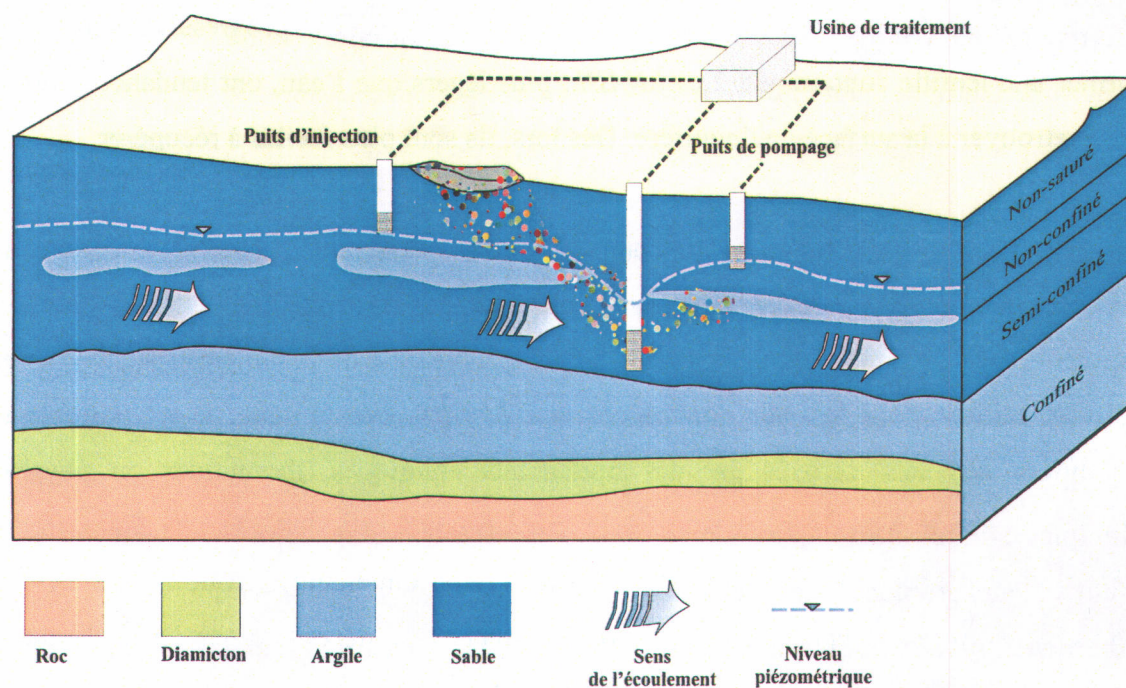
Figure 1.1: Méthode de réhabilitation par "waterflooding" (modifié de Mercer *et al.*, 1990)

Ce procédé est plutôt efficace pour une contamination par des composés légers, dû à leur solubilité dans l'eau. Néanmoins, en présence de composés plus lourds, la méthode du "waterflooding" est peu applicable, étant donné leur faible solubilité et leur mobilité réduite (Mackay et Cherry, 1989).

Plusieurs variantes existent afin d'améliorer le "waterflooding": i) les **méthodes thermiques** et; ii) les **méthodes chimiques**. Elles dérivent notamment de la récupération assistée du pétrole dont l'objectif premier est d'augmenter l'efficacité de récupération des contaminants par un meilleur balayage et un meilleur déplacement. Les méthodes thermiques consistent à injecter de la vapeur, réduisant la viscosité du contaminant et favorisant ainsi son déplacement (Lake, 1989). Les méthodes chimiques jouent préférentiellement sur la mobilité du contaminant ainsi que sur la tension interfaciale entre l'eau et le *NAPL*. Plusieurs procédés chimiques peuvent être répertoriés dans cette catégorie: i) le déplacement miscible, dont le but est d'injecter un fluide miscible à l'huile, formant une phase unique avec celle-ci (solvants, alcools, etc.); ii) l'injection de solutions tensioactives, réduisant la tension interfaciale entre l'eau et le contaminant et; iii) l'injection de polymères, augmentant la viscosité de l'eau et diminuant ainsi le rapport de mobilité, ce qui améliore l'efficacité de balayage (Lake, 1989).

La restauration des aquifères contaminés à l'aide de solutions de lavage a déjà fait l'objet de nombreuses études auparavant (Martel, 1998; Sandiford, 1977; Szabo, 1975b; Gogarty, 1967). Ces solutions nettoyantes sont principalement constituées de tensioactifs, associés dans certains cas à des alcools à chaîne courte et à des solvants. La formulation de ces solutions varie en fonction du type de contaminant. La solution tensioactive est injectée dans le sol et récupérée par un système de pompage en espérant que les *NAPL* aient été contactés par la solution. Celle-ci agit directement sur la tension interfaciale entre l'eau et le *NAPL* en la réduisant de manière significative (Larson *et al.*, 1981). Par cette diminution, il se forme des solutions micellaires ou microémulsions de *NAPL* dans l'eau (processus de dissolution) (Figure 1.2). Des gouttelettes de *NAPL* piégées dans les pores du milieu poreux peuvent également s'agglomérer pour former un banc de *NAPL*, augmentant ainsi leur mobilité (processus de mobilisation).
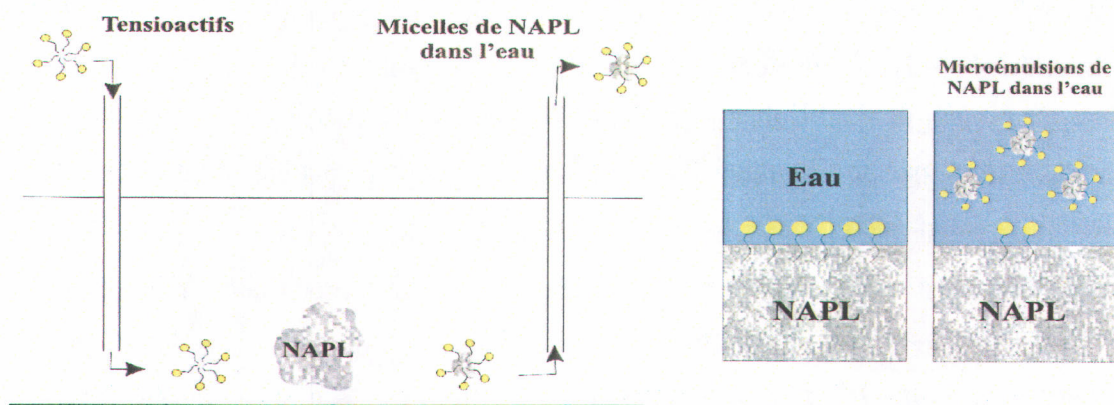
Figure 1.2: Représentation générale du lavage de sol (par dissolution) (modifié de Robert *et al.*, 2006)

Ces solutions de lavage peuvent également déloger les contaminants de la surface des grains de sable en modifiant la mouillabilité du *NAPL*. Enfin, les solvants qui peuvent être ajoutés à la solution nettoyante, transfèrent dans le contaminant, diminuant sa densité et sa viscosité et permettant ainsi d'augmenter la mobilité du *NAPL*.

Malheureusement, la récupération des contaminants par les solutions de lavage n'est pas toujours complète. Pour qu'un site puisse être exempt de toute contamination, il est indispensable que le banc de la solution nettoyante puisse pénétrer et balayer la totalité de la zone contaminée. De nombreux paramètres doivent être considérés lors du lavage de la formation géologique: i) l'hétérogénéité du milieu poreux, favorisant un écoulement à travers les couches plus perméables. Les zones moins perméables (plus fines) ne sont donc pas correctement balayées par les solutions tensioactives, empêchant de déloger les *NAPL* coincés dans les pores (Gupta *et al.*, 1988); ii) les instabilités des fronts de déplacement causées par des contrastes de viscosité et de densité entre l'eau, le *NAPL* et la solution de lavage.

Ces perturbations sont à l'origine de chenaux d'écoulement préférentiel se traduisant par la formation de doigts ("fingering") du fluide déplaçant à travers le fluide déplacé (Hornof et Morrow, 1987) (Figure 1.3).
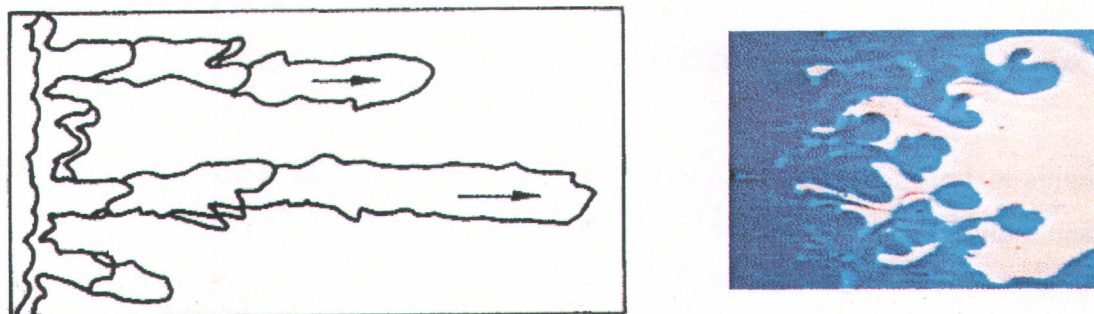
Figure 1.3: Représentation des chenaux d'écoulement préférentiel ("viscous fingering*)* (Pankow et Cherry, 1996)

Le succès de l'application de méthodes de traitement *in situ* pour la réhabilitation des aquifères contaminés par des liquides immiscibles dépend donc principalement de l'efficacité de balayage de la formation géologique contaminée. Deux types de balayage sont répertoriés: i) le **balayage en plan** dont l'efficacité peut être optimisée par l'application d'un patron d'injection et de pompage au moyen de puits verticaux et horizontaux et; ii) le **balayage vertical** dont l'efficacité peut être grandement améliorée par l'utilisation de polymères (Martel *et al.*, 2004). Des études préliminaires ont démontré que l'utilisation de ces polymères solubilisés dans l'eau et injectés en pré traitement de la solution tensioactive, contribuait à un meilleur balayage du milieu poreux. Cette efficacité s'explique par la formation de fronts stables entre les fluides en présence, due à une augmentation de la viscosité du fluide eau/polymère et une diminution du rapport de mobilité entre l'eau (contenant le polymère dissout) et le *NAPL* (Martel, 1998; Sandiford, 1977; Hirasaki et Pope, 1974; Gogarty, 1967). La solution de polymère peut également être injectée derrière la solution nettoyante afin de pousser hors du milieu poreux la solution tensioactive.

Un avantage de l'utilisation de ces solutions de polymère réside dans le fait que ce sont des substances non toxiques facilement dégradables par les bactéries, étant donné leur composition semblable à un sucre. Ceci justifie leurs utilisations dans les applications environnementales.

1.4. Essais de terrain antérieurs

Depuis la fin des années 1980, plusieurs essais à l'aide de solutions de lavage pour la restauration de sites contaminés par les *NAPL* ont été effectués. Le livre intitulé *Technology Practices Manual for Surfactants and Cosolvents* (AATDF, 1997) a répertorié au Canada et aux États-Unis 26 essais de terrain achevés ou en cours de réalisation. Ces tests ont été réalisés dans différents milieux géologiques (sable, gravier, silt argileux, roc fracturé) contaminés par plusieurs types de contaminants. Pour onze d'entre eux, un taux de récupération a été évalué. Ce taux se définit par l'équation suivante (Équation 1.1):

$$Taux\ de\ récupération = \frac{Quantité\ de\ contaminant\ récupérée}{Quantité\ initiale\ de\ contaminant\ en\ place} \qquad \text{Éq. 1.1}$$

Cet indice varie de 0 à 99 % selon la solution tensioactive choisie, le milieu poreux ou encore le contaminant en place. Pour information, une valeur moyenne pour les 26 essais de 58 % de récupération a été obtenue.

Le Tableau 1.1 présente quelques projets de restauration de sites contaminés par injection de solutions de nettoyage.

Tableau 1.1: Essais de terrain antérieurs (AATDF, 1997)

Projets	Milieu poreux	Contaminant	Solutions injectées	Mécanismes de récupération	Taux de récupération
Laramie (petit) (Wyoming/USA) Laramie (grand) (Wyoming/USA)	Sable et/ou gravier	Créosote (*DNAPL*)	Tensioactifs, sels alcalins et polymères	Mobilisation et solubilisation avec contrôle de mobilité	95 % 96 %
Fredricksburg (Virginie/USA)	Silt sableux ou argile silteuse	Créosote (*DNAPL*)	Sels alcalins, tensioactifs et polymères	Mobilisation et solubilisation	Faible récupération car injection lente
L'Assomption (Québec/Canada)	Sable et/ou gravier	Solvants chlorés (*DNAPL*)	Tensioactifs, alcools, solvants et polymères	Mobilisation, émulsification et solubilisation	86 % dans la zone saturée
Paducah (Kentucky/USA)	Sable et/ou gravier	Trichloroéthylène (*DNAPL*)	Tensioactifs	Solubilisation	0 %
Corpus Christi (Texas/USA)	Silt sableux ou argile silteuse	Tétrachlorure de carbone (*DNAPL*)	Tensioactifs	Solubilisation	Non estimé
Hill AFB (Utah/USA)	Sable et/ou gravier	Kérosène avec solvants chlorés (*LNAPL*)	Tensioactifs et cosolvants	Solubilisation (microémulsification)	> 90 %
Hialeah County (Floride/USA)	Roc fracturé	Huiles hydrauliques (*LNAPL*)	Sels alcalins et polymères	Mobilisation avec contrôle de mobilité	65 %

Sur les 26 tests répertoriés par l'AATDF (1997), cinq projets ont utilisé des solutions de polymères parmi lesquels les deux essais de Laramie (Wyoming) et ceux de Fredricksburg (Virginie), de Hialeah County (Floride) et de l'Assomption (Québec). Parmi ces 26 essais, seulement celui de l'Assomption (dans l'aquifère de la Sablière Thouin près de Montréal) a utilisé une solution de polymères en pré et post traitement de la solution tensioactive afin d'évaluer et de contrôler le front de déplacement de la solution de lavage et d'améliorer l'efficacité de balayage à travers l'aquifère (Martel *et al.*, 1998; Hébert, 1998). Le manque de connaissance vis-à-vis de cette pratique constitue donc un grand intérêt quant à la réalisation de ce projet de maîtrise.

1.5. Travaux antérieurs de l'équipe de recherche

La réhabilitation *in situ* des aquifères contaminés par les liquides immiscibles à l'aide de solutions tensioactives avec injection de polymères a déjà fait l'objet de nombreuses études auparavant. Karl-Éric Martel (1995) a en effet étudié l'efficacité de balayage de solutions tensioactives par des essais en bac de sable de 1 850 cm^3 (= 18.7 cm x 5.2 cm x 19 cm) en utilisant une solution de polymère (telle que la gomme de xanthane) comme agent mobilisateur. Différentes solutions ont été injectées à travers un milieu poreux composé de trois couches de sable de granulométrie variable afin d'observer l'effet de l'hétérogénéité sur le balayage. Ces travaux de recherche ont été réalisés en laboratoire afin d'optimiser la technologie d'utilisation des solutions tensioactives et de polymères afin qu'elle soit au point pour des essais pilotes sur le terrain. Cette étude visait essentiellement à évaluer une méthode de restauration *in situ* pour des sites contaminés aux *DNAPL*, notamment pour ceux de Mercier et de l'Assomption (Québec/Canada). Ces essais ont permis de démontrer l'efficacité des solutions de polymères sur le balayage par la formation d'un front de déplacement plus stable à travers les trois couches de sable, (balayage proche de 100 %), comparé à une simple injection d'eau.

D'autres essais en laboratoire à l'aide de colonnes de sable ont également été réalisés dans le but d'approfondir les connaissances entourant la technique de lavage des sols et d'améliorer ainsi l'efficacité de récupération des liquides immiscibles et plus spécifiquement du trichloroéthène (TCE) en phase résiduelle dans les aquifères

contaminés (Saint-Pierre, 2001). Ces travaux ont permis de développer et de sélectionner les solutions de lavage les plus performantes (à l'aide de diagrammes de phase) et d'analyser les différents mécanismes impliqués, soit la solubilisation soit la mobilisation, lors de la récupération des contaminants. Différentes stratégies d'injection ont été proposées afin d'atteindre une récupération maximale du TCE en phase résiduelle dans les sols. Les différentes solutions injectées lors de ces essais en colonne de sable ont permis une récupération du TCE de 1 à 100 %. La mobilisation s'est avérée être la méthode la plus efficace en comparaison avec la solubilisation, en récupérant davantage de TCE tout en injectant moins de solutions nettoyantes.

La plus récente étude a mis en valeur les mécanismes de récupération du TCE par injection d'une solution de lavage associée à une solution de polymère à travers un modèle physique en deux dimensions (Robert *et al.*, 2006). Le montage expérimental était composé d'une chambre de 3 630 cm^3 (= 60.5 cm x 1 cm x 60 cm) munie de parois vitrées permettant ainsi d'observer les mécanismes en cours. Ce modèle d'aquifère consistait principalement à optimiser une stratégie de récupération du trichloroéthène par solubilisation. Le déplacement des différents fluides en présence, l'infiltration du TCE à travers le milieu poreux, sa mobilisation, sa solubilisation ainsi que ses interactions avec les fluides injectés ont été étudiés au moyen de vidéos et de photographies connectées au système. Lors de ces essais, la solution de polymère a joué un rôle important sur le balayage du milieu poreux (balayage estimé à 100 %) tout en évitant la dispersion du TCE à travers les zones non contaminées.

1.6. Objectifs de recherche

Ce mémoire consiste à étudier le comportement de la gomme de xanthane lors de son injection en milieux poreux. Pour y aboutir, deux objectifs sont fixés:

Le premier objectif de ce projet est de réaliser la caractérisation physique de la gomme de xanthane en solution aqueuse pour évaluer son comportement rhéofluidifiant. Des tests en colonne de sable (de granulométrie variable) sont effectués pour mesurer sa viscosité *in situ* en fonction du taux de cisaillement. La compatibilité du polymère avec le milieu

poreux est également observée. Ces essais permettent de mieux comprendre les problèmes liés à l'écoulement en vue d'une utilisation à plus grande échelle.

Le second objectif est d'évaluer l'efficacité de balayage de la gomme de xanthane et la stabilité du front de déplacement lors de son injection en milieux poreux, par des tests en bac de sable rectangulaire. La stratégie d'injection/pompage à utiliser lors de ces essais est estimée par une simulation numérique. Ces travaux se déroulent dans les laboratoires de l'INRS/RDDC-Valcartier situés sur la base militaire de Valcartier à 30 km au nord de Québec.

1.7. Méthodologie

Les propriétés physiques de la gomme de xanthane sont déterminées à l'aide de tests en colonne de sable ainsi que par des essais en bac de sable rectangulaire. Deux sables de granulométrie différente (un sable fin et un sable grossier avec un d_{50} respectivement de 0.45 mm et 0.87 mm) sont utilisés (Filpro Well Gravels sand, U.S. Silica, New Jersey). Le choix du polymère est principalement basé sur son comportement rhéologique, sa faible toxicité, sa grande solubilité aqueuse et son faible coût.

Cinq tests en colonne de sable sont effectués pour déterminer le comportement rhéofluidifiant de la gomme de xanthane: quatre colonnes avec du sable fin et une colonne avec du sable grossier. Un des tests en colonne consiste à injecter pendant trois heures une solution de xanthane, à arrêter l'injection pendant une journée et à redémarrer l'essai le lendemain pendant le même intervalle de temps afin d'observer les éventuels changements de viscosité subis par le polymère après redémarrage. Un autre essai utilise une solution de polymère préalablement cisaillée. Un dernier test consiste à injecter le polymère en continu avec des taux de cisaillement variables. Dans chacun de ces essais, un bactéricide (le sodium azide) est ajouté à la solution de xanthane afin d'empêcher son éventuelle dégradation par les micro-organismes présents dans le milieu poreux. Pour les essais en bac de sable rectangulaire, deux tests sont réalisés pour évaluer et comprendre l'efficacité de balayage de la solution de xanthane: i) un premier essai avec un bac de

sable rempli de sable fin et; ii) un second essai avec un bac de sable composé de trois couches, une couche de sable grossier entre deux couches de sable fin. Trois différents traceurs sont employés pour évaluer la stabilité du front de déplacement: les chlorures, les bromures et l'amarante. Tous ces tests sont faits à charge constante et contrôlés par un système de deux puits en ligne dont un en injection et l'autre en pompage.

1.8. Pertinence scientifique

La mise au point de technologies *in situ* requiert dans la majorité des cas des essais à plusieurs échelles. Les essais de terrain posent souvent de nombreux problèmes tant au niveau du coût qu'au niveau du contrôle des conditions expérimentales. L'échec de bon nombre de projets de restauration a souvent été attribuable au fait que les technologies prometteuses ont failli sur le terrain. Passer du laboratoire au terrain constitue donc le principal problème lié au développement de ces technologies.

L'intérêt de ces travaux de recherche est donc de développer en laboratoire à l'aide d'un bac d'essai de 9 m^3 (= 3 m x 1.5 m x 2 m) un procédé de restauration *in situ* pour la décontamination des sols à l'aide d'une solution de polymère (Chapitre 4). Cette infrastructure unique en bac constitue un excellent moyen de représenter une situation "quasi-réelle" de terrain en trois dimensions en assurant une grande flexibilité dans les modes d'opération tout en réduisant les coûts d'opération par l'automatisation des conditions expérimentales, la réalisation d'un grand nombre d'expériences et une protection de l'environnement assurée en milieu contrôlé. Ce bac d'essai peut également servir à tester différentes géométries d'injection pour différents types de sols et contaminants. Une telle infrastructure permet de réduire considérablement les délais pour le développement des technologies à l'essai et constitue un atout scientifique et économique des plus précieux.

La réalisation de ces essais en bac de sable constitue donc un nouveau défi, tant au niveau de l'infrastructure de l'essai, de la configuration du milieu poreux utilisé et de la géométrie d'injection/pompage mise en place. Le choix d'un milieu poreux hétérogène composé de trois couches de granulométrie variable représente une difficulté

supplémentaire quant au balayage car il tient compte non seulement de l'écoulement des fluides mais également de l'hétérogénéité du milieu. Les essais de cette étude ont pour but de reproduire des conditions de terrains souvent rencontrées de par un arrangement de matériaux difficile à balayer efficacement. Les tests en bac de sable à une couche sont davantage réalisés à titre de base de comparaison afin d'étudier l'écoulement des fluides. La géométrie d'injection/pompage munie d'un seul puits d'injection et d'un seul puits de pompage alignés à chaque extrémité au milieu du bac a également été choisi de façon à rendre l'écoulement des fluides à travers le milieu poreux plus complexe et limiter ainsi les possibilités d'obtenir un balayage complet. Un tel balayage est d'autant plus difficile que les puits d'injection et de pompage n'atteignent pas la base du bac. Toutes ces contraintes ont été originellement fixées afin de mettre en évidence l'efficacité de la solution de polymère sur le balayage à travers un milieu poreux complexe difficile à balayer, proche d'une situation de terrain.

1.9. Organisation du mémoire

Le mémoire est subdivisé en cinq chapitres. Ceux-ci sont rédigés sous forme d'articles scientifiques, à l'exception des deux premières sections qui traitent de la problématique de contamination et des notions élémentaires d'hydrostatique. Le dernier chapitre reprend les conclusions générales tirées des différents articles et présente des recommandations pour les travaux futurs.

Le chapitre 1 présente la problématique de contamination des sols et des eaux souterraines et les techniques de réhabilitation *in situ* des sites contaminés. Le chapitre 2 récapitule les notions de base reliées aux écoulements multiphases en milieu poreux ainsi qu'à la notion d'efficacité de balayage. Le chapitre 3 contient le premier article qui aborde les propriétés physiques des polymères. Ceux-ci sont étudiés afin d'en expliquer le comportement rhéofluidifiant. Ce chapitre met en valeur la caractérisation des polymères par des essais en colonne. Le chapitre 4 traite des essais en bac de sable rectangulaire pour évaluer l'efficacité de balayage des solutions de polymère. Enfin, une conclusion générale et des recommandations terminent cette étude.

CHAPITRE 2
THEORIE

2.1. Introduction

$\mathscr{C}$e deuxième chapitre résume les principes d'écoulements des fluides immiscibles en milieu poreux. Ces concepts théoriques sont nécessaires à la bonne compréhension des mécanismes de piégeage et de récupération des *NAPL* par les solutions de lavage. Ces notions sont principalement tirées du livre de Charbeneau (2000) et du manuel de cours de Lefebvre (2003).

2.2. Notions d'hydrostatique

Dans cette section, il sera question des notions d'hydrostatique afin de mieux cerner la distribution des différents fluides immiscibles dans un milieu poreux à l'équilibre.

La tension interfaciale (σ): il s'agit de l'énergie nécessaire pour générer une nouvelle unité de surface à l'interface entre deux fluides immiscibles.

Cette tension interfaciale se définit comme étant un travail par unité de surface (Équation 2.1):

$$\sigma = \frac{Travail}{Aire} = \frac{F\,dx}{dA}\,[=]\left[\frac{N\,m}{m^2}\right][=]\left[\frac{N}{m}\right][=]\left[\frac{kg}{s^2}\right]$$

Éq. 2.1

La nouvelle unité de surface (*dA*) est créée en appliquant une force (*F*) sur une certaine distance (*dx*) (Figure 2.1):
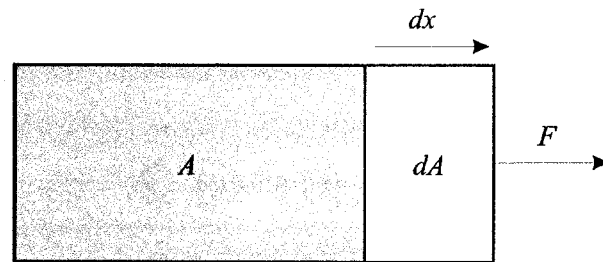
Figure 2.1: Illustration de la tension interfaciale (Lefebvre, 2003)

Ce phénomène d'interface s'explique par un déséquilibre existant entre les forces d'attraction des deux fluides immiscibles.

La mouillabilité d'un fluide: elle se définit comme étant son aptitude relative, lorsque présent avec un autre fluide immiscible, à s'étaler ou à adhérer à une surface solide. Ce paramètre s'exprime par *l'angle de contact (θ)*. Dans un système triphasé composé d'eau (w), d'huile (o) et d'une surface solide (s), la mouillabilité à l'eau ou à l'huile exprime la tendance relative de l'eau ou de l'huile à s'étendre sur la surface solide. Dans le système eau-huile-solide (Figure 2.2), l'expression mathématique mettant en relation la mouillabilité (exprimée par l'angle de contact) et la tension interfaciale s'exprime par l'équation de Young-Dupré (Équation 2.2):

$$\sigma_{os} - \sigma_{ws} = \sigma_{ow} \cos\theta \qquad \text{Éq. 2.2}$$
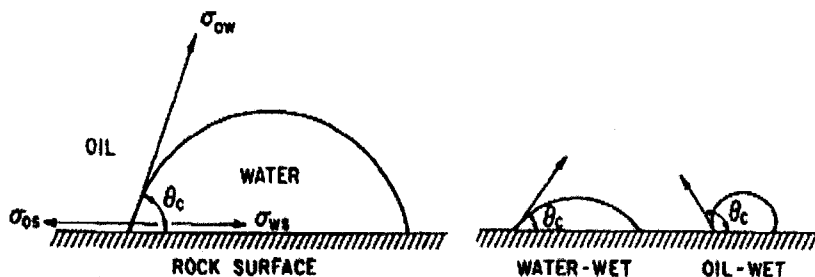
Figure 2.2: Angle de contact et tension interfaciale (Craig, 1971)

La mouillabilité est relativement complexe car elle prend en considération plusieurs facteurs tels que: i) la composition des différents fluides en présence, ii) la caractéristique du milieu poreux et; iii) les conditions physiques de température et de pression.

Les deux paramètres, à savoir la tension interfaciale et la mouillabilité, interviennent directement sur les déplacements des contaminants à travers la formation géologique.

La pression capillaire (P_c): il s'agit de la différence de pression entre deux fluides immiscibles (Équation 2.3):

$$P_c = P_1 - P_2 \, [=] \, [Pa] \, [=] \left[\frac{N}{m^2} \right]$$

Éq. 2.3

Cette pression se mesure à l'interface courbée entre les deux fluides.

Elle est reliée à la tension interfaciale par l'équation de Young-Laplace (Équation 2.4):

$$P_c = \frac{2\sigma}{R} \, [=] \, [Pa] \, [=] \left[\frac{N}{m^2} \right]$$

Éq.2.4

où R représente le rayon de courbure moyen de l'interface.

Dans un tube capillaire, le rayon de courbure (R) s'exprime par le rayon du tube capillaire (r) et par l'angle de contact (θ) selon la loi de Young (Équation 2.5):

$$R = \frac{r}{\cos\theta} \, [=] \, [m]$$

Éq. 2.5

17

En combinant les équations 2.4 et 2.5, la pression capillaire dans un tube capillaire devient:

$$P_c = \frac{2\sigma}{R} = \frac{2\,\sigma\,\cos\theta}{r}$$

La pression capillaire dans un milieu poreux peut être exprimée par l'équation 2.6, en supposant que le milieu soit composé d'une multitude de tubes capillaires dont la distribution des rayons dépend des caractéristiques du milieu (Figure 2.3).
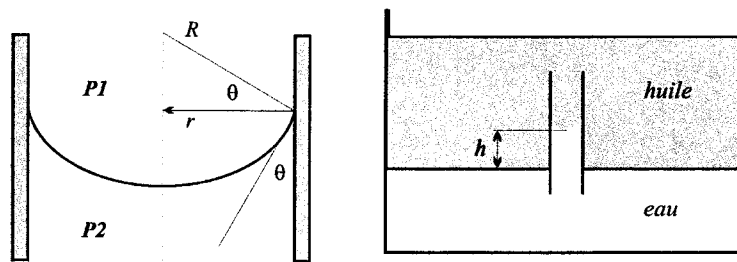
Figure 2.3: Illustration de la pression capillaire pour un tube capillaire (Lefebvre, 2003)

La pression capillaire peut également s'exprimer en prenant la différence de densité ($\Delta\rho$) entre deux fluides immiscibles, l'accélération gravitationnelle (*g*) ainsi que la hauteur de remontée du fluide mouillant (*h*) dans un tube capillaire (Figure 2.3):

$$P_c = \Delta\rho\,g\,h$$

Les propriétés capillaires sont donc fonction du milieu poreux (dimension et distribution des pores) et sont notamment responsables des mécanismes de piégeage des liquides immiscibles.

2.3. Distribution d'un contaminant dans le milieu poreux

Conceptuellement, la majorité des systèmes se composent d'une phase aqueuse (eau), d'une phase organique (*NAPL*), d'une phase solide et en proportions variables, d'une phase gazeuse (en présence dans un milieu non saturé ou partiellement saturé) (Figure 2.4).
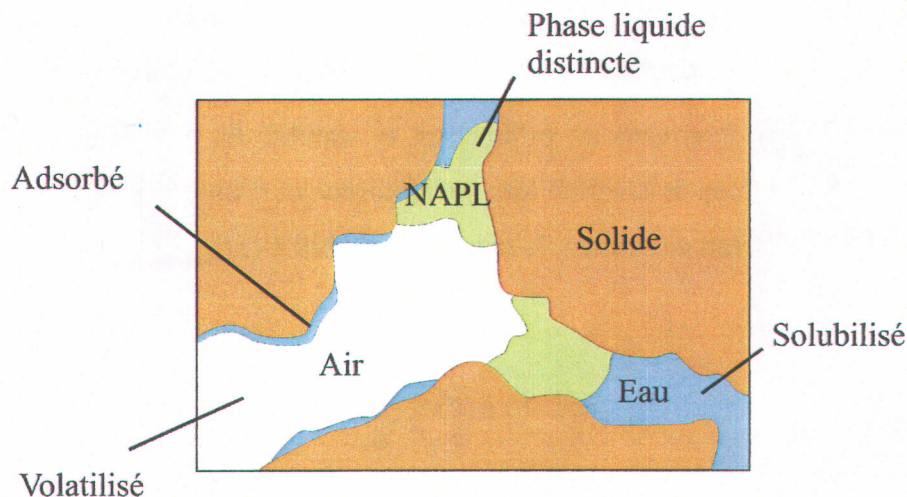
Figure 2.4: Distribution d'un contaminant organique dans un milieu poreux partiellement saturé (modifié de Lefebvre, 2003)

En présence de chacune de ces phases, le contaminant peut se comporter différemment: i) libre en tant que phase distincte, ii) solubilisé dans l'eau, iii) volatilisé dans l'air ou; iv) adsorbé sur le solide.

Le comportement global d'un composé organique à travers la formation géologique s'explique en grande partie par ses propriétés physico-chimiques: i) la migration d'un contaminant est fonction de sa mobilité. Ce mode de migration dépend essentiellement de la viscosité et de la densité du *NAPL*. La mobilité est également influencée par sa solubilité dans l'eau et sa volatilité dans la phase gazeuse; ii) la partition d'un contaminant dépend de sa solubilité, de sa volatilité ou encore de son adsorption sur le solide et enfin; iii) la persistance d'un composé organique est fonction de sa solubilité dans l'eau, de son adsorption sur les grains de la formation et également de son taux de dégradation chimique et biologique.

2.4. Mécanismes de piégeage des NAPL

Il existe quatre grands mécanismes de piégeage des *NAPL* (illustrés à la Figure 2.5) :

Les instabilités des fronts de déplacement ou *instabilités de viscosité* ("viscous fingering"): elles résultent d'un balayage peu efficace du milieu poreux par le fluide de déplacement (dans la majorité des cas l'eau), laissant en arrière du front de petites lentilles de *NAPL* (fluide déplacé). La viscosité et la densité des fluides, de même que la vitesse et le sens de l'écoulement influencent la stabilité du front (Lake, 1989). Pour déterminer les conditions de stabilité lors du déplacement d'un fluide par un autre fluide, il faut définir un nouveau paramètre, le rapport de mobilité (*M*):

$$M = \frac{k_{r1}/\mu_1}{k_{r2}/\mu_2} = \frac{\mu_2}{k_{r2}} \times \frac{k_{r1}}{\mu_1} \qquad \text{Éq. 2.8}$$

où k_r est la perméabilité relative et μ la viscosité.

Un rapport de mobilité inférieur à 1 indique un front de déplacement stable et de ce fait, un balayage plus efficace.

Les instabilités capillaires ("capillary instability"): elles sont présentes uniquement pour des milieux mouillants à l'eau. L'eau tend à demeurer en contact avec le milieu poreux, préférentiellement au *NAPL*. Dès la sortie des fluides d'un pore de faible diamètre, une goutte de *NAPL* reste piégée au centre du pore.

Le contournement de régions par le fluide de déplacement ou *écoulement préférentiel* ("bypassing"): il résulte de la présence de deux voies d'écoulements différentes pour les fluides dans le milieu poreux, se rejoignant par après, causant le piégeage d'un des fluides. En considérant l'eau comme le fluide de déplacement, celui-ci aura tendance à

passer par la voie la plus rapide et couper la voie au *NAPL*. De ce fait, le *NAPL* reste piégé dans le sol.

Le trappage de surface ("surface trapping"): ce phénomène apparaît généralement en surface dans les irrégularités au niveau des pores. Ce piégeage est principalement prononcé pour une mouillabilité aux *NAPL*.

Les instabilités des fronts de déplacement sont fortement influencées par les propriétés des différents fluides en présence. Il est possible de limiter ce type de piégeage en augmentant la viscosité du fluide de déplacement ou en abaissant celle du *NAPL*. Les trois autres mécanismes de piégeage font davantage intervenir les caractéristiques du milieu poreux (porosité, géométrie des pores, etc.) et la mouillabilité des fluides sur les surfaces solides. En abaissant la tension interfaciale entre l'eau et le *NAPL* ou en modifiant la mouillabilité, ces mécanismes de piégeage peuvent être minimisés (Wardlaw, 1982; Morrow, 1979).

La Figure 2.5 illustre de manière schématique les différents mécanismes de piégeage des *NAPL* pour trois mouillabilités différentes: i) mouillant à l'eau; ii) mouillabilité intermédiaire et; iii) mouillant au *NAPL* (Wardlaw, 1982).

Instabilité de viscosité	Instabilité capillaire	Écoulement préférentiel	Trappage de surface

Mouillage à l'eau

Eau ○

Huile ●

Mouillage intermédiaire

Mouillage à l'huile
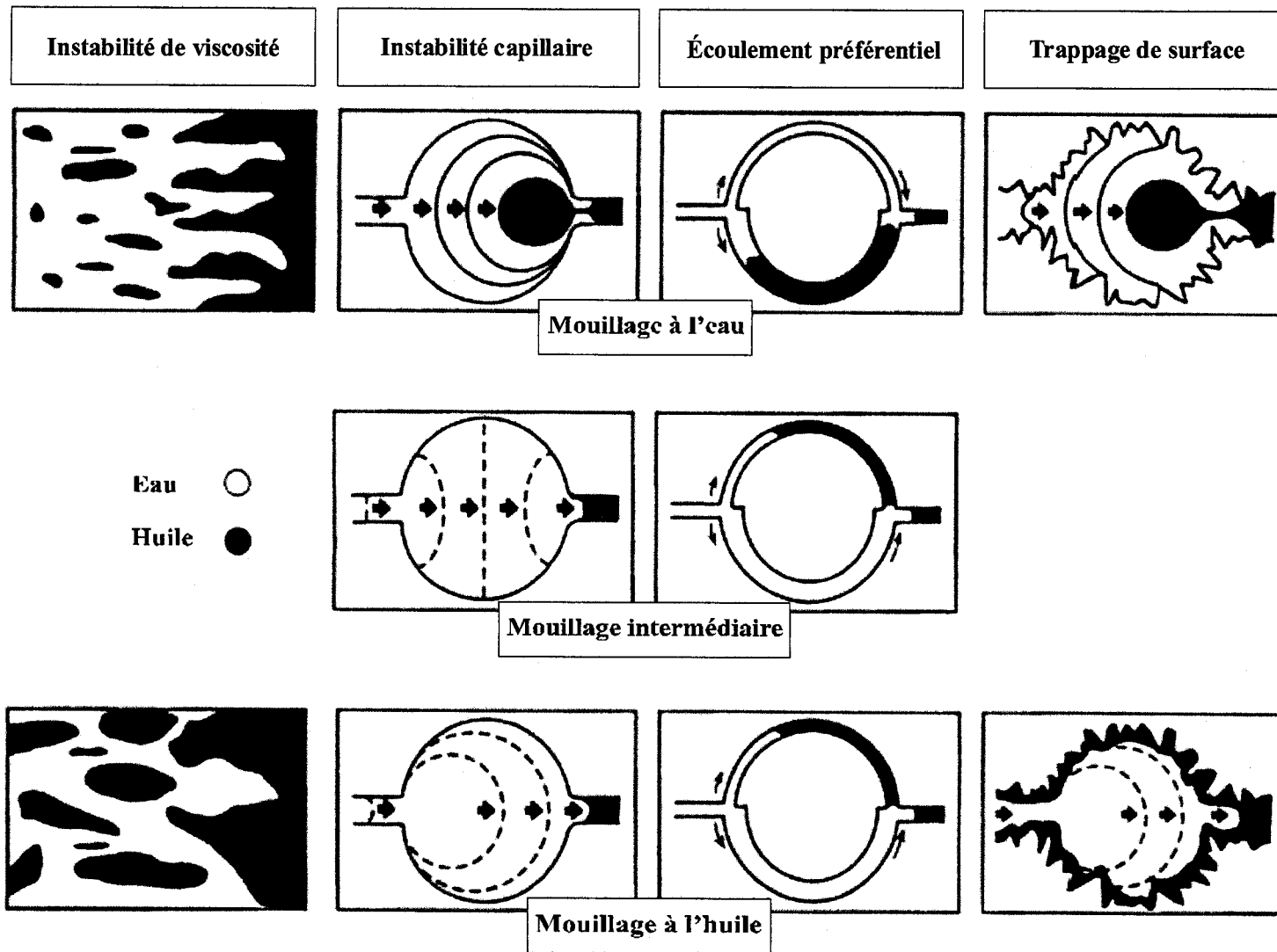
Figure 2.5: Mécanismes de piégeage des *NAPL* (Wardlaw, 1982)

2.5. Mécanismes de récupération des NAPL

2.5.1. Propriétés agissant sur la récupération des NAPL

La récupération des *NAPL* piégés dans le milieu poreux dépend de plusieurs paramètres variables qui interagissent entre eux:

1. Les forces agissant sur le système solide-fluide:

Les forces de viscosité (F_v): elles résultent de l'écoulement du fluide de déplacement qui tend à pousser les *NAPL* hors du milieu poreux. De ce fait, la saturation résiduelle du *NAPL* diminue. Ces forces dépendent principalement de la vitesse de circulation du fluide de déplacement (v) et de sa viscosité (μ) (Équation 2.9). La perméabilité (k) du milieu joue également un rôle:

$$F_v = v\,\mu = k\left(\frac{dP}{dx}\right)$$

Éq. 2.9

Les forces de capillarité (F_c): elles s'expriment par la pression capillaire (Équation 2.6). Elles s'opposent aux forces de viscosité en piégeant les *NAPL* au sein du milieu poreux en empêchant leur mobilisation. La fraction de *NAPL* piégée par les forces capillaires et mobilisée par les forces de viscosité peut se définir par le nombre capillaire (N_c):

$$N_c = \frac{v\,\mu}{\sigma\cos\theta} = \frac{\Delta P\;k}{\Delta L\;\sigma}$$

Éq. 2.10

Les forces de gravité ou flottabilité (F_g): elles font intervenir le facteur gravitationnel. Elles dépendent de la différence de densité des phases en présence ($\Delta\rho$) (phase aqueuse et organique) ainsi que de la dimension des gouttelettes de *NAPL* (h):

$$F_g = \Delta\rho\,g\,h$$

Éq. 2.11

Pour améliorer la récupération des *NAPL*, il est possible d'augmenter les forces de viscosité en augmentant la viscosité du fluide de déplacement ou en diminuant la viscosité du *NAPL*. La modification des forces de flottabilité (densité) est également possible mais peut entraîner un phénomène d'"overriding" ou d'"underriding" du fluide de déplacement lors de la récupération par la formation d'une phase libre de *NAPL* ou de *NAPL* dans une émulsion qui coule plus en profondeur ou qui flotte. Une autre alternative est de jouer directement sur les forces de capillarité en abaissant la tension interfaciale et/ou en modifiant la mouillabilité (Morrow, 1979).

2. Les <u>propriétés</u> des fluides:

La densité, la viscosité ou encore la tension interfacilale des différents fluides en présence influencent fortement la récupération des *NAPL*.

D'autres paramètres non modifiables peuvent également jouer un rôle sur la récupération des *NAPL*, tels que le milieu poreux ou fracturé (porosité, perméabilité, hétérogénéité, topologie, etc.) et les interactions solide-liquide (mouillabilité, perméabilité relative).

2.5.2. Paramètres associés à l'efficacité de récupération

L'efficacité de récupération (E$_R$): elle correspond au ratio entre l'huile récupérée et l'huile présente initialement dans l'aquifère contaminée.

$$\textit{Efficacité de récupération } (E_R) = \frac{\textit{Huile récupérée}}{\textit{Huile initialement en place}} \qquad \text{Éq. 2.12}$$

L'efficacité de récupération peut également s'exprimer par le produit de l'efficacité de déplacement (E$_D$) et de l'efficacité de balayage (E$_B$):

$$E_R = E_D \times E_B \qquad \text{Éq. 2.13}$$

L'efficacité de déplacement (E_D): il s'agit d'un phénomène principalement microscopique. Elle représente la fraction d'huile pouvant être déplacée par le fluide de déplacement et l'huile originellement en place dans le milieu.

$$Efficacité\ de\ déplacement\ (E_D) = \frac{Huile\ déplaçable}{Huile\ initialement\ en\ place} \qquad \text{Éq. 2.14}$$

L'efficacité de balayage (E_B): il s'agit d'un phénomène essentiellement macroscopique. Elle se définit comme la fraction de volume du réservoir mis en contact direct avec le fluide de déplacement.

$$Efficacité\ de\ balayage\ (E_B) = \frac{Volume\ contacté\ par\ le\ fluide\ de\ déplacement}{Volume\ total\ du\ réservoir} \qquad \text{Éq. 2.15}$$

Le balayage dépend essentiellement des forces de viscosité ainsi que des écoulements préférentiels à travers le milieu poreux.

L'efficacité de balayage peut se subdiviser en deux composantes, le balayage vertical (E_{BV}) et le balayage horizontal (E_{BH}). Ces deux paramètres sont des rapports de surface définis par :

$$E_{BV} = \frac{Aire\ verticale\ atteinte\ par\ le\ fluide\ déplaçant}{Aire\ verticale\ totale} \qquad \text{Éq. 2.16}$$

$$E_{BH} = \frac{Aire\ horizontale\ atteinte\ par\ le\ fluide\ déplaçant}{Aire\ horizontale\ totale} \qquad \text{Éq. 2.17}$$

Le produit de l'efficacité de balayage vertical et de l'efficacité de balayage horizontal définit l'efficacité de balayage (E_B) :

$$Efficacité\ de\ balayage(E_B) = balayage\ vertical(E_{BV}) \times balayage\ horizontal(E_{BH}) \qquad \text{Éq. 2.18}$$

Les caractéristiques verticales et horizontales du réservoir jouent donc un rôle important sur le balayage (Figure 2.6) :

(a)   **(b)**
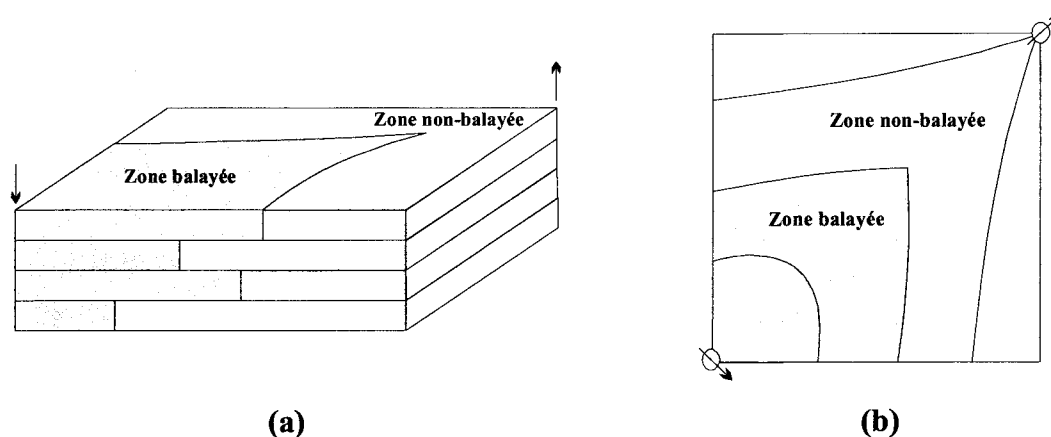
Figure 2.6: Efficacité de balayage vertical (a) et horizontal (b) (modifié de Lake, 1989)

Le balayage vertical (Figure 2.6a), influencé par la viscosité, la densité des fluides et les hétérogénéités du milieu (perméabilité variable, stratifications, etc.) est principalement contrôlé par le rapport de mobilité; le balayage horizontal (Figure 2.6b) dépend de l'anisotropie de la formation ainsi que du patron d'injection.

2.6. Modes de récupération par les solutions de lavage

Il existe deux grands mécanismes de récupération des *NAPL*: i) la **mobilisation** et; ii) la **solubilisation**.

La *mobilisation* est un procédé qui dépend de la capacité d'un tensioactif à abaisser la tension interfaciale entre l'eau et le *NAPL*, lorsque les molécules de tensioactifs se répartissent à la surface du *NAPL* (McCray *et al.*, 2001; Bai *et al.*, 1997; Abdul et Gibson, 1991). Cette diminution a pour but de réduire les forces capillaires responsables du piégeage des *NAPL*. Les gouttelettes de *NAPL* piégées dans les pores du milieu poreux tendent à s'agglomérer pour former un banc de *NAPL*, favorisant leur mobilisation. Le tensioactif transfère également dans le contaminant diminuant sa viscosité et sa densité et augmentant ainsi sa mobilité. Ce mode de récupération est néanmoins très peu employé et ce, malgré son grand potentiel pour la restauration (Bettahar *et al.*, 1999; West et Harwell,

1992). Un des principaux désavantages est que le tensioactif est transféré dans le *NAPL* et est de ce fait, très difficile à recycler.

La *solubilisation* est le mode de récupération des contaminants le plus fréquemment utilisé. L'utilisation d'un tensioactif améliore considérablement la solubilisation. Elle consiste à augmenter la solubilité des contaminants hydrophobes par la formation de micelles. Par ces micelles, le transfert du *NAPL* dans la phase aqueuse est favorisé.

A faible concentration, la solution tensioactive se retrouve sous forme de petites molécules simples, les monomères. Ces molécules ont peu d'effet sur la solubilité des huiles (Pennel *et al.*, 1993). A partir d'une certaine concentration appelée la concentration micellaire critique (CMC), la concentration en monomères n'augmente plus. A partir de ce seuil, les molécules de tensioactifs s'agglomèrent pour former des micelles. Le *NAPL* se retrouve alors enfermé à l'intérieur de la micelle, augmentant sa solubilité apparente dans la phase aqueuse.

La Figure 2.7 illustre la formation des micelles pour des concentrations élevées (supérieures à la concentration micellaire critique).
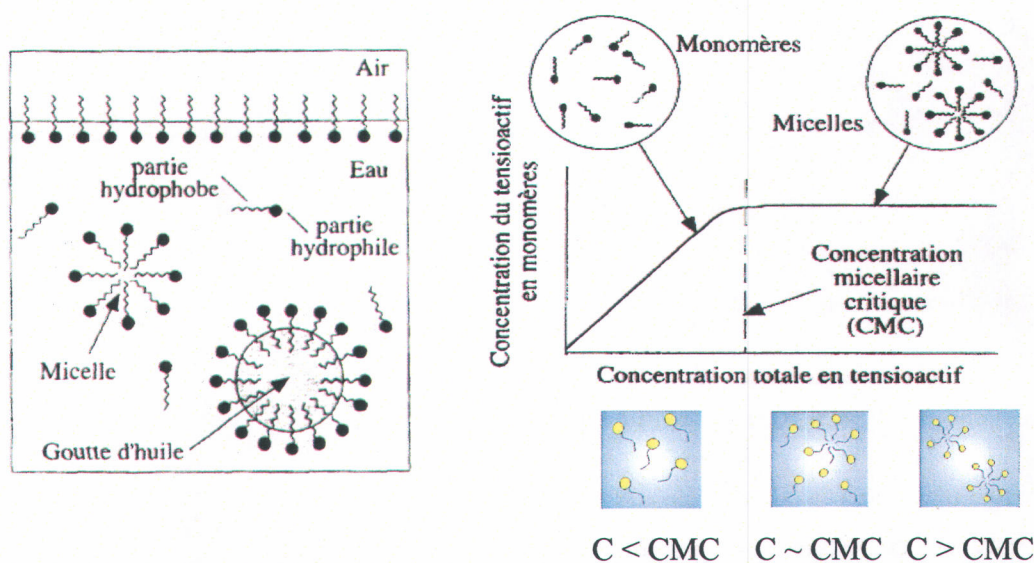
Figure 2.7: Formation des micelles (AATDF, 1997; Lake, 1989)

La solubilisation est un mécanisme qui nécessite l'injection de grandes quantités de tensioactifs, ce qui peut représenter un inconvénient en terme de coût.

CHAPITRE 3
Etude de la gomme de xanthane

3.1. Introduction

$\mathscr{L}$e troisième chapitre de ce mémoire contient le premier article. Il est consacré à la caractérisation physique de la gomme de xanthane pour mieux en connaître ses propriétés intrinsèques. Le choix de ce polymère est basé selon plusieurs critères: ses propriétés rhéologiques, sa grand solubilité aqueuse, sa faible toxicité ainsi que son faible coût. Des essais en laboratoire à l'aide de colonnes de sable de granulométrie variable ont permis de mieux comprendre le comportement rhéofluidifiant de ce polymère lors de son injection à travers un milieu poreux ainsi que ses interactions avec le sable pour une utilisation à plus grande échelle (Essais en bac de sable - Chapitre 4).

L'emploi de polymères solubilisés dans l'eau tels que la gomme de xanthane dans les méthodes de lavage de sols par injection et pompage de solutions tensioactives, contribue à un meilleur balayage de la formation géologique. Cette efficacité s'explique par la formation de fronts stables entre les fluides en présence, due à une augmentation de la viscosité du fluide eau/polymère et une diminution du rapport de mobilité. Cette augmentation de viscosité dépend principalement de la concentration du polymère, de la température ainsi que du taux de cisaillement appliqué sur les différents fluides déplacés.

3.2. Study of the behavior of shear thinning polymers during their injection in porous media

by Michael Haberman, Richard Martel,
Uta Gabriel, René Lefebvre, Luc Trépanier

3.2.1. Abstract

Tests in sand columns confirmed the shear thinning behavior of xanthan gum: the viscosity of this polymer decreases gradually with the shear rate (and thus the flow rate). However, at a fixed shear rate, the viscosity increases due to clogging of the porous medium. This clogging is mainly caused by an accumulation of polymer inside the column. Other tests showed that the intrinsic rheological properties of xanthan gum are modified when it has undergone a first shearing through a porous medium. The polymer then loses its properties.

3.2.2. Résumé

Des essais en colonne de sable ont confirmé le comportement rhéofluidifiant de la gomme de xanthane: la viscosité de ce polymère diminue progressivement avec le taux de cisaillement (et donc la vitesse d'écoulement). Cependant, à partir d'un certain taux de cisaillement, la viscosité augmente à cause d'un colmatage du milieu poreux. Ce colmatage est principalement dû à une accumulation de polymère au sein de la colonne. Les essais ont également montré que les propriétés rhéologiques intrinsèques de la gomme de xanthane sont modifiées lorsque celle-ci a subi un premier cisaillement à travers un milieu poreux. Le polymère perd alors ses propriétés.

3.2.3. Introduction

Non Aqueous Phase Liquids (*NAPL*) causes many difficulties for the remediation of contaminated aquifers. *NAPL* present in an aquifer at saturation varying from full to residual are characterized by a low solubility in water, forming a distinct phase. *NAPL* can be found at the surface of a contaminated aquifer (Light Non Aqueous Phase Liquids, *LNAPL*) or at its base (Dense Non Aqueous Phase Liquids, *DNAPL*) on an impermeable layer. Due to their low aqueous solubility, high toxicity and low biodegradation, *NAPL*-forming substances can be the source of long-term groundwater contamination.

Many processes for the remediation of *NAPL* source zones have already been studied (such as thermal, biological, physico-chemical treatments, etc.) but among the limitations to their uses, there are the extent and the depth of the contamination or still the low temperature of groundwater in cold region (8 °C). Other solutions exist to recover *NAPL* such as "waterflooding". This process consists in injecting water through the geological formation and so pumping the water containing the contaminants that it dislodges. After, this water is treated at the surface. This technique is effective for light compounds but for heavy compounds, this method is not very applicable due to their low solubility and their low mobility (Mackay and Cherry, 1989). *In situ* treatments by soil washing can remediate *NAPL*-contaminated sites and so constitutes a good alternative (Martel *et al.*, 2004; Martel *et al.*, 1998; Sandiford, 1977; Szabo, 1975b; Gogarty, 1967). In soil washing, the use of polymers in the washing solutions or injected alone in pre or post treatment allows a better distribution of contaminants, a better sweep of the geological formation with more contact between the cleaning solution and the porous medium and in this manner, ensures a better recovery of contaminants, avoiding the problems related to displacement front instabilities and preferential viscous fingerings (Robert *et al.*, 2006; Hornof and Morrow, 1987) (Figure 3.1).
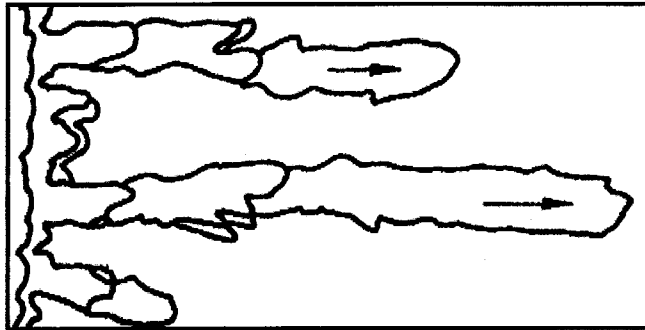
Figure 3.1: Representation of "viscous fingering" (Pankow and Cherry, 1996)

The objective of this study is to better understand the behavior of a polymer (xanthan gum) dissolved in water in porous media. Laboratory tests with sand columns (of various grain sizes) allowed the physical characterization of xanthan gum aqueous solutions and their interactions with the porous media.

3.2.4. Literature review

Previous studies showed that the use of polymers dissolved in water and injected in pre or post treatment contribute to a better sweep of the contaminated aquifer (Martel *et al.*, 1998; Martel, 1995; Sandiford, 1977; Gogarty, 1967). The efficiency is explained by the formation of stable fronts between the different fluids because of an increase of the water viscosity containing polymer and a reduction of the mobility ratio *M* (Lake, 1989):

$$M = \frac{\lambda_{water+polymer}}{\lambda_{NAPL}} = \frac{k_{water+polymer}}{\mu_{water+polymer}} \times \frac{\mu_{NAPL}}{k_{NAPL}} \qquad \text{Eq. 3.1}$$

where k (m^2) is the relative permeability of the porous medium to fluids, μ (Pa.s) is the viscosity of fluids and λ is the mobility (k/μ).

The particularity of polymer solutions (such as xanthan gum) is their shear thinning behavior, i.e. they can thicken the aqueous solution with very low concentrations, thus reducing the fluid relative viscosity when the shear rates are important in order to support the circulation of polymer through a fine porous medium. Also, the fluid relative viscosity is increased when the shear rate is low (in a coarse porous medium). Another advantage of the use of xanthan gum is that it is non toxic and easily biodegradable (Garcia-Ochoa *et al.*, 2000).

Among many research studies realized on the subject, K.E. Martel (1995) evaluated in laboratory the sweep efficiency of polymers solutions such as xanthan gum in water during their injection into a small sand box of 1 850 cm^3 (= 18.7 cm x 5.2 cm x 19 cm). The sand box was made up of three sand layers of different grains size in order to observe the heterogeneity effect. The study allowed to understand the behavior of polymers in porous media and their flow in a two-dimensional system. The realization of these works consisted in optimizing the technology of surfactants and polymers solutions in order to be functional for future pilot tests on the field, notably for the site of Mercier (Québec/Canada) contaminated at residual saturation with oil. These tests showed a stable displacement front during the injection of a xanthan solution, compared to a water injection. Moreover, 100 % of the sand box was swept vertically.

Field tests were also performed in the aquifer at the Thouin Sand Pit (Assomption) near Montreal (Québec/Canada) to study the *in situ* recovering of *DNAPL*. These tests allowed to evaluate an injection/pumping strategy and to test the use of polymer solutions in pre or post treatment of the washing solution. These experiments were carried out in order to evaluate and control the displacement front of the washing solution and to improve the vertical sweep efficiency through the sand unit (Martel et al., 1998; Hébert, 1998). With a system of a central injection well and four pumping wells arranged along a 5-point square pattern, 86 % of initial *DNAPL* saturation was recovered using only 0.9 pore volume of a surfactant solution. Although some zones were not swept, notably in depth in the sand, the vertical sweep was estimated at 95 %.

3.2.5. Methodology

The physical properties of xanthan gum were studied with laboratory tests at 20 °C (± 2 °C) in sand columns to better understand their intrinsic behavior. This section presents characteristics of sands and polymer used and the equipment description.

3.2.5.1. Porous media selection

For the column tests, a medium and a fine sand were used (Filpro Well Gravels sands U.S. Silica, New Jersey). These sands, composed of 99.4 % of quartz, are uniform and the grains are rounded to sub-angular (Table 3.1).

Table 3.1: Characteristics of sands used for tests

Sand	ρ (kg/m^3)	K (m/s)	k (m^2)	d_{50} (mm)	d_{pore} (μm)
FINE	2 650	7×10^{-4}	7.2×10^{-11}	0.45	76
MEDIUM		21×10^{-4}	21.5×10^{-11}	0.87	131

where ρ is the mineral density, K the hydraulic conductivity, k the permeability, d_{50} the mean size diameter of sand particles and d_{pore} the equivalent pore size diameter.

Pore size was calculated as follows (Chauveteau and Zaitoun, 1981):

$$d_{pores} = 2\sqrt{8\frac{k}{n}}$$ Eq. 3.2

where k (m^2) is the intrinsic permeability and n the porosity. The average porosity measured for the used sands is 40 %.

The grain size distribution was characterized according to ASTM D422-63 method (Figure 3.2; Appendix C).
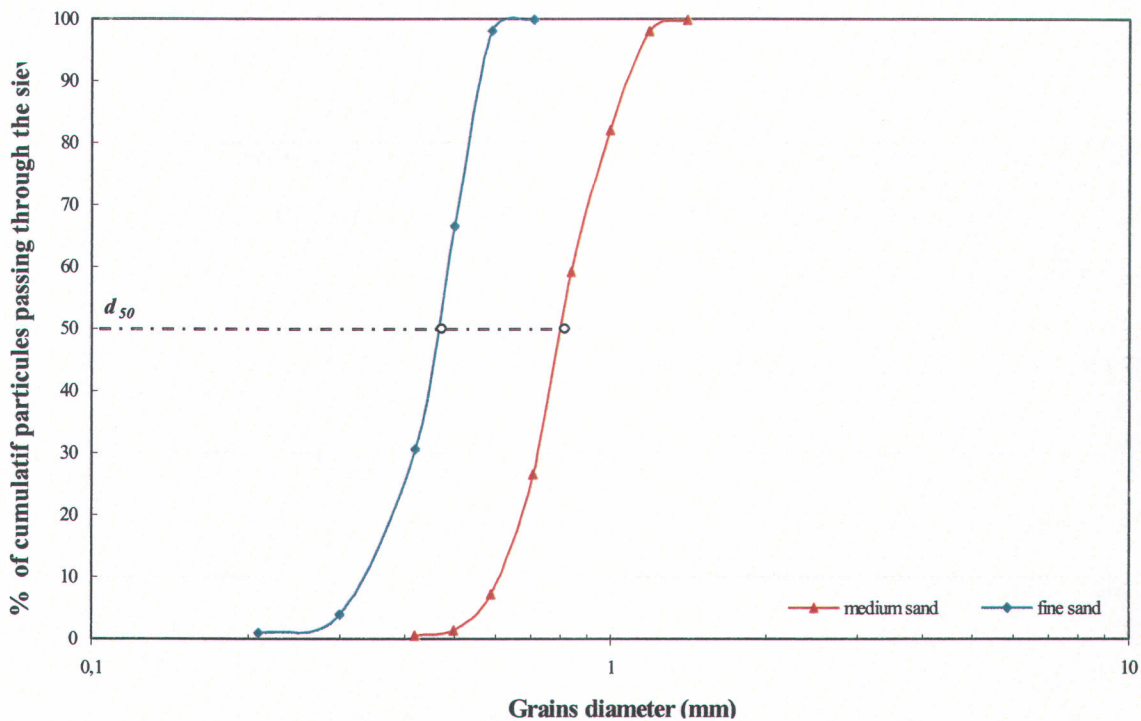
Figure 3.2: Grain size of the selected sands

3.2.5.2. Polymer selection

Xanthan gum was chosen for its rheological behavior, its low toxicity and its low cost. This polymer is characterized by a high aqueous solubility at 20 °C (laboratory temperature) and its shear thinning behavior.

Xanthan gum is a polysaccharides biopolymer. It is made by extra cellular fermentation of glucose with the bacterium *Xanthomonas campestris*. It was isolated for the first time by Jeans *et al.* (1961). Its molecular structure is represented in Figure 3.3.
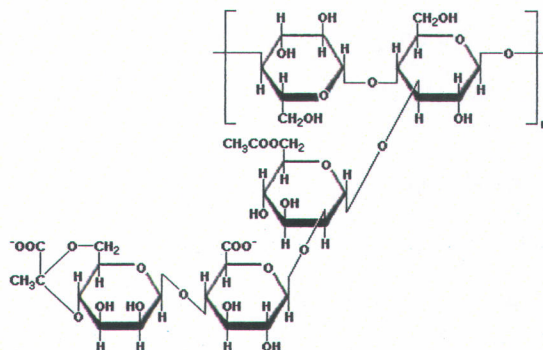
Figure 3.3: Molecular structure of xanthan gum (Roubroeks *et al.*, 2001)

The shear thinning behavior of xanthan gum for different aqueous concentrations was studied by viscosity measurements at 20 °C (±2 °C) with a Brookfield rheometer (Brookfield Engineering Labs, Inc) by increasing progressively the shear rate (Figure 3.4; Appendix A).
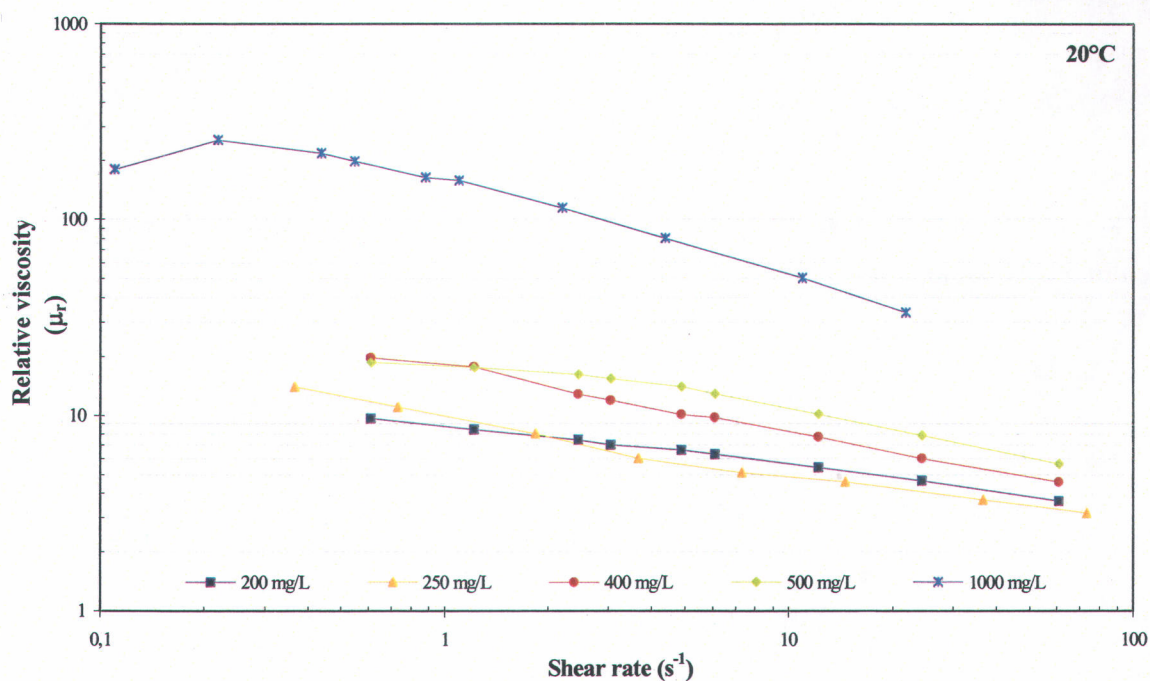
Figure 3.4: Viscosity as a function of shear rate of xanthan gum for different aqueous concentrations

Its molecular weight, measured by light diffusion, is between 1×10^6 and 50×10^6 g/mol depending on the presence of microgels (Chauveteau and Kohler, 1980). The microgels are multimolecular chemical aggregates of 6 μm in size becoming deformed during a rapid flow. For a long time, due to microgels, there was an overestimation of molecular weight obtained by light diffusion. Values between 1×10^6 and 2×10^6 g/mol would be more representative of molecular weight for the xanthan gum

3.2.5.3. Preparation of the polymer solutions

The homogeneity and the viscosity of polymer solutions can be affected by the preparation method (Chen and Sheppard, 1979). For all experiments, a concentrated xanthan solution of 1 000 mg/L was prepared at room temperature by gradually adding the polymer under the form of white powder to degassed distilled water. A slight agitation was necessary to avoid the degradation of rheological properties of the polymer. Because xanthan is an easily degradable polysaccharide, a bactericide (400 mg/L of sodium azide NaN_3) was added to the solution to preserve the solutions for a longer period of time. Finally, the xanthan solution was diluted to 250 mg/L, the concentration used in all the column tests.

3.2.5.4. Experimental equipment

Figure 3.5 schematically represents the set up used for polymer characterization in sand column (Appendix F).
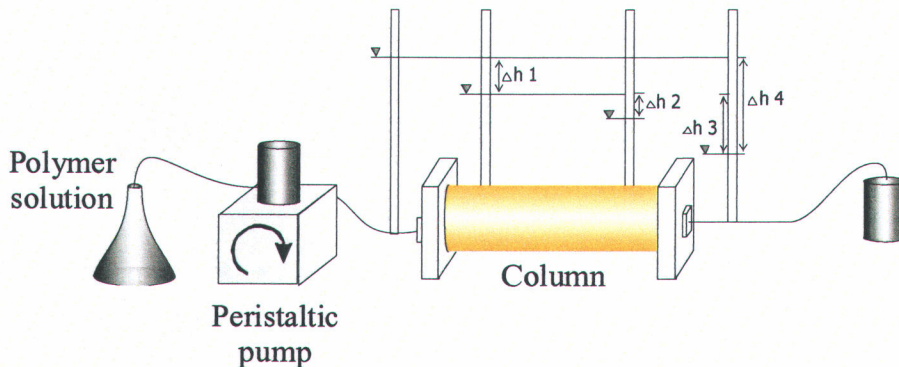
Figure 3.5: Set up for polymer characterization

The column is made of a 14.3 cm long and 3.6 cm diameter Plexiglas cylinder (Figure 3.5). Each extremity consists of two stacked Teflon plates with holes of 1 mm diameter covered with a filter of 160 μm in stainless steel to avoid the sand particles exiting from the column.

Column filling is done with 5 g sand layers introduced into the column and compacted 12 times with a sliding weight of 204 g attached to a vertical stem and dropped from a 13 cm height. The surface of the layer is scarified to ensure a link with the next layer. This process is repeated until complete filling of the column. The column is then flushed with carbon dioxide (CO_2) to eliminate ambient air trapped before the saturation of the column with degassed water.

The polymer solution is injected into the sand column using a peristaltic pump. Two vertical tubes connected to the Plexiglas cylinder allow the measurement of hydraulic heads in the sand (Δh_2). Two other tubes are put outside the column to measure the external heads (Δh_4) (Figure 3.5). A laser beam (Black & Decker) is used to provide a reference level. By measuring the height of fluid in each tube, it is possible to witness by difference the hydraulic head between the different tubes. Knowing the dimensions of the column and the mass of sand and water inside and by measuring the flow, the hydraulic heads and the sand properties (porosity and hydraulic conductivity), it is possible to calculated the applied shear rate through sand grains and to evaluate the viscosity of the polymer solution.

Sand column tests were characterized by injecting water. Flow rate and water heights inside each vertical tube were measured to calculate the hydraulic head differences (Δh_2 and Δh_4) (Figure 3.5) and to determine the corresponding hydraulic conductivity of the porous medium (Table 3.2) according to Darcy's law:

$$K = \frac{Q}{\Delta h} \times \frac{\Delta L}{A}$$

Eq. 3.3

where K (m/s) is the hydraulic conductivity, Q (m^3/s) the flow rate, Δh (m) the difference in hydraulic heads (Δh_2 or Δh_4), ΔL (m) the length of the porous medium and A (m^2) the column surface area.

The relative viscosity (μ_r) of polymer solutions is calculated from the following equation:

$$\mu_r = \frac{K_{water}}{K_{xanthane}}$$

Eq. 3.4

where K_{water} is the hydraulic conductivity to water and $K_{xanthan}$ is the hydraulic conductivity to xanthan solution in the column.

All the experiments consider only the hydraulic head difference inside the column (Δh_2) and the permeability k is supposed constant during all the tests.

Five sand column tests were carried out to determine the physical properties of xanthan gum: four column tests with fine sand and one column with medium sand (medium sand; column 3) (Table 3.2). Among these tests, one consisted in stopping the injection for one day and restarting the injection the day after to see if change in polymer viscosity is observed after restarting (injection restarted; column 1). Another test used an already sheared polymer that had undergone shearing by flowing through a sand tank (sheared polymer; column 4). Another column test consisted in injecting a xanthan solution continually with variable flow rates (increasing-decreasing-increasing shear rates) to observe the hysteretic effect (cycled polymer; column 5).

Table 3.2: Characteristics of tests realized and hydraulic conductivity according to hydraulic heads (Δh_2)

Column	Characteristics	Hydraulic conductivity K associated to Δh_2 (m/s)
1	Fine sand [Xanthan] = 250 mg/L (restarted)	9.62×10^{-4}
2	Fine sand [Xanthan] = 250 mg/L	5.89×10^{-4}
3	Medium sand [Xanthan] = 250 mg/L	21.1×10^{-4}
4	Fine sand [Xanthan] = 250 mg/L (sheared)	5.35×10^{-4}
5	Fine sand [Xanthan] = 250 mg/L (cycled)	5.89×10^{-4}

3.2.6. Results

Five tests in sand column determined the physical properties of xanthan gum and identified the intrinsic characteristics of the tested sands (Appendix E).

3.2.6.1. Evolution of viscosity after stopping and restarting

A xanthan gum solution at 250 mg/L was injected through a column during three hours with the same flow rate (column 1). The experiment was then stopped during a day. A second injection was made with the same conditions than the first one. Finally a third injection finished the test with the same flow rate after another stop of one day (Figure 3.6). The viscosity varies very little during this test.
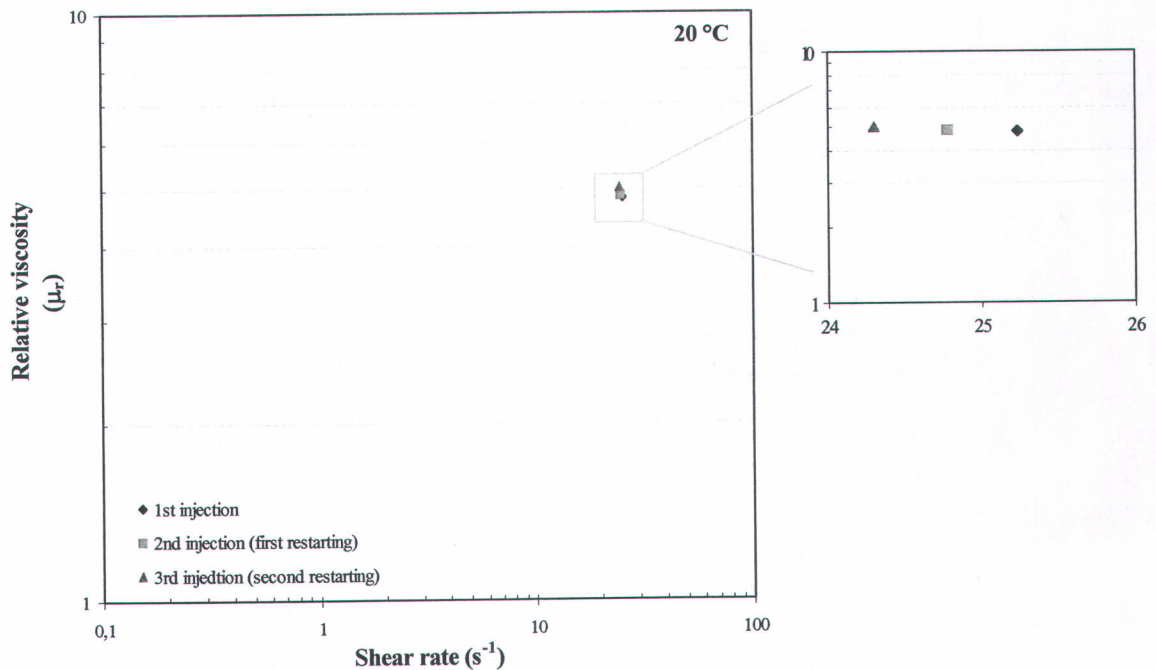
Figure 3.6: Evolution of viscosity after restarting the injection in sand column 1

Table 3.3 shows the values of relative viscosity for each restarted injection. The viscosity variation is insignificant. In fact, the weak viscosity increase between each test is related to a very small decrease in shear rate (flow rate).

Table 3.3: Relative viscosity for each start up with the shear rate

Start	Shear rate (s^{-1})	Relative viscosity
1	25.23	4.83
2	24.78	4.87
3	24.30	5.02

3.2.6.2. Shear thinning behavior of 250 mg/L polymer solutions

For shear rates between 0.1 and ~ 3 to 6 s^{-1}, the decrease in viscosity is function of the increase in shear rate (and so increase in injection flow rate), and confirms the shear thinning behavior of xanthan gum (Figure 3.7). For shear rates higher than 6 s^{-1} (indicated by the vertical line on Figure 3.7), the shear thinning behavior is lost and viscosity tends to increase with shear rate, due to a clogging phenomenon.
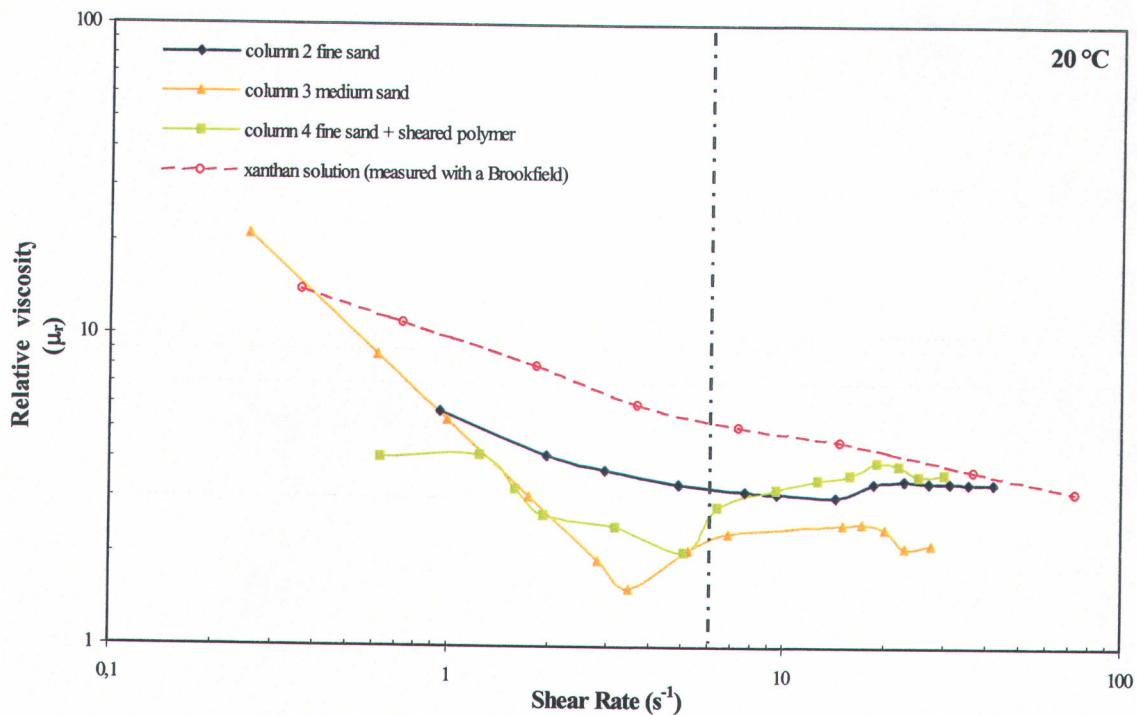
Figure 3.7: Shear thinning behavior of xanthan gum solutions at 250 mg/L

Measured viscosities in sand columns are compared to viscosities of a xanthan solution at 250 mg/L measured with a Brookfield that was not circulated in sand (Figure 3.7). Measured viscosities in fine and medium sands are compared to a theoretical curve with a constant slope based on the observed viscosities at low share rates (Figure 3.8).
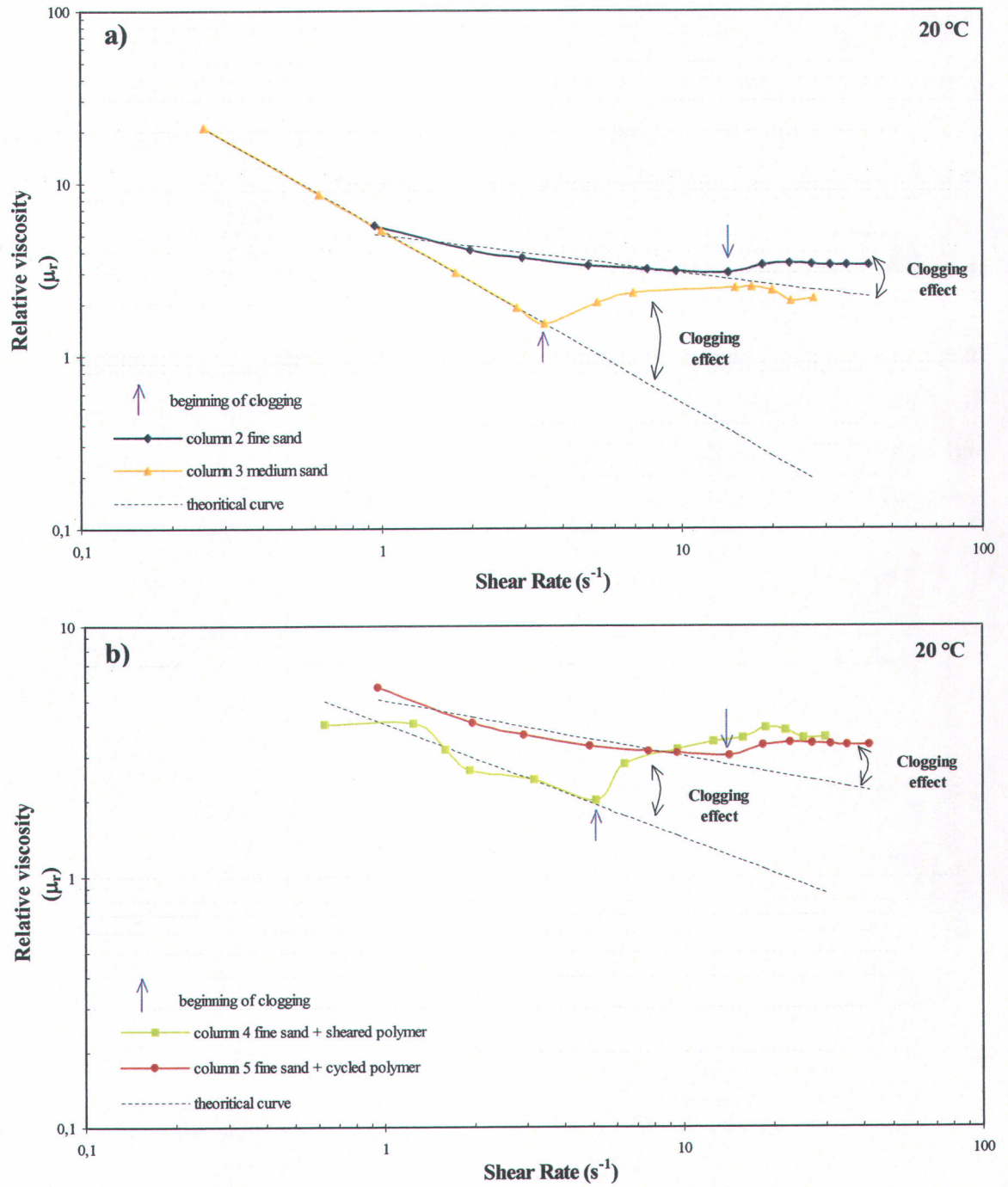
Figure 3.8: Experimental data and theoretical curve of relative viscosity of 250 mg/L aqueous xanthan gum solution as a function of shear rate

There is a clogging effect for each test caused by the polymer in the column. The clogging occurs earlier for the medium sand at a shear rate of 3.5 s^{-1} (column 3) and is more marked (Figure 3.8a). As the shearing is weaker in a coarser porous medium due to grains size, the viscosity is higher and so the polymer solution tends to block more easily the medium pores. For the same shear rate, μ_r is higher in the fine sand than in the medium sand because the polymer loss is more important in the medium sand and so the polymer concentration decreases. In the column 4 and 5, the shear thinning behavior is also respected until the clogging occurs (Figure 3.8b). For each column, the shear thinning behavior follows theoretical data until clogging.

3.2.6.3. Clogging process

In all column tests, clogging cannot be explained by the presence of microgels because of their small size (6 μm) compared to pore size (respectively of 76 μm and 131 μm for fine and medium sand) and the mesh size of the metallic screen at the inlet and the outlet of columns (160 μm) as shown in Figure 3.9 (Appendix D).
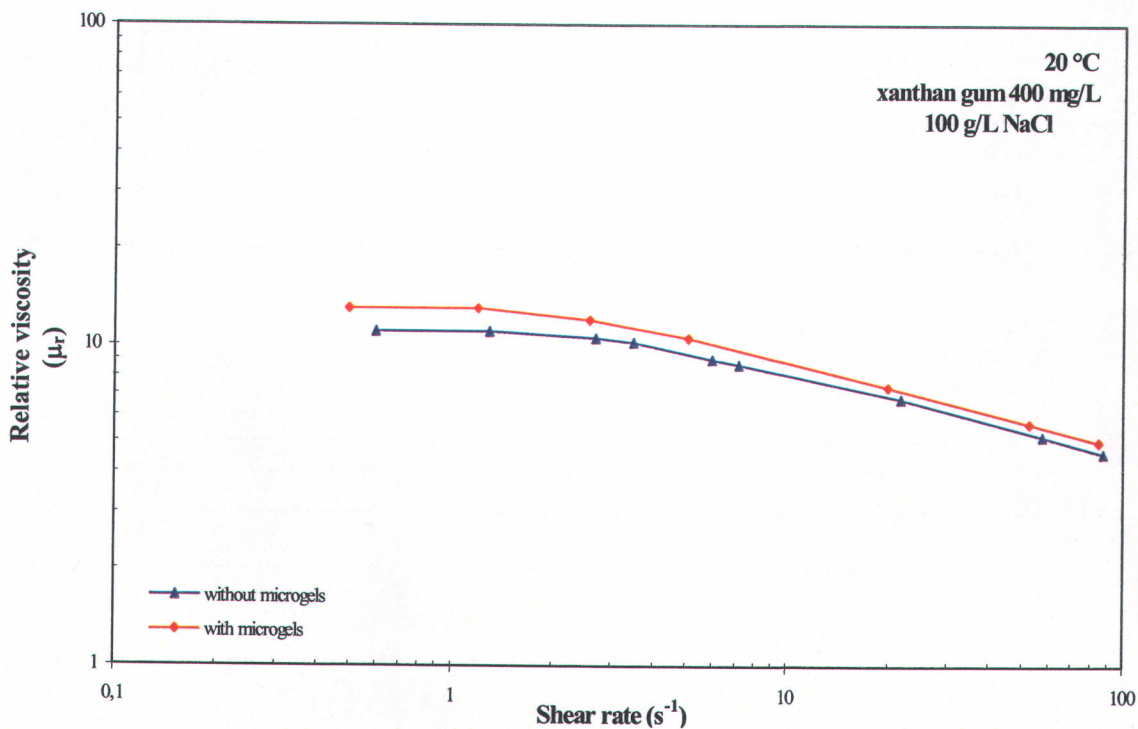
Figure 3.9: The effects of microgels on shear viscosity (adapted from Chauveteau and Kohler, 1980)

The presence of microgels does not influence very much the viscosity of polymer solutions, mainly at the highest shear rates as shown in Figure 3.9 made by Chauveteau and Kohler from direct measurements of relative viscosity on a xanthan gum solution at 400 mg/L with a rheometer.

Two hypotheses are considered for the clogging process: i) polymer accumulation inside columns or ii) obstruction of pores in the screens at the inlet and outlet of columns.

To understand the clogging process, a polymer solution at 250 mg/L was injected into different sand columns. The flow rate (and so the shear rate) was progressively increased. The two vertical tubes connected to the column allowed to measure the hydraulic heads in the sand (Δh_2) and the two other tubes put outside the column allowed the measurements of the external heads (Δh_4). Therefore, by measuring the height of fluid in each tube for different shear rates, the hydraulic head was determined by difference between the four tubes (Figure 3.5).

Figures 3.10 to 3.13 show the hydraulic head differences observed inside and outside of the different columns.
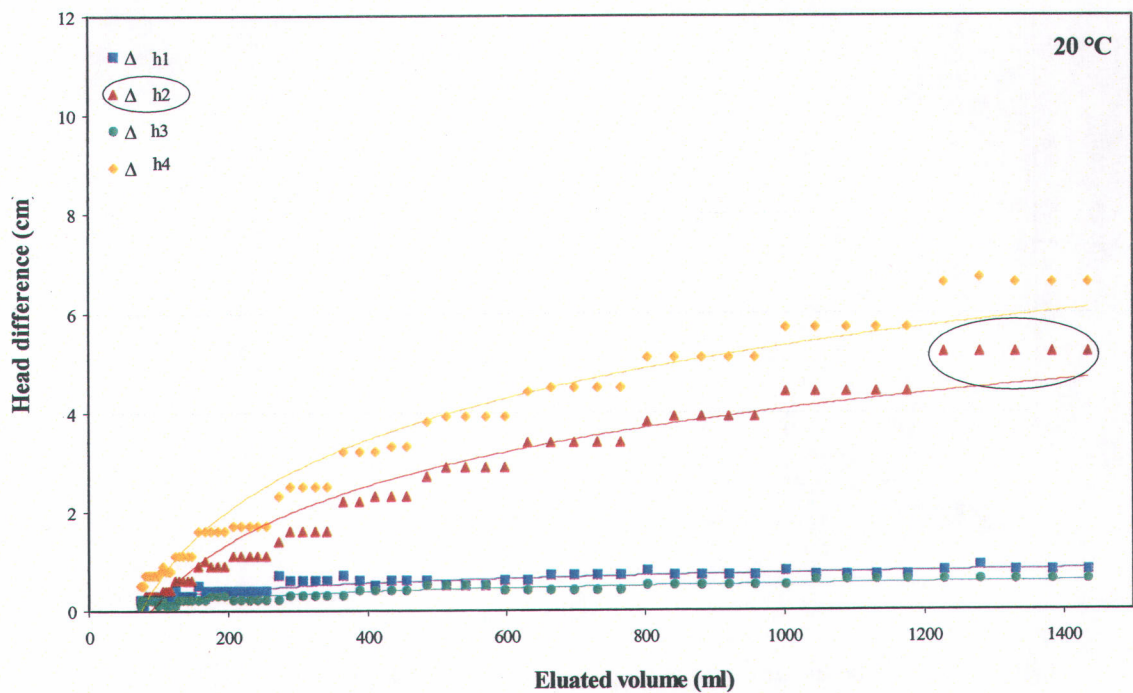
Figure 3.10: Head difference in column 2 (fine sand test)
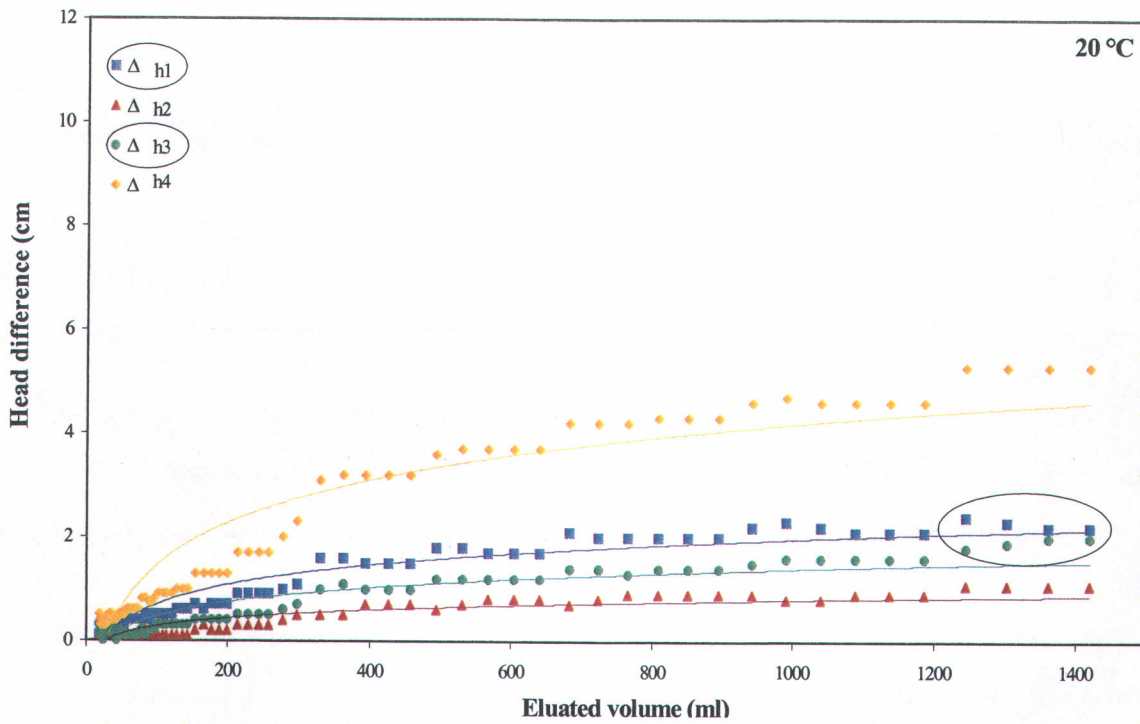
Figure 3.11: Head difference in column 3 (medium sand test)
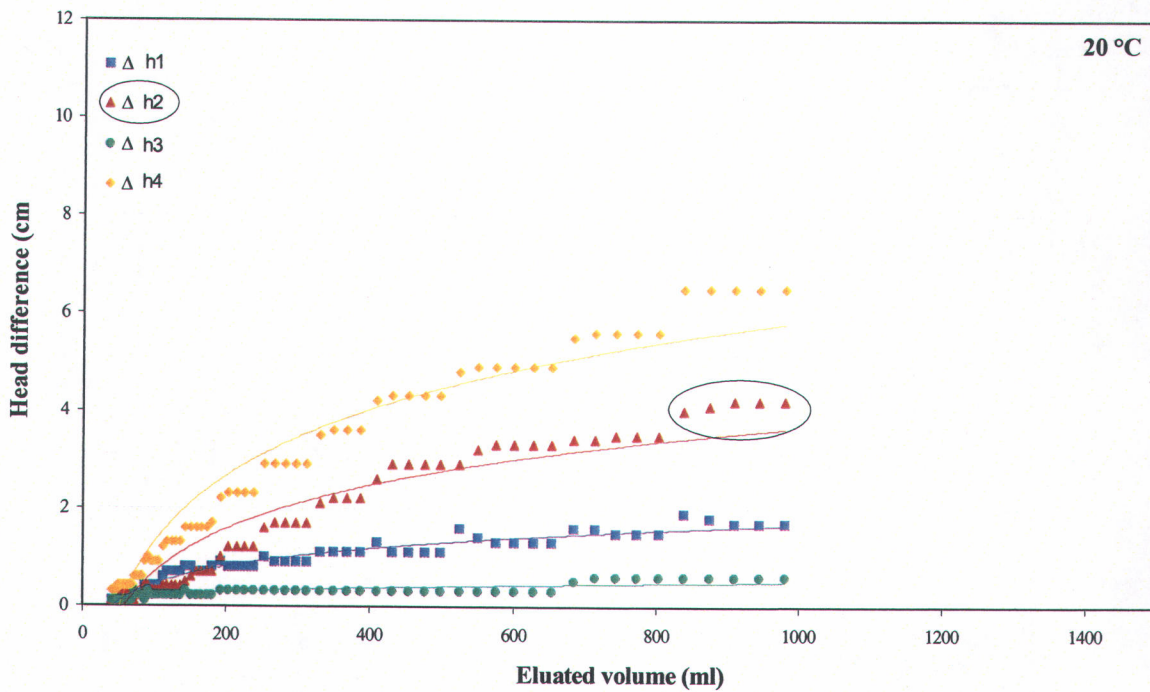
Figure 3.12: Head difference in column 4 (fine sand – sheared polymer test)
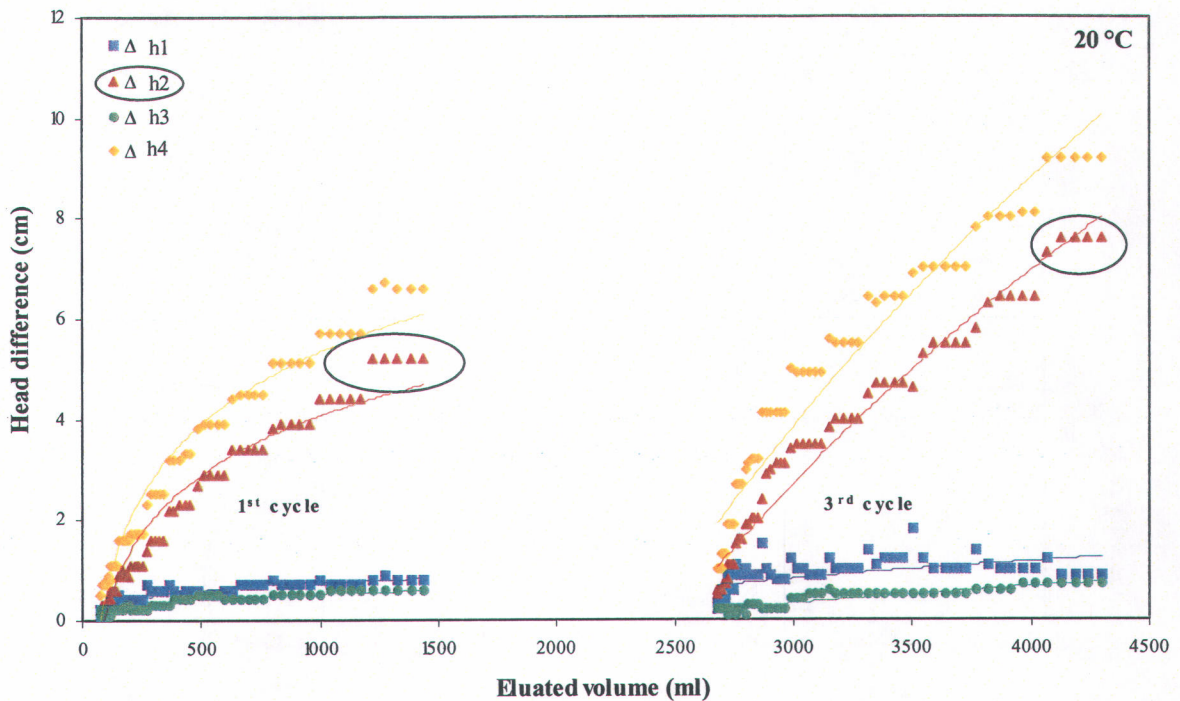
Figure 3.13: Head difference in column 5 (fine sand – cycled polymer test)

The hydraulic head difference in each test increases with the volume. For the fine sand column tests (Figures 3.10, 3.12 and 3.13), the contribution of Δh_2 on the global clogging of the column (Δh_4) is more important than the contribution of Δh_1 and Δh_3. This observation confirms that the clogging is essentially caused by an accumulation of polymer inside the column in the pores of the porous medium and not by an obstruction of the screen pores at the inlet and outlet of columns. At the opposite, for column 3 with medium sand (Figure 3.11), the contribution of Δh_1 and Δh_3 is more important than the contribution of Δh_2. This shows well that the screen is clogged. A bad preparation of the xanthan solution or a bad homogenization during the solution preparation could be the main reasons. In order to verify these last hypotheses, a second test in sand column with medium sand was carried out and showed the same results.

To better illustrate the clogging phenomenon, we traced down the viscosity ratio curve (ratio of measured to calculated viscosity) as a function of time (Figure 3.14). We noticed in all cases that the viscosity ratio is relatively stable during the shear thinning behavior

of xanthan gum part of the curve (flat curve). When the viscosity ratio is superior to 1, the clogging occurs. The clogging is observed in all column tests.
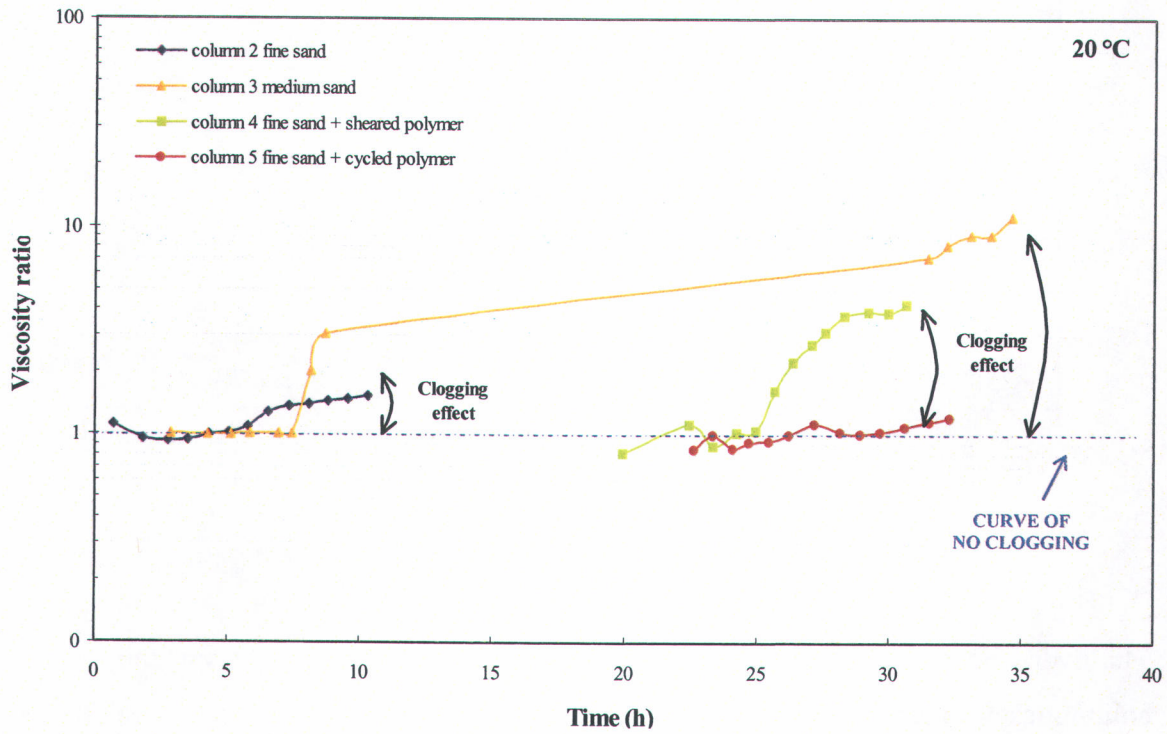
Figure 3.14: Viscosity ratio as a function of time

3.2.6.4. Evolution of the hydraulic conductivity

Clogging can also be illustrated by the evolution of the hydraulic conductivity to xanthan solution (Figures 3.15 to 3.18).
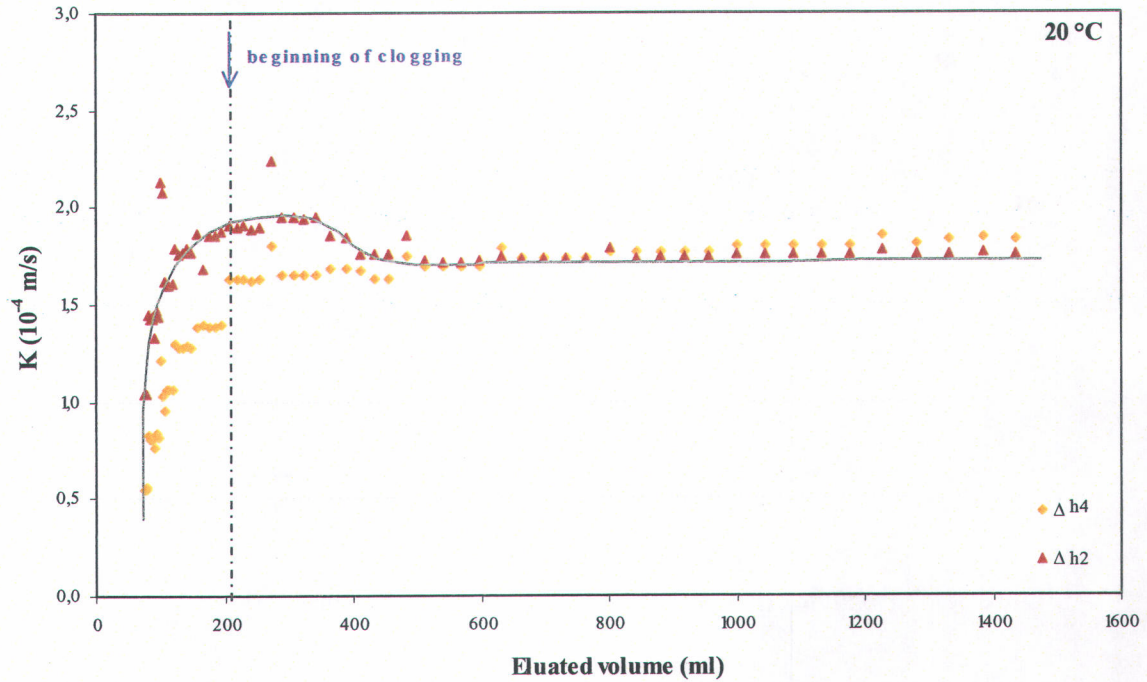
Figure 3.15: Behavior of K for column 2 (fine sand test)
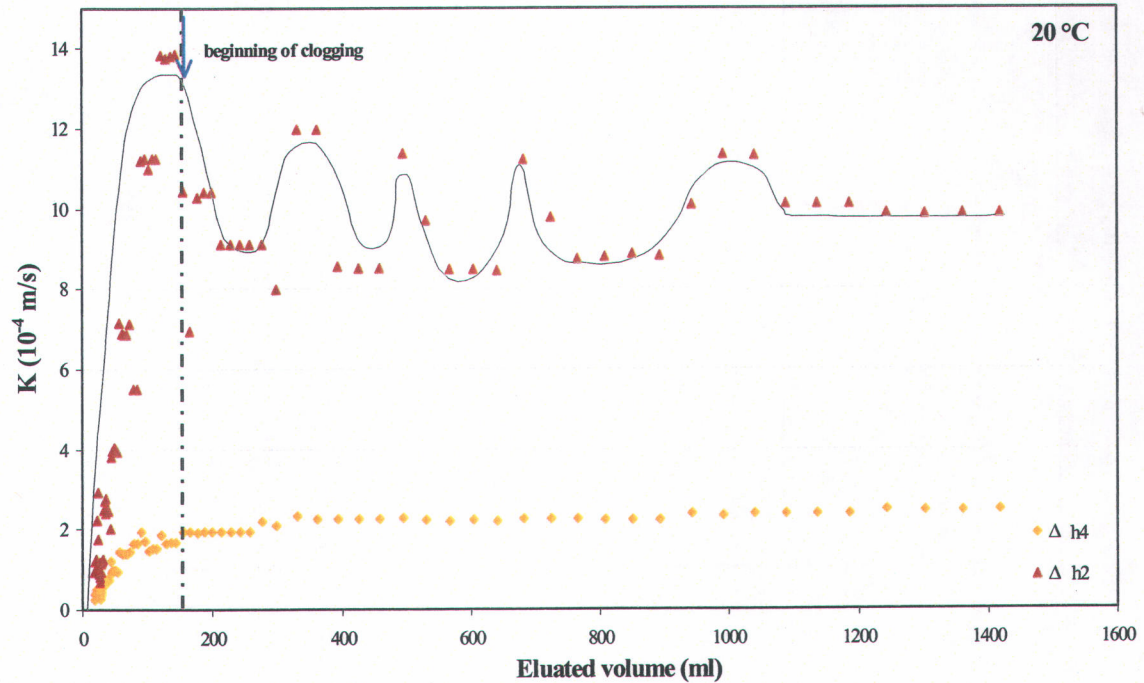
Figure 3.16: Behavior of K for column 3 (medium sand test)
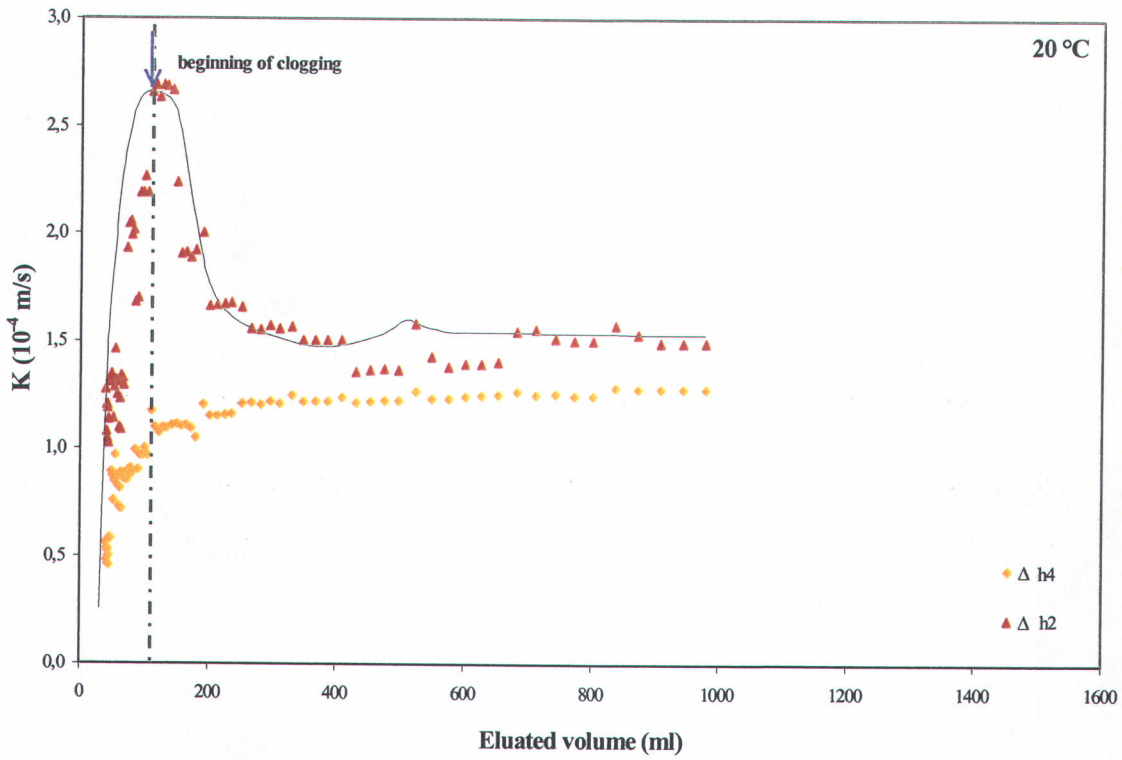
Figure 3.17: Behavior of K for column 4 (fine sand – sheared polymer test)
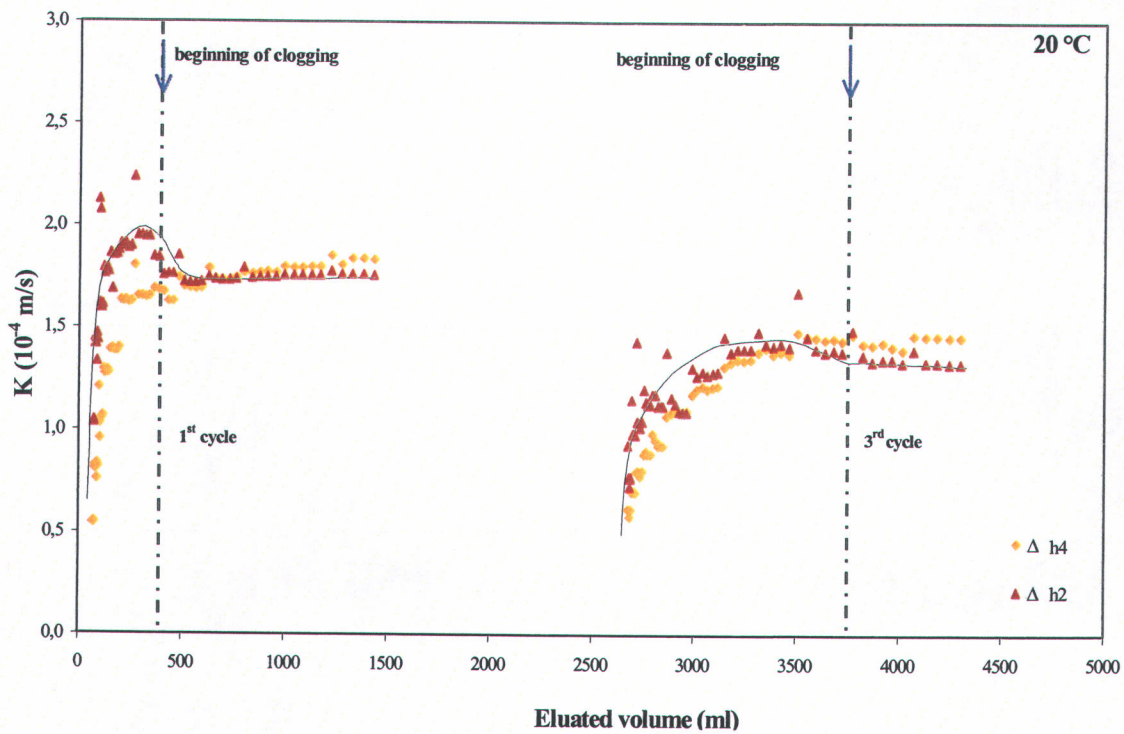
Figure 3.18: Behavior of K for column 5 (fine sand – cycled polymer test)

Each figure shows a progressive increase in hydraulic conductivity with time as calculated as follows:

$$K = k \frac{\rho\, g}{\mu}$$

<div align="right">Eq. 3.5</div>

where K (m/s) is the hydraulic conductivity to the tested fluid, k (m^2) the intrinsic permeability of the porous medium, ρ (kg/m^3) the fluid density, g (9.81 m/s^2) the gravitational acceleration and μ (Pa.s) the viscosity of the tested fluid.

Hydraulic conductivity is inversely proportional to the viscosity of the injected solution (Equation 3.5). A viscosity reduction (by the shear thinning behavior of xanthan gum) leads to an increase in hydraulic conductivity. A hydraulic conductivity decrease is observed when the column begins to clog as showed by the vertical lines in Figures 3.15 to 3.18. When the hydraulic conductivity is constant, there is no more shear thinning effect. However, the difference between Δh_2 and Δh_4 is low in each test except for column 3 with medium sand.

When the hydraulic heads in the sand (Δh_2) are higher than the external heads (Δh_4), a hydraulic conductivity is more important inside the sand column compared to the global set up. So, a hydraulic conductivity loss occurs at the ends of the column. When Δh_2 is similar to Δh_4, a hydraulic head loss in the sand column can explain the loss of hydraulic conductivity.

3.2.6.5. Influence of shearing on the rheological properties of polymer

To understand the effect of shearing on the physical properties of xanthan gum, an intact polymer solution (column 2) and sheared polymer solution (column 4) were injected through two different sand columns (Figure 3.19).
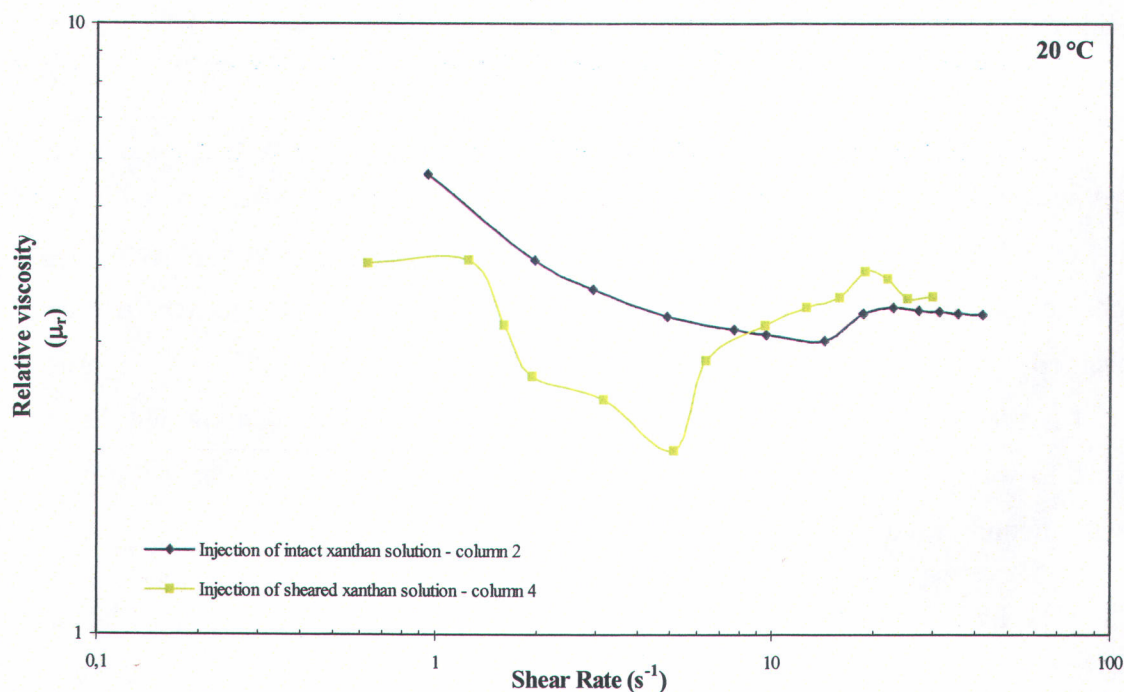
Figure 3.19: Influence of the shearing on the polymer properties

The sheared xanthan solution has a slightly lower viscosity than the intact one. That can be explained by a loss of the intrinsic polymer properties. Because the polymer solution flowed already through the sand in a sand tank, it is possible that the solution has not the initially injected xanthan concentration. It is also possible that the sand adsorbed some polymer in the sand tank (adsorption of xanthan gum on Cape May sand varies from 3 to 16 μg/g of dry sand for concentrations between 100 and 500 mg/L as shown in Martel *et al.*, 1998) or that the polymer is trapped mechanically in the pores of the sand tank. A dilution of xanthan solution by water present in pores of the sand tank prior to the test can be also the reason of a viscosity decrease. So, the initial concentration of xanthan gum in

column 4 test is modified from 237 mg/L to 182 mg/L according to the adsorbed xanthan gum mass. The loss of polymer properties can also be due to a modification of the chemical structure of xanthan gum, notably by chain break off. The shear thinning behavior is nevertheless present in each column.

3.2.6.6. Influence of Shear Rate

The hysteretic effect on relative viscosity of the polymer solution is showed by applying three successive cycles: i) increase of the shear rate (1st cycle), ii) reduction of the shear rate (2nd cycle) and finally; iii) again increase of the shear rate (3rd cycle). These cycles are obtained by increasing and decreasing the injection flow rate in the column (column 5) (Figure 3. 20).
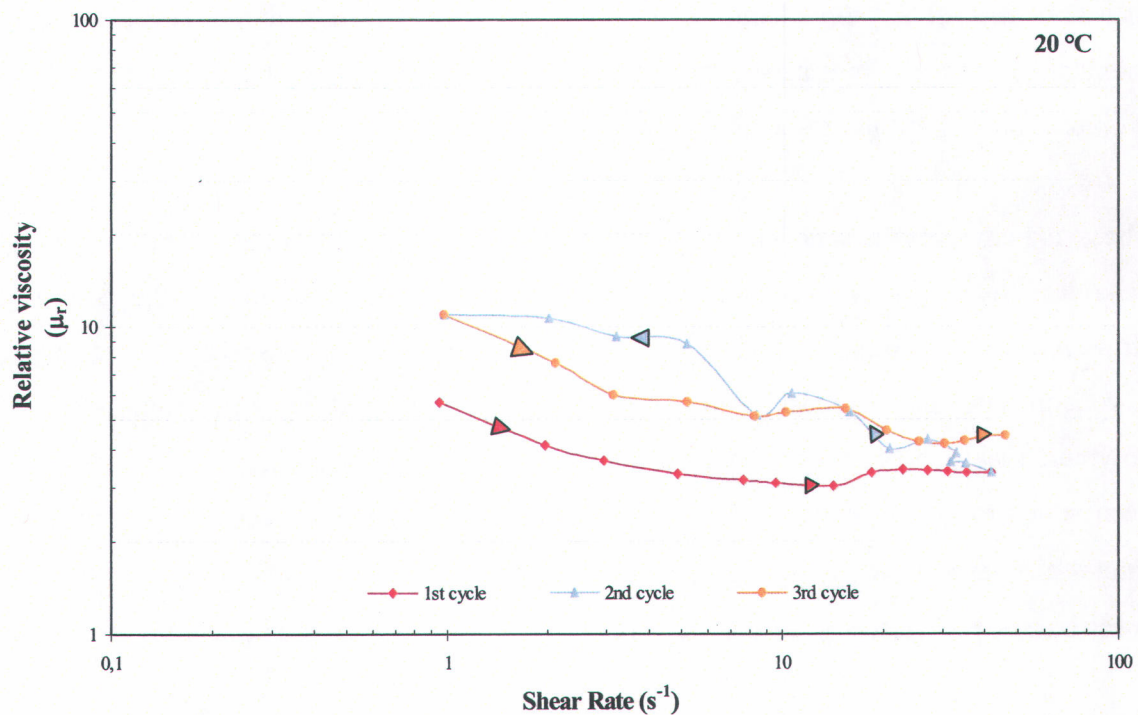
Figure 3.20: Hysteretic effect on relative viscosity for a xanthan solution sheared (fine sand column 5) (arrows indicate the increasing or decreasing shear rate on the solution)

The shear thinning behavior of xanthan gum is observed during the 1st cycle during the increase of the shear rate. By decreasing the shear rate (2nd cycle), clogging is noticed by an increase of relative viscosity. This is explained by an accumulation of polymers inside the column. When the shear rate is increased again (3rd cycle), the shear thinning behavior is again observed but with a higher viscosity than in the first cycle. We can consequently describe this phenomenon as "memory" or hysteresis. The xanthan gum keeps its properties after having undergone two cycles.

3.2.7. Conclusions

This study principally consisted in understanding the intrinsic behavior of xanthan gum during its injection in porous media. Laboratory tests with sand columns of variable grain sizes allowed to study the physical characterization of xanthan gum aqueous solutions by measurements of *in situ* viscosity as a function of shear rate and to evaluate their interactions with the porous medium. These tests allowed also to better understand the problems related to the flow with a view to an use on a large scale.

These experiments in sand columns confirmed that the polymer has a shear thinning behavior: the viscosity decreases with an increase in shear rate for all the columns. However, after a certain volume, a partial pores clogging effect starts to occur, leading to a general viscosity increase. Clogging is principally caused by an accumulation of polymers inside the column. Clogging is not due to bacterial growth as a bactericide has been added to all xanthan solutions to avoid its degradation. The presence of microgels cannot also explain the clogging because of their small dimension (6 µm) compared to pore size and the mesh size of the metallic screen at the inlet and the outlet of columns.

The comparison between a previously sheared polymer and an intact polymer showed a loss of the rheological properties of the sheared polymer. The viscosity of the sheared polymer is slightly lower than the intact solution. This can probably be explained by a decrease of polymer concentration by adsorption of xanthan on the porous medium of the sand tank where the solution was previously injected, a mechanical trapping, a dilution of

the solution with water present in the sand tank or a modification of the chemical structure of xanthan gum by chain break off.

A hysteretic behavior of the polymer ("memory effect") in the sand column was observed when xanthan gum solution was injected continuously with three cycles of increasing-decreasing-increasing flow rate (shear rate). The polymer keeps its rheological properties during the third cycle. The second cycle is marked again by the clogging phenomenon.

The results obtained with the sand column tests were conclusive but also showed the limits of their use. Two important problems were observed during the different tests: the clogging effect and the loss of rheological properties of xanthan gum.

To avoid the clogging phenomenon in the porous medium, it would be preferable to inject the polymer solution at lower flow rates (and so at lower shear rates). The clogging occurs at shear rates higher than 6 s^{-1} for the fine sand and higher than 3.5 s^{-1} for the medium sand. Therefore, according to the configuration of the porous medium and the grains size, the flow rate has to be adapted. Moreover, the volume of polymer solution injected through the sand column also has to be controlled in order to prevent the accumulation of polymers in the sand, leading to pores clogging.

The loss of rheological properties of xanthan gum during its flow through the sand tank was estimated between 5 and 27 % according to the adsorbed xanthan gum mass on the sand grains. The polymer degradation could be minimized by decreasing the injection flow rate. Nevertheless, in saturated porous media (as often seen on the field), the effect of dilution can lead to properties loss of polymer.

The polymer degradation due to a modification of the chemical structure by an eventual chain break off can be verified by the use of the mass spectroscopy. It seems to be an excellent analytical tool to quantify the polymer and to precisely elucidate the chemical structure of the xanthan molecule.

In the future, xanthan gum could be added to washing solutions for the remediation of contaminated aquifers. However, sand tank tests could be carried out to evaluate and understand the sweep efficiency and the displacement front stability of the xanthan solution. Indeed, the beneficial effect of xanthan gum on the sweep cannot be represented in sand column tests because they only take into account the horizontal flow (one-dimensional model) compared to sand tank tests (three-dimensional model). Before performing tests on a large scale in sand tank, it would be preferable to carry out other column tests at 8 °C (groundwater temperature) to observe the temperature effect on the polymer solution in a sandy porous medium.

For the future field works, the clogging effect and the polymer properties degradation could be avoid by playing on the distance between the injection and the pumping wells, on the diameter of wells or on the stay time of the polymer solution in the porous medium. A wider diameter for the injection and the pumping wells and a shorter distance between them could allow the decrease of the flow rate and the shear rate. Moreover, a low stay time in the porous medium could barely influence the polymer properties. All these criteria are necessary for a good realization of field tests by avoiding the problems related to clogging and polymer properties degradation.

3.2.8. References

Chauveteau G. and N. Kohler 1980. Influence of microgels in xanthan polysaccharide solutions on their flow through various porous media, 55th Annual Fall Technical Conference and Exhibition of the SPE of AIME (Dallas, TX, USA), SPE 9295, 1-13.

Chauveteau G. and A. Zaitoun 1981. Basic rheological behavior of xanthan polysaccharide solutions in porous media: effects of pore size and polymer concentration, European Symposium on Enhanced Oil Recovery (Bournemouth, England), 197-214.

Chen C.S.H. and E.W. Sheppard 1979. Conformation and hydrolytic stability of polysaccharide from *Xanthomonas campestris*, Journal of Macromolecular Science and Chemistry, **2**, (13), 239-259.

Garcia-Ochoa F., V.E. Santos, J.A. Casas and E. Gomez 2000. Xanthan gum: production, recovery and properties, Biotechnology Advances, **18**, 549-579.

Gogarty W.B. 1967. Mobility control with polymer solutions, Society of Petroleum Engineers Journal, **7**, (2), 161-173.

Hébert A. 1998. Etude du comportement des fluides lors d'un essai de décontamination in situ à l'aide d'une solution tensioactive à l'Assomption, Québec, Mémoire pour l'obtention du grade de maître ès sciences, Août, Département de géologie et génie géologique, Université de Laval, (Québec, Canada).

Hornof V. and N.R. Morrow 1987. Gravity effects in the displacement of oil by surfactant solutions, Reservoir Engineering Society of Petroleum Engineers, **2**, (4), 627-633.

Jeanes A.R., J.E. Pittsley and F.R. Senti 1961. Polysaccharide B-1459: A new hydrocolloid polyelectrolyte produced from glucose by bacterial fermentation, Journal of Applied Polymer Science, **5**, 519-26.

Lake L.W. 1989, Enhanced oil recovery, Prentice-Hall Inc, (New Jersey, USA), 550 pp.

Mackay D.M. and J.A. Cherry 1989. Groundwater contamination: pump-and-treat remediation, Environment Science Technology, **23**, (6), 630-636.

Martel K.E., R. Martel, R. Lefebvre and P.J. Gélinas 1998. Laboratory study of polymer solutions used for mobility control during *in situ NAPL* recovery, Groundwater Monitoring and Remediation, **18**, (3), 103-113.

Martel R. and P.J. Gélinas 1996. Surfactant solutions developed for *NAPL* recovery in contaminated aquifers, Groundwater, **34**, 143-154.

Martel R., P.J. Gélinas et L. Saumure 1998c. Aquifer washing by micellar solutions: 3 - Field test at the Thouin Sand Pit (Québec, Canada), Journal of Contaminant Hydrology, **30**, 33-48.

Martel R., A. Hébert, R. Lefebvre, P.J. Gélinas and U. Gabriel 2004. Displacement and sweep efficiencies in a *DNAPL* recovery test using micellar and polymer solutions injected in a five-spot pattern, Journal of Contaminant Hydrology, **75**, 1-29.

Pankow J.F. and J.A. Cherry 1996. Dense chlorinated solvents and other *DNAPL* in groundwater, Waterloo Press, (Portland, USA), 522 pp.

Robert T., R. Martel, S.H. Conrad, R. Lefebvre and U. Gabriel 2006. Visualization of TCE recovery mechanisms using surfactant polymer solutions in a two-dimensional heterogeneous sand model, Journal of Contaminant Hydrogeology, **86**, 3-31.

Roubroeks J.P., R. Andersson, D.I. Mastromauro, B.E. Christensen and P. Aman 2001. Molecular weight, structure and shape of oat (1→3), (1→4)-β-d-glucan fractions obtained by enzymatic degradation with (1→4)-β-d-glucan 4-glucanohydrolase from Trichoderma reesei, Carbohydrate Polymers, **46**, (3), 275-285.

Sandiford B.B. 1977. Flow of polymers through porous media in relation to oil displacement: Improved oil recovery by surfactant and polymer flooding. Shah, D.O. and Schechter R.S. (eds.). Academic Press inc., New-York, USA, 487-509.

Szabo M.T. 1975b. Laboratory investigation of factors influencing polymer flood performance, Society of Petroleum Engineers Journal, **15**, (4), 338-346.

CHAPITRE 4

Réhabilitation in situ de sites contaminés

4.1. Introduction

$\mathscr{L}$e quatrième chapitre de ce mémoire constitue le second article. Il traite de l'efficacité de balayage et de la stabilité du front de déplacement de la gomme de xanthane lors de son injection à travers un bac de sable rectangulaire. Il s'agit d'une représentation à plus grande échelle des essais en colonne de sable définis au chapitre 3.

Deux essais en bac de sable sont effectués: i) injection du polymère à travers un milieu poreux formé d'une seule couche de sable fin (une couche) (essai réalisé en collaboration avec Uta Gabriel) et; ii) injection du polymère à travers un milieu poreux composé d'une couche de sable grossier entre deux couches de sable fin (trois couches). Différentes concentrations pour la gomme de xanthane sont injectées à travers la formation géologique pour évaluer les contrastes de viscosité des différentes solutions en présence et leur effet sur le balayage. Plusieurs traceurs sont également utilisés pour assurer correctement le suivi du front de déplacement à travers le milieu poreux. La stratégie d'injection/pompage utilisée lors de ces essais est développée sur la base d'une simulation numérique à l'aide du logiciel UTCHEM.

Ces travaux se déroulent dans les laboratoires de l'INRS/RDDC-Valcartier situés sur le complexe expérimental de Recherche et Développement pour la Défense Canada – Valcartier à 30 km au nord de Québec.

4.2. Behavior of xanthan gum solutions injected in a sand tank with a doublet line drive pattern

by Michael Haberman, Richard Martel,
Uta Gabriel, René Lefebvre, Luc Trépanier

4.2.1. Abstract

To evaluate and understand the sweep efficiency and the displacement front stability of xanthan gum solutions during their injection into porous media, two sand tank tests with two different sands were carried out: a first test in a porous medium made up of fine sand (one-layer sand tank test) and a second test within a porous medium made up of a medium sand layer between two fine sand layers (three-layer sand tank test). The sand tank tests with a doublet line drive pattern confirmed the role played by xanthan gum in improving porous media sweep compared to a water injection: the geological formation is better swept with a xanthan solution due to a stable and vertical displacement front. Moreover, in the one-layer sand tank test, no clogging phenomenon is observed. For the three-layer sand tank test with four monitoring wells and nine sampling points, the sweep is monitored in each of the three layers. The fluid circulation is faster in the middle layer, due to a higher permeability. With water injection, some zones, principally in the fine layers, are poorly swept, notably for a well near the pumping well. That can be explained by the fine sand texture where the flow rate is lower than in the coarse sand layer. A wall effect can also be the reason. With xanthan injection, all sampling wells are swept. Finally, the displacement front was observed by the use of chlorides and bromides as tracers. The other tracer, amaranth, is delayed compared to chlorides and bromides, caused by its organic chemical structure, which tends to form hydrogen links between the oxygen atoms of the amaranth and the water molecules of porous medium, leading to a decrease of amaranth concentration during its injection. However, the color of amaranth allows a simple visual follow up of the test.

4.2.2. Résumé

Pour évaluer et comprendre l'efficacité de balayage et la stabilité du front de déplacement de solutions de gomme de xanthane lors de leurs injections en milieux poreux, deux essais en bac de sable de granulométrie différente ont été réalisés: un premier essai avec un bac de sable rempli de sable fin (bac de sable à une couche) et un second essai avec un bac de sable composé d'une couche de sable grossier entre deux couches de sable fin (bac de sable à trois couches). Les essais en bac de sable à l'aide d'un patron d'injection/pompage en ligne ont confirmé le rôle joué par la gomme de xanthane sur le balayage d'un milieu poreux en comparaison avec une simple injection d'eau: le balayage de la formation géologique par injection d'une solution de xanthane est beaucoup plus complet, dû à un front de déplacement plus stable et plus droit. De plus, dans le test en bac de sable utilisant une seule couche, aucun phénomène de colmatage n'est observé. Pour le test en bac de sable utilisant trois couches (avec quatre puits d'observation et neuf points d'échantillonnage), le balayage se fait dans chacune des trois couches. La circulation des fluides est plus rapide dans la couche centrale, dû à sa texture grossière et

sa perméabilité plus élevée. Avec l'injection d'eau, certaines zones, principalement dans les couches fines, sont peu balayées, notamment pour un puits d'observation à proximité du puits de pompage. Ceci peut s'expliquer par la granulométrie du sable fin dont le débit passant est beaucoup moins important par rapport à la couche de sable grossier. Un effet de paroi peut également en être la cause. Avec l'injection de xanthan, tous les puits d'échantillonnage sont balayés. Enfin, le suivi de l'avancée du front de déplacement a été observé en utilisant les chlorures et les bromures comme traceurs. Un retard de l'autre traceur, l'amarante, en comparaison avec les chlorures et les bromures, est constaté, étant donné sa structure chimique organique qui lui donne une tendance à former des ponts hydrogènes avec les molécules d'eau présentes dans le milieu poreux, amenant à un abaissement de la concentration d'amarante lors de son injection. Par contre, la coloration de l'amarante permet un suivi visuel simple de l'essai.

4.2.3. Introduction

Nowadays, groundwater contamination by Non Aqueous Phase Liquids (*NAPL*) is one of the major challenges in hydrogeology. Due to their low solubility in water, their high toxicity and their low biodegradation, these compounds can be found in aquifers forming a distinct phase making the *NAPL* a free flowing or immobile at residual saturation. So, these compounds can be the source of groundwater contamination for many decades. Among the *NAPL*, the substances denser than water (Dense Non Aqueous Phase Liquids, *DNAPL*) pose many problems for their recovery because they tend to migrate to the base of the aquifers by gravity until reaching an impermeable layer. Moreover, during its advance to the bottom of the aquifer, *DNAPL* can be trapped at the grains surface or inside the pores. At the top of impervious layers, *DNAPL* thus accumulates slowly to form contaminated pools. *LNAPL* (Light Non Aqueous Phase Liquids) are lighter than water and tend to float at the surface of the water table and, therefore, their recovery is easier.

The remediation of contaminated aquifers by *NAPL* can be achieved by different processes such as thermal, biological or physico-chemical treatments (Laliberté *et al.*, 2002). Unfortunately, the extent, the depth of the contamination and the low temperature of groundwater limit the use of many techniques. Among the proposed solutions to improve the recovery of contaminants, the "waterflooding" can be considered. The process consists in injecting water through the porous medium and recovering the water

containing the contaminants that are dislodged by increasing the viscous forces. Nevertheless, the low solubility of heavy organic compounds in water and their low mobility can cause some difficulties of remediation by this method. *In situ* treatments by soil washing constitutes a good alternative to remediate *NAPL*-contaminated sites (Martel *et al.*, 2004; Martel *et al.*, 1998; Sandiford, 1977; Szabo, 1975b; Gogarty, 1967). Previous studies demonstrated that the use of polymers in the washing solution or dissolved in water and injected alone in pre or post treatment allows a better distribution of contaminants, a better sweep of the geological formation with more contact between the cleaning solution and the porous medium and in this manner, ensure a better recovery of contaminants, minimizing the problems related to displacement front instabilities and preferential viscous fingerings (Robert *et al.*, 2006; Hornof and Morrow, 1987) (Figure 4.1).
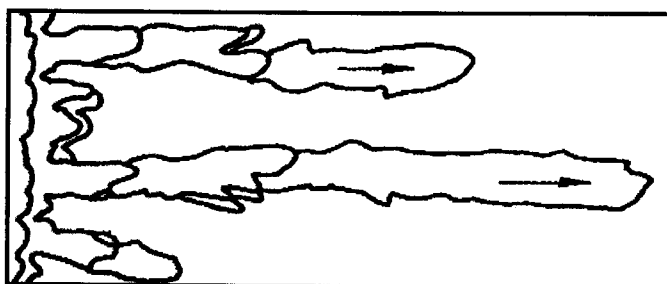
Figure 4.1: Representation of "viscous fingering" (Pankow and Cherry, 1996)

The objective of this study is to evaluate the sweep efficiency and the displacement front stability of a shear thinning polymer such as xanthan gum compared to water during their injection into a porous medium. Laboratory tests with sand tank of 9 m^3 allowed to understand the behavior of the polymer through a geological formation of variable grains size. Two different sand tank tests are carried out: a first test in a porous medium made up of fine sand (one-layer sand tank test) and a second test in a porous medium made up of a medium sand layer between two fine sand layers (three-layer sand tank test). Three different tracers (chlorides, bromides and amaranth) are used and added to the injected solutions (water and xanthan gum) to observe the breakthrough of tracers in the sand tank and so to evaluate the sweep efficiency of each solution. The sand tank is equipped with a doublet line drive pattern. The injection/pumping strategy for theses tests is estimated by numerical simulation with the software UTCHEM.

In most cases, the development of *in situ* treatments requires tests at many scales. The field tests often lead to many difficulties such as the cost and the control of experimental conditions. The main reasons of the failure of remediation projects is that the promising technologies were not enough tested at the laboratory scale. The principal problem related to the development of these processes is to scale up from laboratory to field applications.

The interest of these research works is in the use of sand tank. Indeed, this infrastructure constitutes an excellent way to represent a "quasi-real" field situation in three dimensions by ensuring a great flexibility in the modus operandi. It allows to reduce the operation costs by automation of experimental conditions, to realize or reproduce a large number of experiments and to guarantee the environmental protection insured by the confinement of the experiment in a tank. The sand tank can be used to test various injection/pumping strategies for different porous media with many types of contaminants at the desired temperature. Such an infrastructure allows to reduce considerably the time for the development of technologies in progress and constitutes a great scientific and economic advantage.

The choice of porous medium composed of three layers of different grain sizes (three-layer sand tank test) represents an additional difficulty for the sweep due to the heterogeneity of the porous medium. This test allows to reproduce conditions often met in the field with an arrangement difficult to sweep effectively. The injection/pumping strategy with one injection well and one pumping well aligned at each end in the middle of the tank is also selected to limit the possibilities to obtain a complete sweep of the tank and to lead a complex fluid flow through the porous medium. Such a sweep is still more difficult when the injection and the pumping wells do not reach the base of the sand tank.

All these constraints are originally fixed in order to evaluate the efficiency of a polymer solution on the sweep compared to a water injection through a complex porous medium difficult to sweep, near a field situation.

4.2.4. Literature review

The success of the application of *in situ* treatment methods using fluids injection for the remediation of contaminated aquifers by *NAPL* depends mainly on the sweep efficiency of the contaminated aquifer:

$$Sweep\ efficiency = \frac{Volume\ of\ reservoir\ contacted\ by\ the\ displacement\ fluid}{Total\ volume\ of\ reservoir} \qquad \text{Eq. 4.1}$$

This sweep efficiency can be largely improved by the use of polymers dissolved in water and injected in pre or post treatment (Martel *et al.*, 1996; Sandiford, 1977; Gogarty, 1967).

This is explained by the formation of stable fronts between the different fluids in presence, due to an increase of fluid viscosity (water/polymer) and a reduction of the mobility ratio *M* (Lake, 1989):

$$M = \frac{\lambda_{water+polymer}}{\lambda_{NAPL}} = \frac{k_{water+polymer}}{\mu_{water+polymer}} \times \frac{\mu_{NAPL}}{k_{NAPL}} \qquad \text{Eq. 4.2}$$

where k (m^2) is the relative permeability of the porous medium to fluids, μ (Pa.s) is the viscosity of fluids and λ is the mobility (k/μ).

The particularity of polymer solutions (such as xanthan gum) is their shear thinning behavior, i.e. they can increase the relative viscosity of the aqueous solution at low shear rates and so slow down the circulation of fluids in a coarse porous medium. At the opposite, for important shear rates, the relative viscosity is reduced to facilitate the circulation of polymer through a fine porous medium. The xanthan gum is often used for environmental applications because of its non toxicity and its easy biodegradability (Garcia-Ochoa *et al.*, 2000).

The use of polymers in the washing solutions or injected alone in pre or post treatment for the *in situ* remediation of contaminated aquifers by *NAPL* was already studied by many authors (Robert *et al.*, 2006; Martel *et al.*, 1998; Martel, 1995; Sandiford, 1977; Gogarty, 1967). Different tests in laboratory and in the field allowed to confirm the benefit effect of polymer solutions on the sweep of porous media.

Tests in laboratory with a small sand box of 1 850 cm^3 (= 18.7 cm x 5.2 cm x 19 cm) were carried out to understand and evaluate the efficiency of polymers solutions such as xanthan gum in water on the sweep in a two-dimensional model (Martel, 1995). Different solutions were injected into the sandy porous medium composed of three layers of various grain sizes to observe the heterogeneity effect. This research work was performed in order to improve the technology of surfactant and polymer flooding for the *in situ* remediation of *DNAPL* contaminated sites such as Thouin and Mercier sites (Québec/Canada). The results of this study showed that the displacement front of a xanthan solution injected following a water injection in a three-layer sand box (a middle layer of medium sand and two layers of fine sand) was "deformed" but stable. Xanthan gum solution circulated more in the permeable middle layer than in the fine sand layers. The proportion of liquid circulated in the middle layer was reduced by the use of polymer compared to a water injection. In this experiment, 100 % of the sand box was swept vertically by the xanthan gum solution after the injection of 1.5 pore volumes but the breakthrough in the middle layer was observed after the injection of 0.8 pore volume.

The recovery mechanisms of trichloroethene (TCE) in sand during the injection of washing solutions containing surfactants and xanthan gum were showed in a two-dimensional physical model by Robert *et al.* (2006). The experimental set up of 3 630 cm^3 consisted of a two-dimensional chamber of 1 cm thick, 60.5 cm wide and 60 cm tall. This research focused on the recovery of TCE by dissolution. The chamber was filled with four types of sand and glass walls allowed to observe the displacement of different injected fluids, the infiltration of TCE in the porous medium, its mobilization, its dissolution and the interactions between the washing solution, the polymer and the TCE in a saturated heterogeneous porous medium. Photographs and digital image analysis

were used to illustrate these phenomena. In this test, xanthan gum was included in the washing solutions. The solutions were injected with a concentration gradient in surfactant but with a constant concentration of xanthan gum. The polymer played an important role on the sweep in preventing the invasion of non contaminated zones by mobile TCE during the flooding. 100 % of the chamber was swept by the washing solution. The chamber was also more evenly swept vertically with a xanthan solution compared to water injection with a slug of 0.3 pore volume deformed, instable and with fingering.

Many field tests were also carried out to evaluate the efficiency of washing solutions prior and after polymers injection for the remediation of contaminated aquifers by *NAPL*. The book *Technology Practices Manuel for Surfactants and Cosolvents* (AATDF, 1997) listed twenty-six field tests in Canada and in United States with different geological media and contaminants such as the Laramie tests (in Wyoming/USA), Fredricksburg (in Virginia/USA) and the Assomption (in Québec/Canada). Among them, the particularity of this last test is the use of polymers solutions injected in pre and post treatment of the surfactant solution. This field test was realized more exactly in the aquifer of the Thouin Sand Pit near Montreal. The objective of this study was to evaluate the *DNAPL* recovery mechanisms, the efficiency of the washing solution developed and the sweep efficiency of a 5-spot pattern during this pilot test (Martel *et al.*, 1998; Hébert, 1998). The injection/pumping system was composed of a central injection well and four pumping wells arranged along a square pattern. The 0.9 pore volume of surfactant solution recovered 86 % of the initial *DNAPL* saturation. The areal sweep was evaluated by the observation of the arrival time of washing solution in a monitoring system and the numerical modeling of the injection/pumping system was evaluated near to 100 %. The vertical sweep was estimated at 95 % based on the washing solution arrival at observation and pumping wells. The non swept zones was located at depth in the sand where the clay base was deeper than the base of the injection well. The volumetric sweep efficiency of the 5-spot pattern test was around 95 %.

4.2.5. Methodology

Two sand tank tests were carried out to evaluate and understand the sweep efficiency and the displacement front stability of a 100 mg/L, 250 mg/L and 500 mg/L xanthan gum solutions during their injection into a porous medium: i) a first test in a porous medium made up of fine sand (one-layer sand tank test) and; ii) a second test within a porous medium made up of a medium sand layer between two fine sand layers (three-layer sand tank test). The temperature of the laboratory was controlled at 8 °C ($\pm$ 0.5 °C) during all the duration of the tests to represent a "quasi-real" field situation (where the groundwater temperature is approximately at 8 °C).

The porous medium composed of a single layer was chosen as reference to observe only the flow of fluids in the sand. The sand tank test with three sand layers of two different grain sizes was realized to evaluate the sweep efficiency of polymers solutions in a porous medium difficult to sweep due to the heterogeneity, similar to field conditions.

This section presents the characteristics of sands, polymer and the equipment used.

4.2.5.1. Porous media selection

For the sand tank tests, a fine and a medium sands were used (Filpro Well Gravels sands U.S. Silica, New Jersey). These sands are uniform, mainly composed of quartz (99.4 %) and their grains are rounded to sub-angular (Table 4.1).

Table 4.1: Characteristics of sands used for sand tank tests

Sand	ρ (kg/m^3)	K (m/s)	k (m^2)	d_{50} (mm)	d_{pore} (μm)
FINE		7×10^{-4}	7.2×10^{-11}	0.45	76
MEDIUM	2 650	21×10^{-4}	21.5×10^{-11}	0.87	131

The density (ρ) is the quartz density from Handbook (Lide, 2000). The hydraulic conductivity (K) is measured during sand column tests with water injection (Chapter 3).

The permeability (k) is derived from the general equation related to hydraulic conductivity:

$$K = k \frac{\rho g}{\mu}$$

Eq. 4.3

where g (9.81 m/s^2) is the gravitational acceleration and ρ and μ are respectively the density and the dynamic viscosity of water at 20 °C (Table 4.2).

Table 4.2: Physical properties of water at atmospheric pressure

T (°C)	ρ (kg/m^3)	μ (10^{-3} kg/m.s)
20	998.29	1.003

The equivalent pore size diameter (d_{pore}) was calculated from Chauveteau and Zaitoun equation (1981):

$$d_{pores} = 2 \sqrt{8 \frac{k}{n}}$$

Eq. 4.4

where n is the porosity. The average porosity measured for the used sands with column tests is 40 % (Chapter 3).

The mean grain size (d_{50}) is from the grain size curve that was made according to ASTM D422-63 method (Figure 4.2; Appendix C).
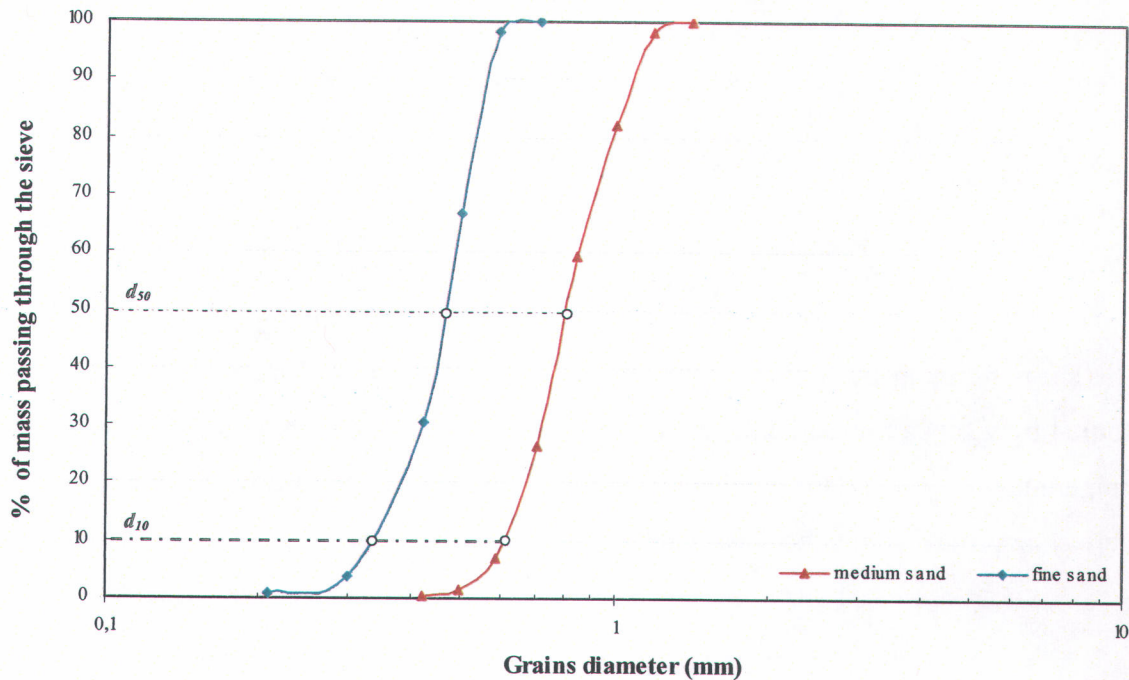
Figure 4.2: Grain size of the selected sands

4.2.5.2. Polymer selection

The selection criteria for xanthan gum were related to its rheological behavior (more particularly its shear thinning behavior), its high aqueous solubility, its low toxicity and its low cost. This polymer was also chosen for his many previous applications in laboratory tests (Martel *et al.*, 1998; Martel, 1995), in two-dimensional sand box tests (Robert *et al.*, 2006) and in field tests (Martel *et al.*, 2004; Hébert, 1998).

Xanthan gum is a polysaccharide biopolymer. It comes from the extra cellular fermentation of glucose by the bacterium *Xanthomonas campestris* and it was isolated and characterized for the first time by Jeans *et al.* (1961). Its molecular structure presented in Figure 4.3 is made of glucose cycles linked by oxygen atoms.
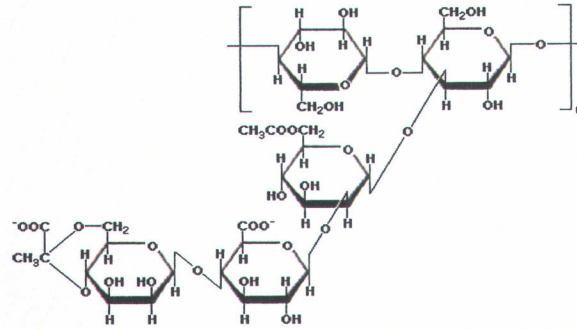
Figure 4.3: Molecular structure of xanthan gum
(Roubroeks *et al.*, 2001)

The shear thinning behavior of xanthan gum for different aqueous concentrations was studied by viscosity measurements at 8 °C ($\pm$ 0.5 °C), corresponding to the groundwater temperature, with a Brookfield rheometer (Brookfield Engineering Labs, Inc) by increasing progressively the shear rates (Figure 4.4; Appendix B).
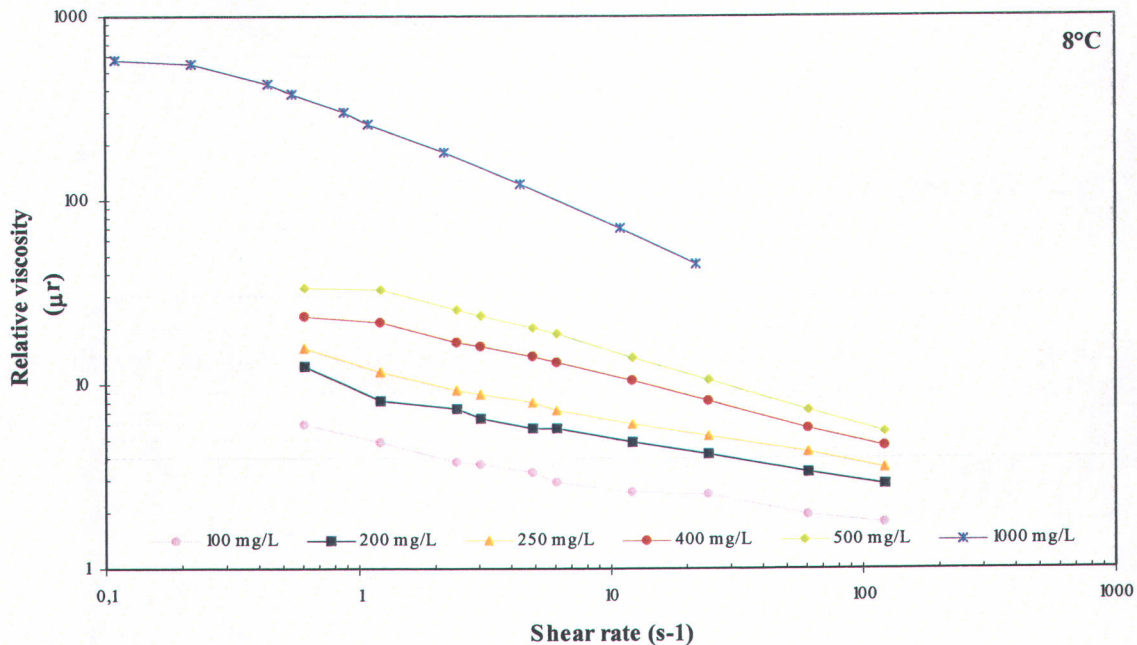
Figure 4.4: Viscosity as a function of shear rate for different aqueous concentrations of xanthan gum

The molecular weight of xanthan gum was measured by light diffusion by many authors (Chauveteau and Kohler, 1980). It varies between 1×10^6 and 50×10^6 g/mol depending on the presence of microgels. The microgels are multimolecular chemical aggregates of

large size (6 µm) in static conditions but they become deformed during filtration at high flow rate. For this reason, they are more difficult to filtrate than the cellular debris or the other solid particles coming from the fermentation process. For a long time, the microgels caused the overestimation of the molecular weight. A molecular weight for the xanthan gum between 1 x 10^6 and 2 x 10^6 g/mol would be more representative.

4.2.5.3. Preparation of the injected solutions

According to Chen and Sheppard (1979), the preparation method of polymer solutions can affect their homogeneity and their viscosity. In our case, the process used for the preparation of xanthan gum solutions was by dissolution.

The injected fluids were prepared in three different stainless steel reservoirs of ~2.23 m^3. Each reservoir is equipped with a stirrer. For the two sand tank tests, three different concentrations of xanthan gum (100 mg/L, 250 mg/L and 500 mg/L) were prepared. All the solutions were obtained by progressively adding the polymer under the form of white powder to deaerated distilled water. A slight agitation was necessary to homogenize the solution and to avoid the degradation of rheological properties of the polymer. The temperature of solutions was controlled with a thermostat at 8 °C ± 0.5 °C.

Three different tracers were added to solutions used for the tests to observe the breakthrough of tracers in the sand tank: chlorides with a concentration of 1 g/L, bromides with a concentration of 0.1 g/L and amaranth with a concentration of 0.1 g/L. Amaranth is a red organic compound regularly used as food additive. For the sand tank test with a single layer of fine sand, six solutions were injected at different flow rates (Table 4.3): five water solutions and one xanthan solution at 100 mg/L, followed by two xanthan solutions at 250 mg/L. For the sand tank test with three sand layers (Table 4.4), one water solution was injected and followed by one xanthan solution at 250 mg/L, followed by a xanthan solution at 500 mg/L, followed by a second xanthan solution at 250 mg/L and finally a water solution to finish the experiment. No bactericide was added to all solutions.

Tables 4.3 and 4.4 show the fluids injected in the sand tank for each test.

Table 4.3: Fluids injected in the one-layer sand tank test

Tests	Fluids	Flow rate (10^{-5} m³/s)	Volume injected (m³)	Vp with tracer	Total Vp	Δh (m)	Tracers added to injected fluids
A	water	1.39	10.2	1.9	3.9	0.045	chloride/bromide
B	water	2.66	8.9	1.2	3.4	0.089	chloride/bromide
C	water	0.85	6.3	1.4	2.4	0.030	chloride/bromide
D	water	1.73	6.3	2.2	2.4	0.063	chloride/bromide
E	water	2.31	8.7	1.3	3.3	0.085	chloride/bromide
F	xanthan 100 mg/L	1.56	2.2	0.85	0.85	0.107	chloride/bromide
	xanthan 250 mg/L		4.4	1.7	1.7		

where Vp is the pore volume and Δh the difference of hydraulic heads between the injection and the pumping wells (Figure 4.5).

Table 4.4: Fluids injected in the three-layer sand tank test

Tests	Fluids	Flow rate (10^{-5} m³/s)	Volume injected (m³)	Vp with tracer	Total Vp	Δh (m)	Tracers added to injected fluids
A	water	2.89	19.6	1.00	9.00	0.0206	chloride/amaranth
B	xanthan 250 mg/L	2.08	3.5	1.59	1.59	0.0366	chloride/amaranth
C	xanthan 500 mg/L	0.62	2.6	1.13	1.13	0.0297	bromide
D	xanthan 250 mg/L	0.87	3.4	1.55	1.55	0.0606	chloride
E	water	2.20	3.3	1.54	1.54	0.0420	-

where Vp is the pore volume and Δh the difference of hydraulic heads between the monitoring well OBS 2 and the monitoring well OBS 3 (Figure 4.6a).

The viscosity of water and xanthan gum measured at 8 °C (± 0.5 °C) with a Brookfield rheometer are illustrated in the Table 4.5.

Table 4.5: Viscosity of water and polymer solutions at 8 °C at no shear rate

Fluids	water	xanthan 100 mg/L	xanthan 250 mg/L	xanthan 500 mg/L
Viscosity (10^{-3} kg/m.s)	1.39	6.0	15.6	33.6

Chloride and bromide concentrations in the samples collected during the tests were measured by ion chromatography (ICS-2000 ionic chromatography system, DONEX). The use of standard solutions of chlorides and bromides (SCP Science) allowed to calibrate the equipment. The amaranth samples were measured by spectrophotometer (spectrophotometer spectronic 601, Bausch and Lomb/Milton Roy) at a wavelength of 522.5 nm and the calibration was done with solutions containing known concentrations of amaranth in water varying from 10^{-4} g/L to 10^{-1} g/L.

All the water injection tests were carried out to characterize the flow in the porous medium. The xanthan solutions injection tests consisted in evaluating the sweep efficiency through a geological formation compared to a water injection and understanding the problems related to viscosity contrasts between the different injected fluids.

4.2.5.4. Experimental set up

Figure 4.5 schematically represents the set up used for water and polymer solutions injection in the sand tank (Appendix G).
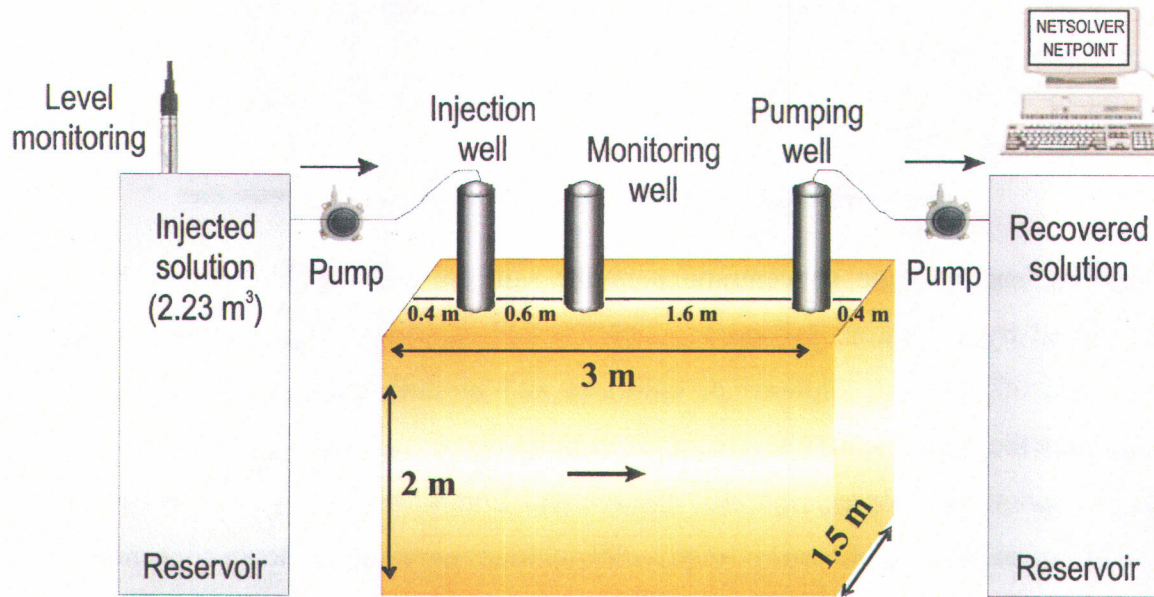
Figure 4.5: Set up for water and polymer solutions injection in the one-layer sand tank

The sand tank (3 m x 1.5 m x 2 m) made of stainless steel contained quartz sand: i) for the one-layer sand tank test, 1.5 m thick of Temisca 30 (a fine sand similar to the one described in Table 4.1) and; ii) for the three-layer sand tank test, 1.29 m thick of Filpro Well Gravels sands U.S. Silica (fine and medium). For the three-layer test, the porous medium is made up of a medium sand layer of 0.41 m thick between two fine sand layers of 0.44 m of thick. The one-layer sand tank was used as reference to observe the flow of fluids. The three-layer sand tank test was carried out to lead an additional difficulty for the sweep due to the heterogeneity of the porous medium. These different geometries were chosen to reproduce at best field conditions in order to evaluate the sweep efficiency of polymer solutions through a porous medium difficult to sweep.

The tank is in a laboratory at controlled temperature (8 °C ± 0.5 °C). For each test, the sand was introduced using barrels (300 kg of sand and 4 L of water per barrel). Water was added to the sand to facilitate the compaction of sand. Each barrel can make a layer of

about 4 cm in the tank. The sand was compacted between each layer using 7.2 kN compactor (Mikasa MVC-40G) and each layer was scarified before introducing the following one. This operation was repeated about 37 times to fill the tank. The mobile water fraction was drained using two openings of 10 mm at the bottom of the sand tank on each side. The sand tank was covered with a plate and a slight vacuum was applied. The sand tank was saturated with carbon dioxide (CO_2) before applying the vacuum again. Five CO_2-vacuum cycles flushing were done to completely remove air from the porous medium. Finally, the sand tank was saturated with deaerated tap water from the bottom-up to minimize air invasion.

Table 4.6 summarizes the physical characteristics of the sand layers after filling and compaction of the sand tank for the two tests.

Table 4.6: Physical characteristics of sand layers in the sand tank

	One-layer sand tank	Three-layer sand tank		
Sand mass (kg)	10 980	9 633		
Sand volume (m^3)	6.75	5.81		
Porosity	0.39	0.37		
Pore volume (m^3)	2.60	2.17		
Dry bulk density (kg/m^3)	1 630	1 658		
Thickness (m)	1.5 (fine sand)	1.29	top layer	0.44 (fine sand)
			middle layer	0.41 (medium sand)
			bottom layer	0.44 (fine sand)

For the one-layer sand tank test, three wells made of stainless steel were placed and aligned in the middle (central line) of the tank: one injection well, one monitoring well and one pumping well (Figure 4.5). Each well of 5 cm diameter measured 2 m in length with a 1.2 m screen length installed at 20 cm from the bottom of the sand tank (screen openings of 0.25 mm).

For the three-layer sand tank test, all the wells were made of stainless steel except for the injection and the pumping wells made of PVC. There were in total twenty-nine wells installed at different positions in the sand tank (Figure 4.6a): one injection well, one pumping well, four monitoring wells and twenty-three sampling wells. The injection well, the pumping well and the four monitoring wells were placed and aligned in the middle (central line) of the tank. The injection and the pumping wells of 1.9 cm diameter had a 2 m length with a screen located across the thickness of the sand tank, at 20 cm from the bottom of the tank (screen openings of 0.25 mm). The monitoring wells (OBS 1 to OBS 4) were similar to the ones used in the one-layer sand tank test but with a screen length of 30 cm located at 20 cm from the bottom of the sand tank. Finally, the sampling wells of 9.8 mm in diameter were placed at nine different locations in the sand tank designated by the wells 1 to 9 (Figure 4.6a). At each sampling point (wells 1 to 7), three observation wells were installed at different depths in the tank with a screen installed in the middle of each layer (one well in the bottom layer within fine sand, one well in the middle layer within medium sand and one well in the top layer within fine sand). Two other wells (wells 8 and 9) were installed deeper than the injection and the pumping wells (~5 cm below them) (Figure 4.6b). For all observation wells, the screen length measured 15 cm with openings of 2 mm. A filter mesh of 160 μm in stainless steel was put inside the screen of each observation well to avoid any sand particles infiltration into the well.

In the two sand tank tests, each monitoring well was equipped with a pressure transducer (KPSI Pressure Systems, Inc.). For the one-layer sand tank test, the injection and the pumping wells were also equipped with a pressure transducer. In each sand tank test, the injection well also contained a water level detector, which was used as an additional shut down criteria. A constant head between the injection and the pumping wells was kept by positioning a tube (pumping tube) in the pumping well (Figure 4.6b).
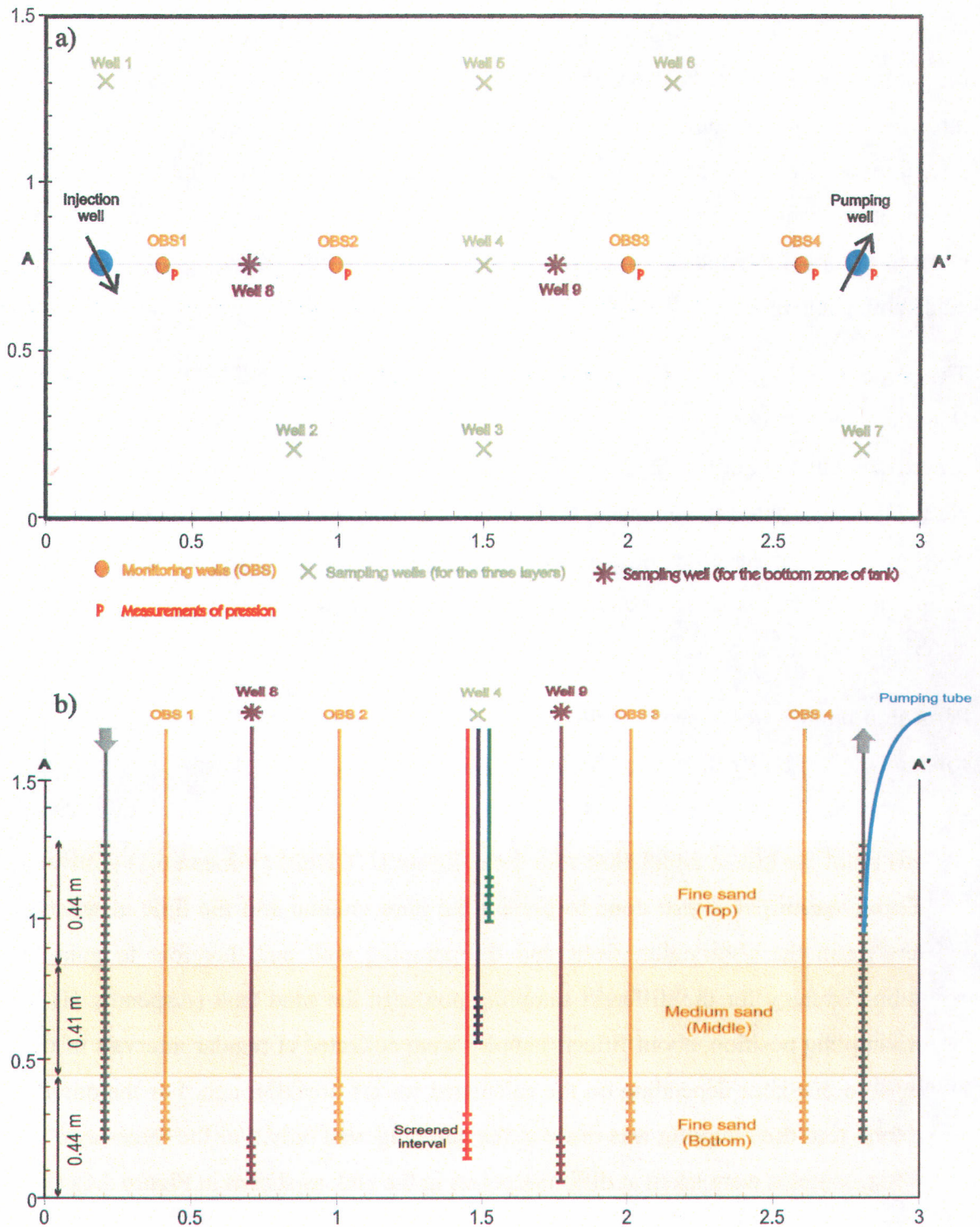
Figure 4.6: Set up for the three-layer sand tank test: a) plan view - b) cross section view

For each test, the fluids were mixed in three reservoirs of ~2.23 m^3 and then pumped in the sand tank through the screen of the injection well with a compressed air membrane pump (Marathon Pump, IDEX Corporation). The pumping well was also equipped with the same type of pump. Each reservoir was provided with an automated valve and was interconnected to the others to ensure a continuous flow into the sand tank without interruption of the experiment. Four water level detectors and pressure transducers put in the three reservoirs were used for the calculation of the flow rates and to monitor the pumped volume of liquid into the sand tank. Manual flow rate measurements were also made at the tank outlet.

The experimental set up was controlled by two softwares: NETSOLVER (Cutler-Hammer, 1999) to control the set up (valves opening, change of reservoirs, etc.), to verify the experimental conditions and to collect data from the different measurement devices; NETPOINT (Cutler-Hammer and PC Soft International, Version 7.51) as the interface with the user to visualize measured parameters (hydraulic heads in wells, time of sampling, tracers concentrations), results and to modify parameters during the experiment.

Peristaltic pumps were used to automatically collect 250 ml samples controlled by the software NETSOLVER at selected times or according to chloride and bromide concentrations. Amaranth was used for its red color in order to ensure a simple visual follow up of the test. A simulation with the software UTCHEM (Version 6.1) (University of Texas, Austin) was also done to predict the pore volume and the time at witch the tracers reach the observation wells and the pumping well and therefore to guide the sampling strategy for the different sampling points in the sand tank (Appendix H). For each sampling position, about fifteen samples were collected at regular intervals of thirty minutes to one hour depending on the calculated tracers breakthrough. For the one-layer sand tank test, the sampling was made at the pumping well only. For the three-layer sand tank test, samples were taken at different points in the tank as shown in Figure 4.6a (wells 1 to 9).

All tests were done at constant head according to the pressure fixed in the injection well by the transducer and the position of the pumping tube in the pumping well (Figure 4.6b).

Hydraulic heads were continuously monitored in each monitoring well and the pumping well (indicated by the symbol P on the Figure 4.6a). The injected solutions into the sand tank (water and xanthan solutions) were pumped and stirred into a 1 L overflowing beaker containing two ion selective probes (TempHion2, Instrumentation Northwest, Chloride - Bromide) to evaluate the tracers concentrations injected. These selective probes were calibrated with standard solutions of chlorides and bromides (SCP Science) with concentrations of 10 mg/L, 50 mg/L, 100 mg/L, 500 mg/L and 1 000 mg/L. The calibration was done before each test to ensure a maximal precision of the measurements. The tracers concentrations measured with these selective probes were used to observe the tracers breakthrough in the pumping well. Tracers concentrations presented in the following section were measured by the ionic chromatography.

The hydraulic heads in each well, the temperature of injected solutions, the tracers concentrations, the reservoir number during the fluids injection and the water levels in the reservoirs were recorded continuously during the test.

4.2.6. Results

4.2.6.1. One-layer sand tank tests

In the one-layer sand tank, two tests were carried out: i) one test with water injection at different flow rates and ii) one test with a xanthan solution at 100 mg/L, followed by two xanthan solutions at 250 mg/L. The use of chlorides and bromides as tracers added to the injected solutions allowed to evaluate the sweep efficiency and the displacement front stability of xanthan gum compared to a water injection at the pumping well (Appendix E).

Evolution of hydraulic head difference and hydraulic conductivity

Figure 4.7 shows the evolution of hydraulic head difference between the injection and the pumping wells and hydraulic conductivity for three water injections. In each test, the hydraulic head difference was kept constant between the injection and the pumping wells (Figure 4.7a). The little variations of hydraulic head observed on the Figure 4.7a, particularly for the test E, are principally due to fluctuations of flow rate at the beginning

77

of the test before reaching the steady state. The hydraulic conductivity estimated from Equation 4.5 is also constant during all the test (Figure 4.7b). However, in some cases, the hydraulic head difference reaches a zero value corresponding to the temporary shut down of the experiments.
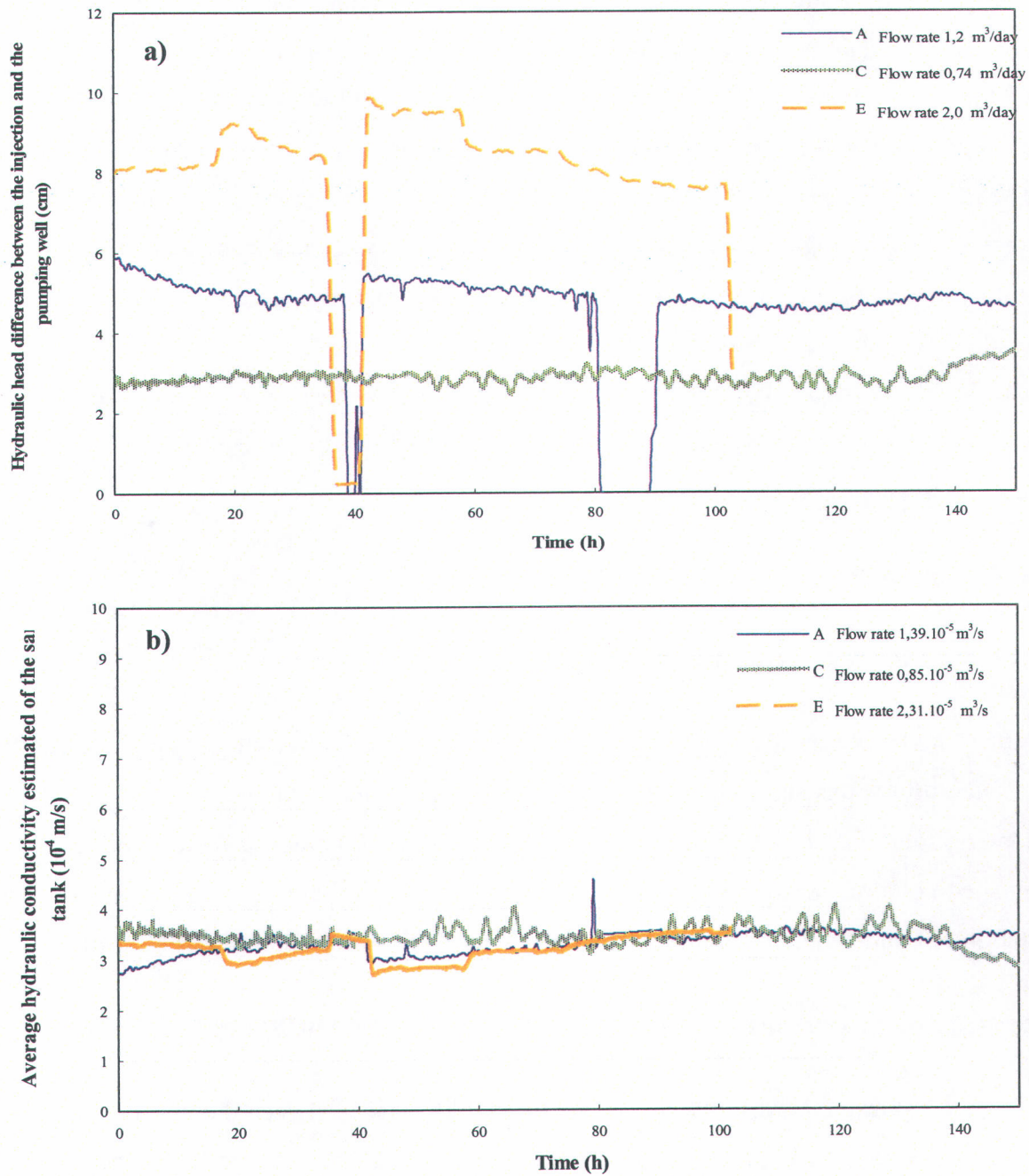
Figure 4.7: Evolution of a) hydraulic head difference and b) hydraulic conductivity for three water injections in the one-layer sand tank

The hydraulic conductivity in the sand tank was estimated between the monitoring well and the pumping well by considering a linear flow through the porous medium:

$$Q = K\, A\, \frac{\Delta h}{\Delta L} = k\, \frac{\rho\, g}{\mu}\, A\, \frac{\Delta h}{\Delta L}\, [=]\left[\frac{m^3}{s}\right]$$

Eq. 4.5

where Q (m³/s) is the flow, K (m/s) the hydraulic conductivity, A (m²) the porous medium surface, Δh (m) the hydraulic head difference and ΔL (m) the distance between the monitoring well and the pumping well.

The average hydraulic conductivity estimated in the one-layer sand tank test for the water injection (Figure 4.7b) is in agreement with the value obtained in the sand column tests (Table 4.1).

The hydraulic conductivity of the fine sand with water and 250 mg/L xanthan solution obtained with the sand column tests and the one-layer sand tank test, are noticed in the Table 4.7.

Table 4.7: Hydraulic conductivity of the fine sand with water and 250 mg/L xanthan solution

Fluids	water (sand column tests) *Table 4.1*	water (one-layer sand tank test) *Figure 4.7b*	xanthan at 250 mg/L (one-layer sand tank test) *Figure 4.8*
K (10^{-4} m/s)	7.0	~ 3.5	~ 0.6

During the injection of xanthan solutions, the hydraulic head difference between the injection and the pumping wells increased continuously with time (Figure 4.8). Moreover, the corresponding effective hydraulic conductivity decreased steadily during the injection of xanthan solutions. Following the injection of the 100 mg/L xanthan solution, the decrease of the hydraulic conductivity continued for the first reservoir of the 250 mg/L xanthan solution.

According to Equation 4.6, the hydraulic conductivity is inversely proportional to the viscosity of injected solutions. A viscosity increase (due to the injection of xanthan solution compared to water) leads to a decrease in hydraulic conductivity.

$$K = k \, \frac{\rho \, g}{\mu} \, [=] \left[\frac{m}{s} \right]$$

Eq. 4.6

where K (m/s) is the hydraulic conductivity of the injected fluid, k (m^2) the intrinsic permeability of the medium, ρ (kg/m^3) the fluid density, g (9.81 m/s^2) the gravitational acceleration and μ (Pa.s) the viscosity of the injected fluid.
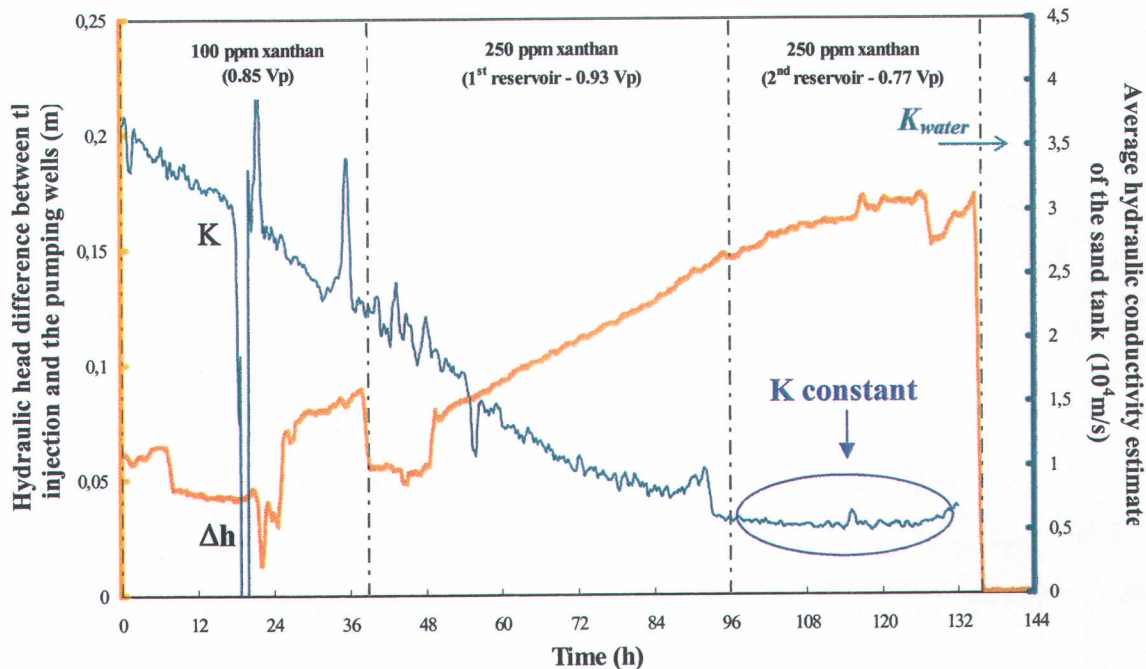
Figure 4.8: Evolution of hydraulic head difference between the injection and the pumping wells and hydraulic conductivity with time

By considering a linear flow (similar to a column test), the flow is directly proportional to the hydraulic conductivity and to the hydraulic head difference between the injection and pumping wells (Equation 4.5). As the flow is imposed at the beginning of the test at a constant value, if the hydraulic conductivity decreases by the use of polymer, the hydraulic head difference must increase to keep a constant flow rate (Figure 4.8).

80

For the second reservoir with 250 mg/L xanthan solution, the hydraulic conductivity became constant, indicating that the tank reached a steady state. Neither pore clogging nor polymer accumulation was observed in the sand tank as shown by the constant hydraulic conductivity value (Figure 4.8).

Hydraulic conductivity between sand column and sand tank tests

The hydraulic conductivity of the fine sand measured in sand column tests and estimated in the one-layer sand tank test for the water injections were compared to the value obtained with 250 mg/L xanthan solution by calculation, knowing the viscosity of each solution at 8 °C (Table 4.5).

The hydraulic conductivity of the fine sand with water and 250 mg/L xanthan solution are calculated by the Equations 4.7 and 4.8:

$$K_{water} = k \frac{\rho_{water}\, g}{\mu_{water}} \qquad\qquad \text{Eq. 4.7}$$

$$K_{xanthan} = k \frac{\rho_{xanthan}\, g}{\mu_{xanthan}} \qquad\qquad \text{Eq. 4.8}$$

Knowing the hydraulic conductivity of the fine sand with water in the one-layer sand tank ($K_{t\ water}$) (Table 4.7) and the viscosity ratio between water and the 250 mg/L xanthan solution (Table 4.5):

$$K_{t\ water} = 3.5 \times 10^{-4}\ m/s \quad \text{and} \quad \mu_{xanthan} \approx 11 \times \mu_{water} \qquad \text{Eq. 4.9}$$

The hydraulic conductivity of the fine sand with 250 mg/L xanthan solution in the sand tank ($K_{t\,xanthan}$) can be calculated according to the Equation 4.10:

$$K_{t\,xanthan} = K_{t\ water}\, \frac{\mu_{water}}{\mu_{xanthan}} = \frac{K_{t\ water}}{11} = \frac{3.5 \times 10^{-4}}{11} = 3.2 \times 10^{-5}\ m/s = 0.32 \times 10^{-4}\ m/s \qquad \text{Eq. 4.10}$$

The hydraulic conductivity of the fine sand with water obtained in the sand column tests ($K_{c\ water}$) (Table 4.7) can be used to calculate the hydraulic conductivity for 250 mg/L xanthan solution ($K_{c\ xanthan}$):

$$K_{c\ xanthan} = K_{c\ water}\ \frac{\mu_{water}}{\mu_{xanthan}} = \frac{K_{c\ water}}{11} = \frac{7 \times 10^{-4}}{11} = 6.4 \times 10^{-5}\ m/s = 0.64 \times 10^{-4}\ m/s \quad \text{Eq. 4.11}$$

Table 4.8 resumes the hydraulic conductivity for 250 mg/l xanthan solution between the observed and calculated data.

Table 4.8: Hydraulic conductivity of the fine sand for 250 mg/L xanthan solution

Fluids	xanthan at 250 mg/L (sand column tests) *calculated eq.4.11*	xanthan at 250 mg/L (one-layer sand tank test) *calculated eq.4.10*	xanthan at 250 mg/L (one-layer sand tank test) *observed on figure 4.8*
K **(10^{-4} m/s)**	0.64	0.32	0.6

There is a good agreement between the values observed on Figure 4.8 and the results calculated by the Equations 4.10 and 4.11.

Displacement front stability

The displacement front stability of each injected solution was evaluated through the one-layer porous medium on the basis of tracers concentrations measured at the pumping well (Figure 4.9). Two tracers were added to the solutions: chlorides at a concentration of 1 g/L and bromides at a concentration of 0.1 g/L (Table 4.3). The collected samples at the pumping well containing the tracers were analyzed by ion chromatography to determinate their concentrations in order to evaluate the tracers breakthrough and so their sweep efficiency.

The displacement front for the xanthan solution is more vertical and less dispersed compared to different water injections, indicating that the front is more stable. Therefore,

the breakthrough (at $C/C_0 = 0.5$) of tracers in water is observed before the breakthrough of the xanthan solution, meaning that the porous medium is better swept with the xanthan solution.
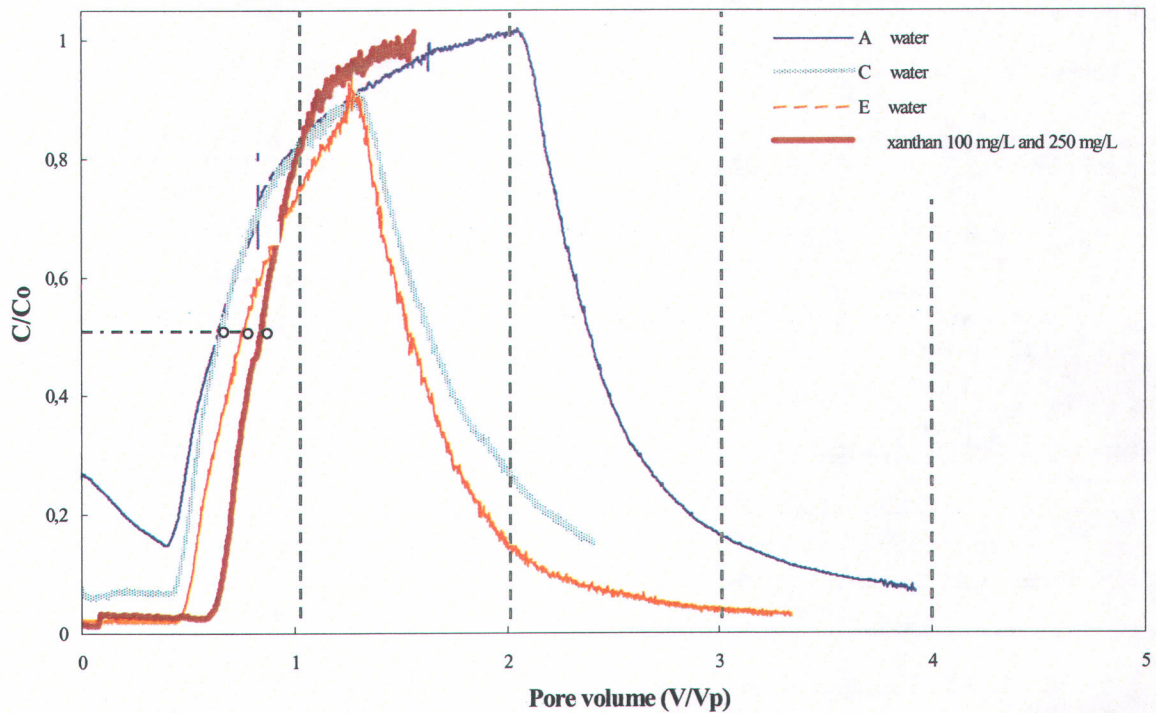
Figure 4.9: Evaluation of displacement front stability based on tracer arrival at the pumping well for three water injection tests and the xanthan solution injection test

Nevertheless, in each case, the tracers breakthrough is viewed before the injection of one pore volume, which means the sweep of the geological formation is not complete. Some zones are not swept, due notably to a radial effect near injection and pumping wells.

Table 4.9 and 4.10 resume the characteristics of the one-layer sand tank test and give an idea of sweep efficiency for each injected solution based on tracers arrival at the pumping well.

Table 4.9: Characteristics of the one-layer sand tank test

Tests	Fluids	Flow rate (10^{-5} m^3/s)	Vp injected with tracer	Vp injected without tracer	Tracers added to injected fluids (mg/L)	
					chlorides	bromides
A	water	1.39	1.9	2.0	1.0	0.1
C	water	0.85	1.4	1.0	1.0	0.1
E	water	2.31	1.3	2.0	1.0	0.1
F	xanthan 100 mg/L	1.56	0.85	-	1.0	0.1
	xanthan 250 mg/L		1.7	-		

Table 4.10: Sweep efficiency at breakthrough in the one-layer sand tank

Tests	Fluids	Flow rate (10^{-5} m^3/s)	Vp at breakthrough ($C/C_0 = 0.5$)	Sweep efficiency (%)
A	water	1.39	0.64	64
C	water	0.85	0.65	65
E	water	2.31	0.75	75
F	xanthan 100 mg/L	1.56	0.84	84
	xanthan 250 mg/L			

Although the tracers breakthrough (at $C/C_0 = 0.5$) is observed before the injection of one pore volume (corresponding to a perfect sweep), the sweep is more effective with the xanthan solution (84 %) compared to water injections (64 to 75 %). The benefit effect of xanthan gum on the sweep is so confirmed.

4.2.6.2. Three-layer sand tank tests

Two tests were made with the three-layer sand tank: i) one test with water injection and ii) one test with a xanthan solution at 250 mg/L, followed by a xanthan solution at 500 mg/L, followed by a second xanthan solution of 250 mg/L. Finally, a water injection completed this experiment. Many observation wells were installed at different locations inside the sand tank to evaluate the sweep efficiency and the displacement front stability when solutions are injected in the three sand layers.

Evolution of hydraulic head difference

During the test, the hydraulic head difference was imposed between the injection and the pumping wells. However, Figure 4.10 represents the evolution of hydraulic head difference between the monitoring well OBS 2 and monitoring well OBS 3 (Figure 4.6a) with water injection test. The total injected pore volume of water is 9.0 m^3. The hydraulic head difference was kept constant during all the test. The variations observed on the Figure 4.10 are due to little fluctuations in the flow rate before reaching the steady state.
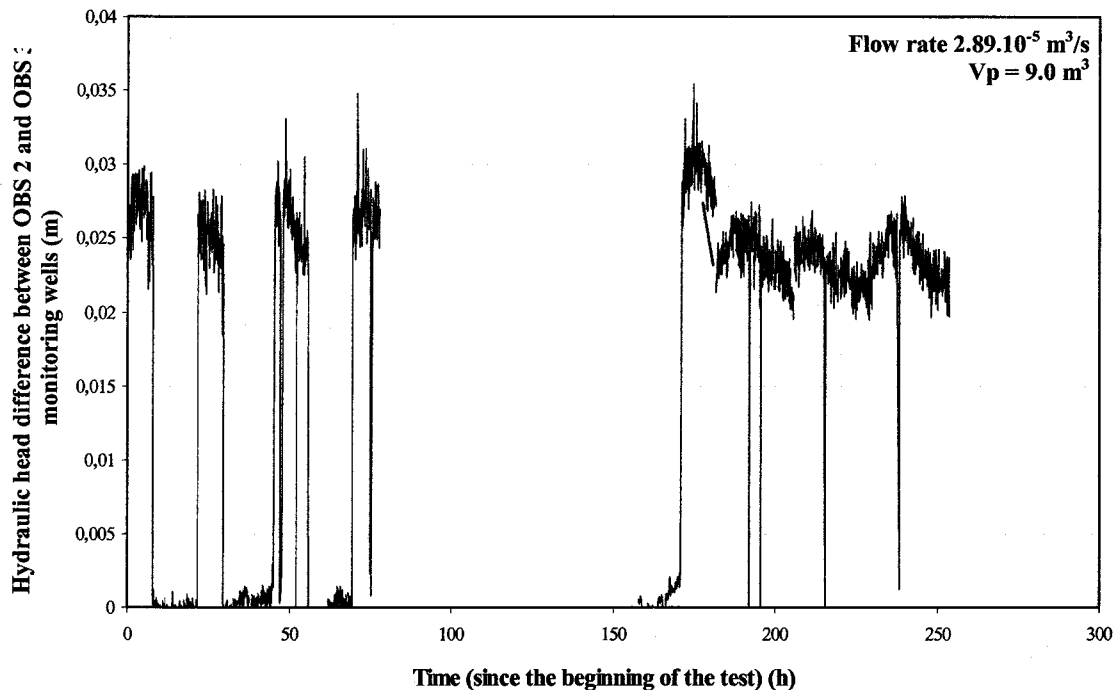
Figure 4.10: Evolution of the hydraulic head difference between OBS 2 and OBS 3 monitoring wells during the water injection in the three-layer sand tank test

An average value of 2.5 x 10^{-2} m is obtained for the hydraulic head difference between OBS 2 and OBS 3 monitoring wells. The hydraulic head difference had sometimes a zero value, due to the shut down of the test at night or during holidays. The diffusion of injected solutions through the porous medium during the shuts down is supposed to be nil and therefore, there are not mass loss in the three dimensions of the sand tank.

Evolution of hydraulic conductivity with water

The evolution of the hydraulic conductivity was calculated during all the test to confirm the values obtained in sand column tests and in the one-layer sand tank test (Figure 4.11). The hydraulic conductivity was estimated in the sand between OBS 2 and OBS 3 monitoring wells by considering a linear flow in the tank, by knowing the length (ΔL) between OBS 2 and OBS 3 monitoring wells, the surface (A) of the tank and the hydraulic head difference (Δh) and by measuring the injection flow (Q) according to the Equation 4.12.

$$K = \frac{Q}{\Delta h} \times \frac{\Delta L}{A} \qquad \text{Eq. 4.12}$$

where K (m/s) is the hydraulic conductivity of injected fluid, Q (m^3/s) the flow, Δh (m) the hydraulic head difference between OBS 2 and OBS 3 monitoring wells and ΔL (m) the length between OBS 2 and OBS 3 monitoring wells.
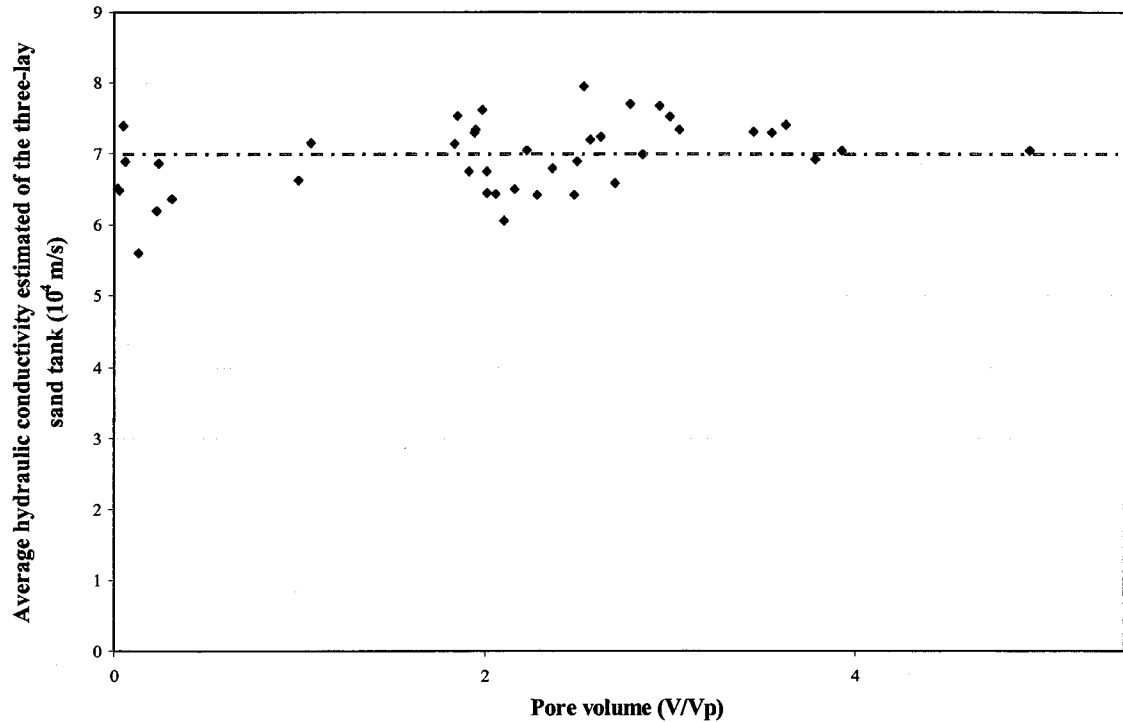
Figure 4.11: Evolution of the hydraulic conductivity with water injection in the three-layer sand tank

The hydraulic conductivity is kept constant during the test. An average hydraulic conductivity value around 7×10^{-4} m/s is obtained. By knowing the hydraulic conductivity of each sand layer and their thickness (Table 4.11), it is possible to calculate the global hydraulic conductivity through the three layers in the sand tank (Equation 4.13):

$$K = \frac{\sum_{i=1}^{n} b_i K_i}{\sum_{i=1}^{n} b_i}$$

Eq. 4.13

where K_i is the hydraulic conductivity of the sand layer i and b_i the thickness of the sand layer i.

Table 4.11: Hydraulic conductivity of each sand layer with their thickness

Sand layer	K (m/s)	b (m)
FINE (TOP)	3.5 x 10^{-4} *(from previous one-layer sand tank test – Table 4.7)*	0.44
MEDIUM (MIDDLE)	21 x 10^{-4} *(from sand column test – Table 4.1)*	0.41
FINE (BOTTOM)	3.5 x 10^{-4} *(from previous one-layer sand tank test – Table 4.7)*	0.44

$$K = \frac{\sum_{i=1}^{n} b_i K_i}{\sum_{i=1}^{n} b_i} = \frac{(0.44 \times 3.5.10^{-4}) + (0.41 \times 21.10^{-4}) + (0.44 \times 3.5.10^{-4})}{(0.44 + 0.41 + 0.44)} = 9 \times 10^{-4} m/s \quad \text{Eq. 4.14}$$

The hydraulic conductivity calculated at Equation 4.14 is compared to the value observed on Figure 4.11 and shows a good agreement between the values.

Sweep efficiency with water

The sweep efficiency and the displacement front stability was evaluated through the three layers in the sand tank. Two tracers were used for the water injections to observe the breakthrough of tracers in water: chlorides with a concentration of 1 g/L and amaranth with a concentration of 0.1 g/L. The characteristics of different tests are showed in Table 4.4. Many observation wells were installed at different locations in the sand tank to evaluate the sweep efficiency and the displacement front stability when solutions are injected into the three sand layers. At each positions, about fifteen samples are collected and analyzed. The samples containing the chlorides tracers were analyzed by ionic chromatography, the amaranth samples by spectrophotometer. For the pumping well, the values obtained with the selective probes were compared to those measured by ionic chromatography (Figure 4.15).

Figures 4.12 to 4.15 represent the breakthrough of tracers for some sampling points (well 1, well 4, well 7 and the pumping well) in the three sand layers after the injection of 1.0 pore volume water with tracers.

The question marks indicated on Figures 4.12 to 4.15 mean that at some times, the sampling was not done. So, hand lines were drawn to smooth the curves. Consequently, the top of the curve represents a virtual picture of what could happen. The background does not always reach a zero value, meaning that the samples contained still a little concentration of tracers.
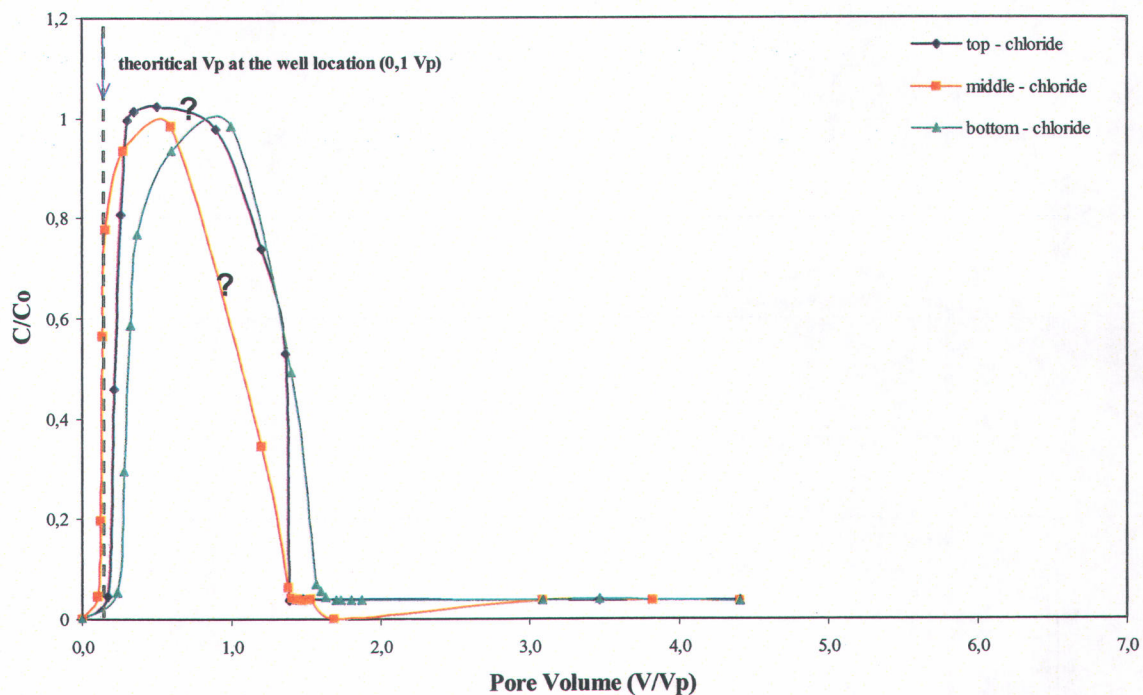
Figure 4.12: Breakthrough of tracers at well 1 with water injection
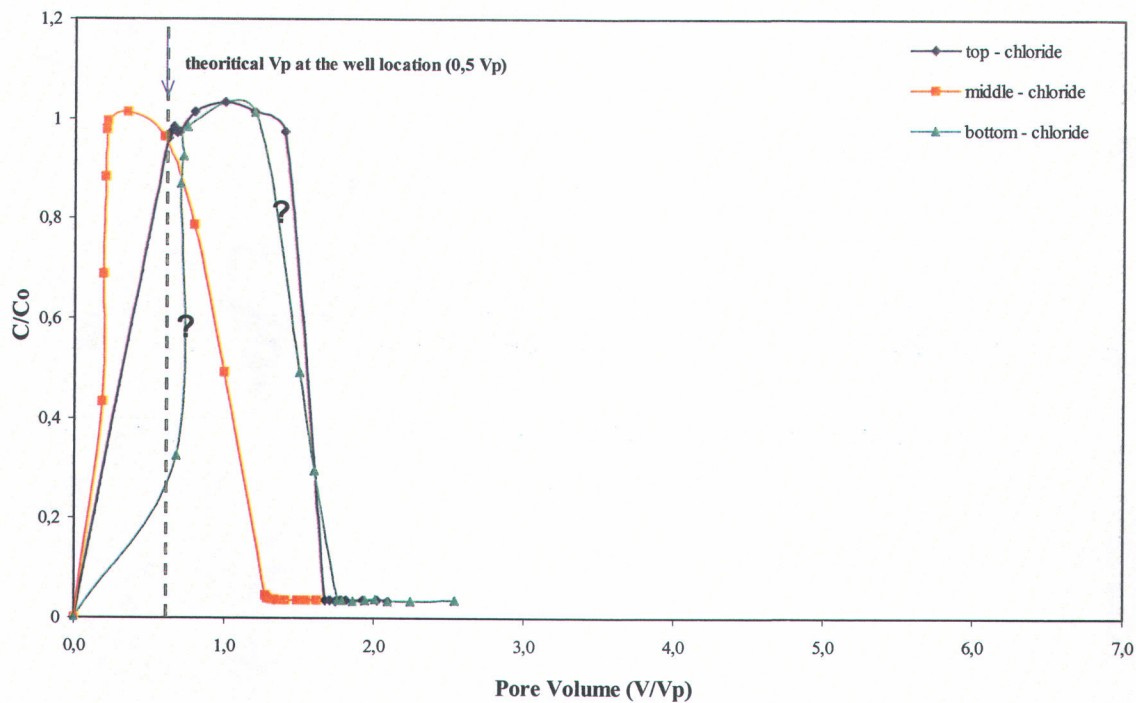
Figure 4.13: Breakthrough of tracers at well 4 with water injection
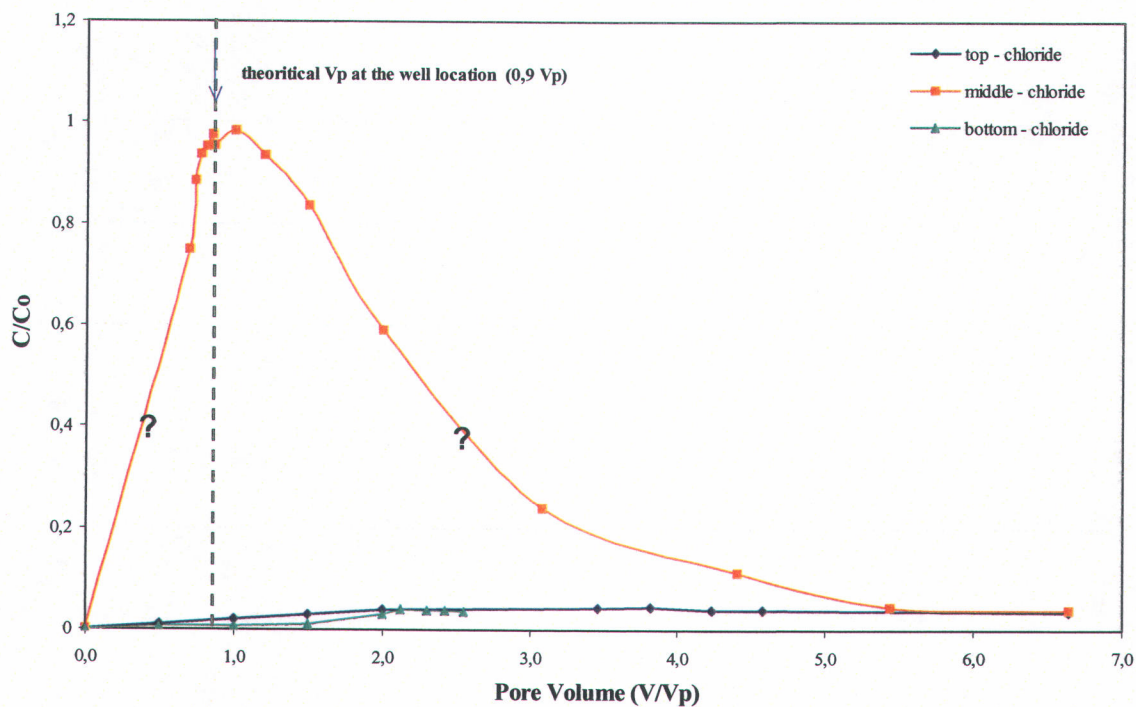
Figure 4.14: Breakthrough of tracers at well 7 with water injection
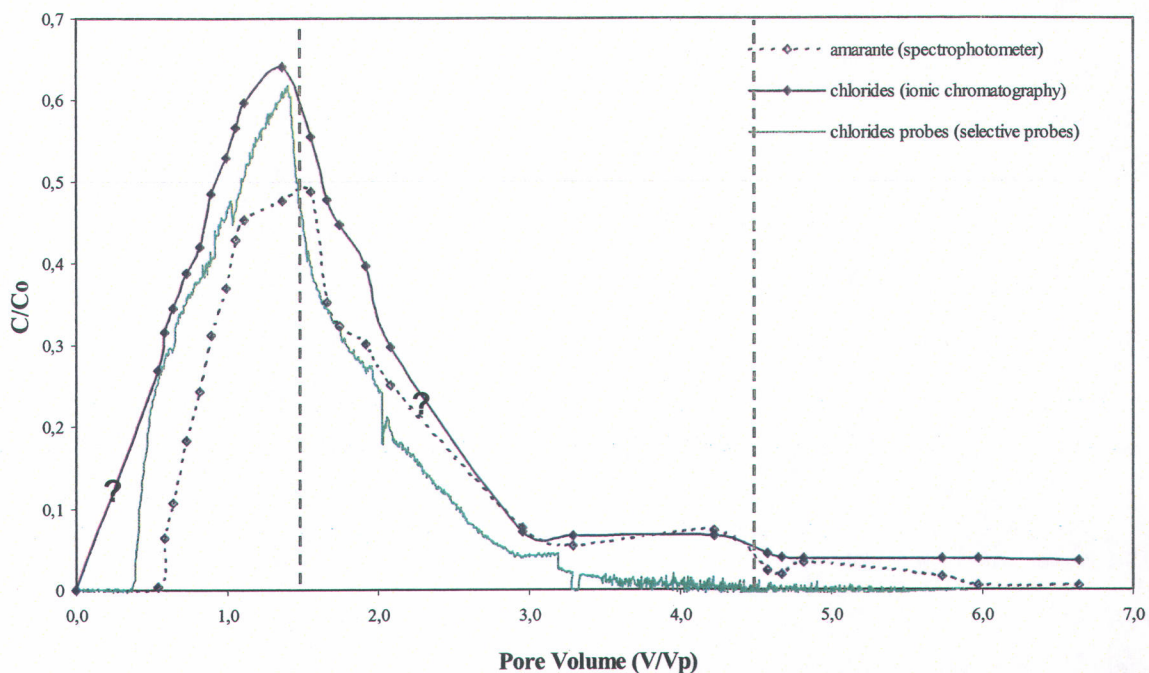
Figure 4.15: Breakthrough of tracers at the pumping well for collected samples compared to the data obtained with the selective probes with water injection

In all cases except for the sampling well 7 as shown in Figure 4.14, the tracer arrival is observed. The three sand layers at well 1 and well 4 are swept and only the middle layer at well 7 is swept. The maximum concentration of chlorides tracer (1g/L) is often reached (ratio C/C_0 near 1). At the opposite, for the amaranth (with an initial concentration of 0.1 g/L), the ratio C/C_0 is lower. This low concentration ratio is due to the chemical structure of the amaranth (Figure 4.16).
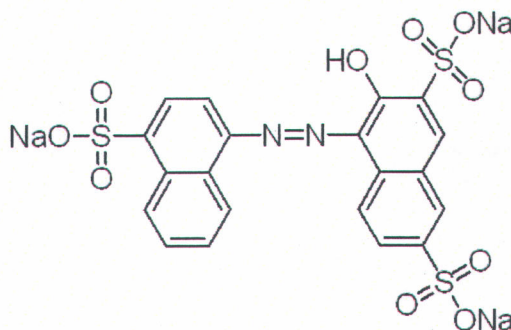
Figure 4.16: Chemical structure of amaranth

In fact, it is an organic compound and so tends to form hydrogen links between the oxygen atoms of the amaranth and the water molecules present in the pores of porous medium, leading to a decrease of amaranth concentration during its injection. Consequently, the amaranth undergoes a mass loss. In the following of the study, only the results obtained by ionic chromatography with chloride tracers will be provided. In the pumping well (Figure 4.15), the maximum concentration of tracers is not reached because the pumped solution comes from the three layers with a different front position according to the grain size (faster in the medium sand). A dilution of the solution is occurring during its way through the sand tank.

Based on the breakthrough of tracers in wells, the areal sweep of the sand tank is not perfect with a doublet (Figure 4.17), due to a radial effect near injection and pumping wells. The not swept zones, particularly in the corners of the sand tank or along the walls, was estimated between 10 and 20 %.
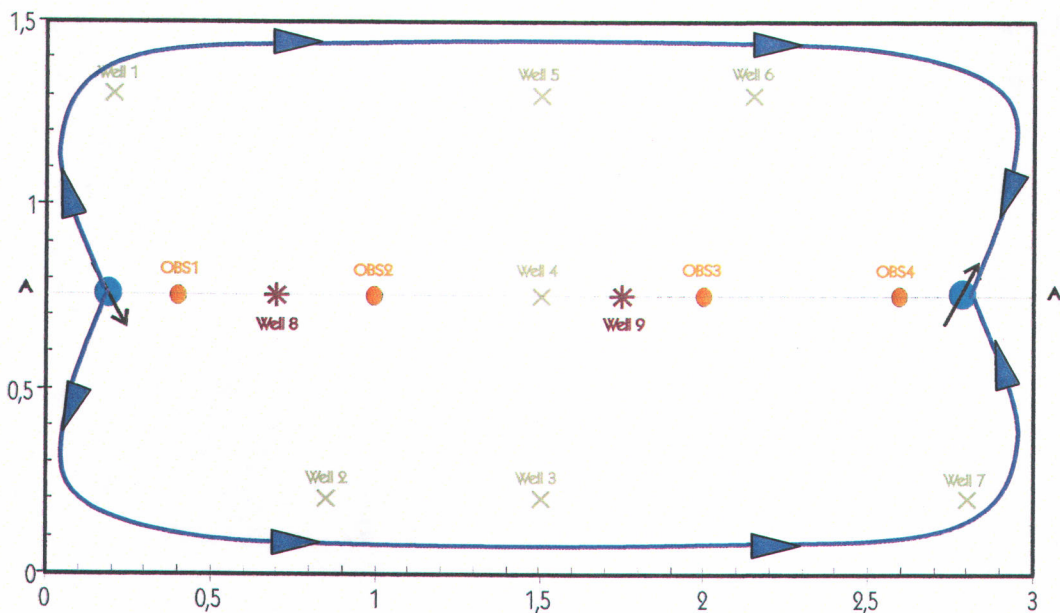
Figure 4.17: Areal sweep of the sand tank during water injection in the middle layer

Tables 4.12 and 4.13 resume the characteristics of the three-layer sand tank test and give an idea of sweep efficiency with water.

Table 4.12: Water injection in the three-layer sand tank test

Tests	Fluids	Flow rate $(10^{-5} m^3/s)$	Vp of water injected with tracer	Vp of water injected without tracer	Tracers added to water solution (mg/L)	
					chlorides	amaranth
A	water	2.89	1.0	8.0	1.0	0.1

Table 4.13: Sweep efficiency at breakthrough in the three-layer sand tank

Tests	Fluids	Flow rate $(10^{-5} m^3/s)$	Theoritical Vp at breakthrough for chlorides $(C/C_0 = 0.5)$		Sweep order
A	water	2.89	well 1	top layer	0.23	Second
				middle layer	0.12	First
				bottom layer	0.27	Third
			well 4	top layer	0.32	Second
				middle layer	0.22	First
				bottom layer	0.68	Third
			well 7	top layer	0.00	Not swept
				middle layer	0.46	First
				bottom layer	0.00	Not swept

In the three observations wells, the breakthrough occurs first in the middle layer and in last in the bottom layer. At well 7 (Figure 4.14) at the tank end, the top and the bottom layers are not swept with water. A lower flow rate in the fine sand layers is the main reason but a wall effect can also explain this result.

The advancement of the displacement front between the chloride tracer and amaranth is slightly different. The samples with chlorides are collected before the samples with amaranth (Figure 4.15). It is caused by a dilution of amaranth samples with water present in the pores of porous medium (the delay factor varies between 1.1 and 1.3 compared to chloride tracer). Moreover, the advancement of the solution is faster through the medium sand than in the two fine sand layers, due to the sand grains size and so to a higher pore volume (more important flow rate).

By comparing the measured values by ion chromatography and spectrophotometer and the data obtained by the selective probes (Figure 4.15), the curves shape is similar. The maximal value for the chloride tracer is reached after 1.5 Vp and finished after 4.5 Vp (indicated by the vertical lines). There is a good agreement between the direct experimental data (selective probes) and the results obtained by ion chromatography and spectrophotometer. However, the sweep efficiency of water at the pumping well (at C/C_0 = 5) reaches almost a value of 100 %, due notably to the fact that the pumping well is aligned with the injection well and that the majority of the injected solution flows through the middle layer of the sand tank (Figure 4.15).

Among all the observation wells, an only one was not treated (well 6 in the top layer with fine sand) due to an installation problem or a clogging of the screen by fine particles.

Evolution of hydraulic conductivity with xanthan

The evolution of the hydraulic conductivity with different xanthan solutions injections was estimated according to Equation 4.12 during all the test, considering a linear flow between OBS 2 and OBS 3 monitoring wells. These results were compared to those obtained in sand column tests and in the one-layer sand tank (Figure 4.18).
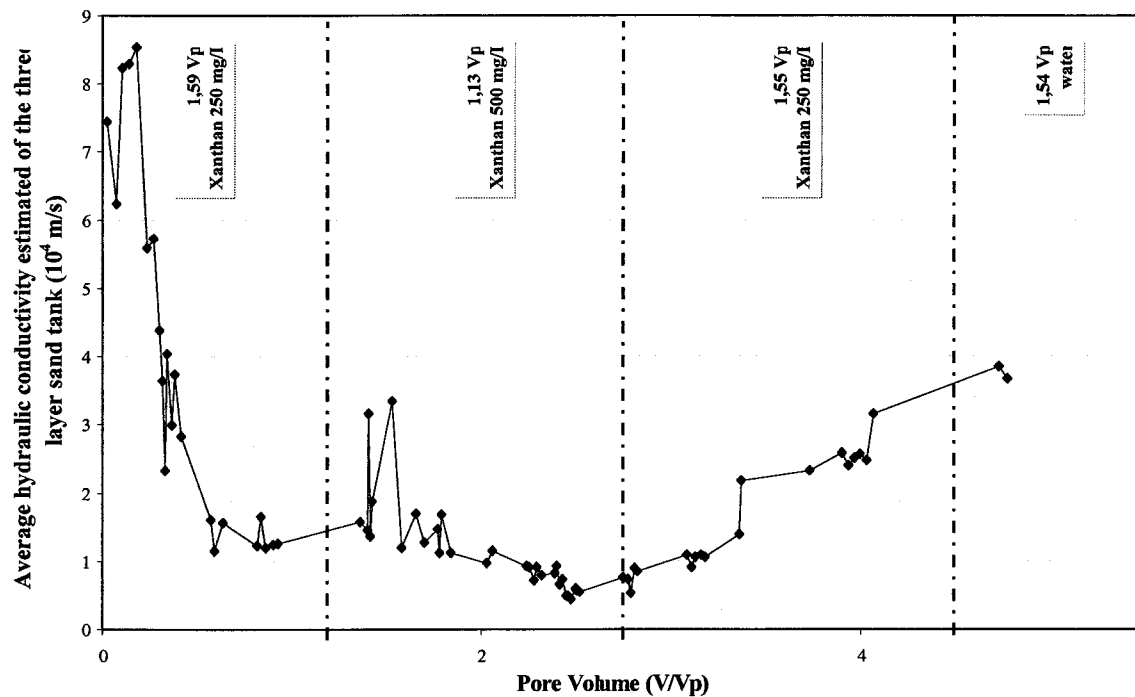
Figure 4.18: Evolution of the average global hydraulic conductivity during xanthan injection

The effective hydraulic conductivity decreases drastically with the first xanthan injection at 250 mg/L. As the hydraulic conductivity is inversely proportional to the viscosity, if the viscosity increases, the hydraulic conductivity decreases. It is the same phenomenon after xanthan solution injection at 500 mg/L, due to a still higher viscosity. With the second xanthan injection at 250 mg/L, the viscosity is lower and so, the hydraulic conductivity increases again and continues to increase with water injection.

Knowing the viscosity of water and 500 mg/L xanthan solution (Table 4.5) and so the ratio between these two solutions (the viscosity of water is twenty-four times lower than xanthan solution), it is possible to calculate the hydraulic conductivity for 500 mg/L xanthan solution by Equation 4.15:

$$K_{xanthan} = K_{water} \frac{\mu_{water}}{\mu_{xanthan}} = \frac{K_{water}}{11} = \frac{3.5 \times 10^{-4}}{24} = 1.4 \times 10^{-5} \ m/s = 0.14 \times 10^{-4} \ m/s \quad \text{Eq. 4.15}$$

Table 4.14 resumes the hydraulic conductivity for all the injected solutions into the three-layers sand tank.

Table 4.14: Hydraulic conductivity for water, 250 mg/L xanthan solution and 500 mg/L xanthan solution

Fluids	water *observed on Figure 4.7b*	xanthan 250 mg/L *calculated eq.4.10*	xanthan 500 mg/L *calculated eq.4.15*
K $(10^{-4}$ m/s)	~ 3.5	~ 0.32	~ 0.14

More the viscosity of the injected solution is high, more the hydraulic conductivity is low. The fluid has more difficulties to flow through the porous medium.

Sweep efficiency of xanthan gum

Different solutions of xanthan with three different tracers were injected into the sand tank to evaluate the sweep efficiency through the three sand layers (Table 4.15). The samples with chloride and bromide tracers were measured by ion chromatography, the amaranth samples by spectrophotometer.

Table 4.15: Xanthan solutions injection in the three-layer sand tank test

Tests	Fluids	Flow rate (10^{-5} m³/s)	Vp injected with tracer	Tracers added to xanthan solution (mg/L)	
				chlorides / bromides	amaranth
B	xanthan 250 mg/L	2.08	1.59	1.0 / -	0.1
C	xanthan 500 mg/L	0.62	1.13	- / 0.1	-
D	xanthan 250 mg/L	0.87	1.55	1.0 / -	-
E	water	2.20	1.54	-	-

Figures 4.19 to 4.21 represent the breakthrough of tracers for well 1, well 4 and well 7 in the different layers after the injection of the two first xanthan solutions at 250 mg/L and 500 mg/L for a total of 2.72 Vp.
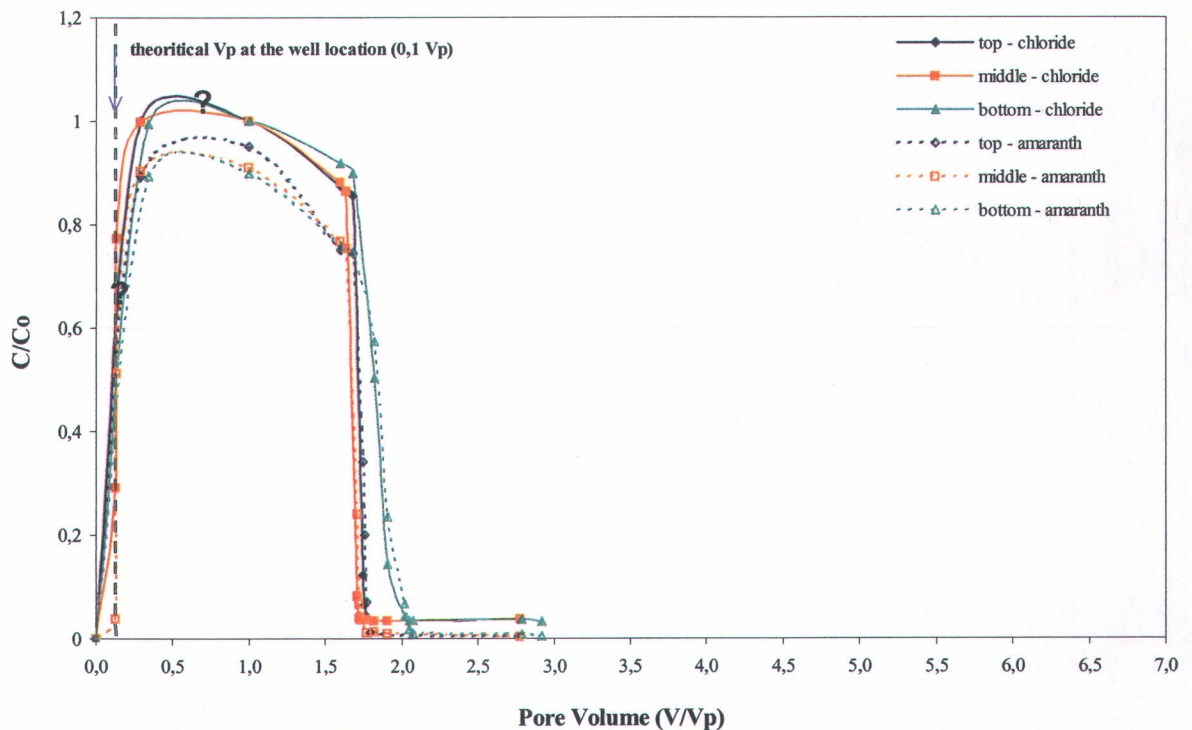
Figure 4.19: Breakthrough of tracers in xanthan at 250 mg/L at well 1
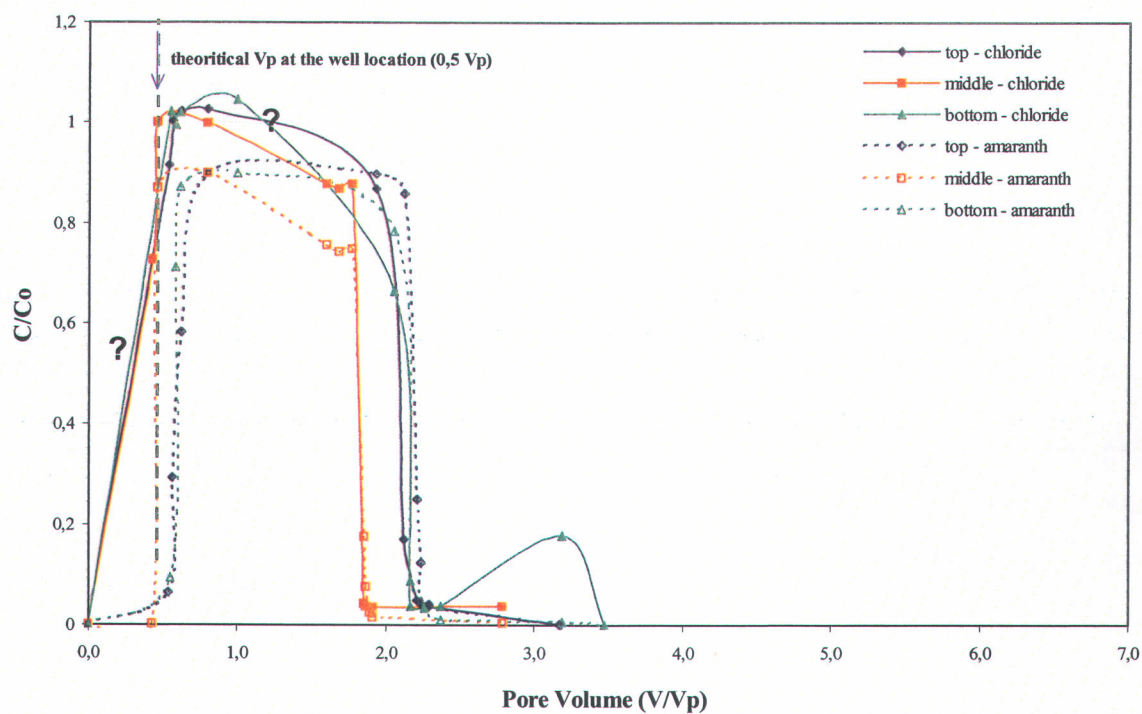
Figure 4.20: Breakthrough of tracers in xanthan at 250 mg/L at well 4
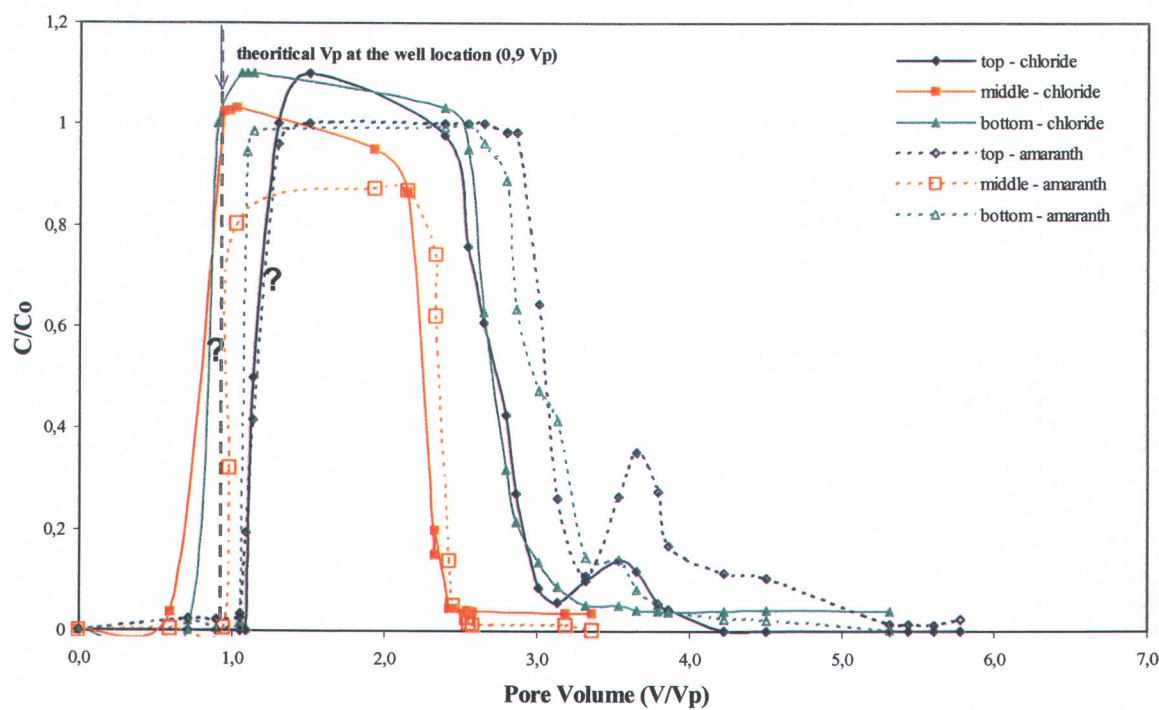
Figure 4.21: Breakthrough of tracers in xanthan at 250 mg/L at well 7

Table 4.16 gives an idea of sweep efficiency of the first 250 mg/L xanthan solution.

Table 4.16: Breakthrough in the three-layer sand tank for 250 mg/L xanthan solution

Tests	Fluids	Flow rate $(10^{-5}\,m^3/s)$	Theoritical Vp at breakthrough for chlorides $(C/C_0 = 0.5)$		Sweep order
B	250 mg/L xanthan solution	1.6	well 1	top layer	0.12	Same time
				middle layer	0.12	
				bottom layer	0.12	
			well 4	top layer	0.50	Third
				middle layer	0.40	First
				bottom layer	0.47	Second
			well 7	top layer	0.94	Second
				middle layer	0.83	First
				bottom layer	0.94	Second

In each case, even for the well 7 near the pumping well, the xanthan injection ensures a better sweep of porous medium through the three sand layers, due to a displacement front more stable and straighter. The breakthrough of tracers at each sampling well occurs practically at the same time through the three sand layers with the same velocity. The benefic effect of the xanthan gum on the sweep is so confirmed. The xanthan gum ensures a better sweep through the porous medium compared to a water injection by reducing the flow in the coarse layer (more permeable) and by increasing the flow in the finer layers

99

(less permeable). However, like during water injection, the front advancement is slightly faster in the middle layer (medium sand), due to a flow rate more important and a higher permeability.

For the well 1, well 4 and well 7, the upward and downward fronts are straight in the three sand layers, indicating stable fronts. At well 1, there is no delay at the arrival of xanthan in the three layers. At well 4, xanthan solution arrives earlier in the middle layer compared to the top and the bottom layers (with a delay of 0.1 pore volume), where the front advances simultaneously because the breakthrough of the front in the middle layer occurs before those of two other layers. At the well 7, 250 mg/L xanthan solution bank circulating in the middle layer is thinner compared to water injection in the same middle layer and in the two others sand layers. The delay is more important at the outlet of 250 mg/L xanthan solution bank. The use of polymer allows to sweep the well 7 whereas the water injection cannot do it. However, there is a kick off at the end of the curve. This can be explained by the late arrival of the xanthan solution circulating near walls and/or flooding at the back of the injection well. The three-layer sand tank test also showed that the wells installed deeper than the injection and the pumping wells (wells 8 and 9) were also swept with xanthan injection.

Table 4.17 summarizes the sweep efficiency for water and 250 mg/L xanthan solution injections.

Table 4.17: Breakthrough in the three-layer sand tank for water and 250 mg/L xanthan solution

		Vp at breakthrough for water injection	Vp at breakthrough for 250 mg/L xanthan injection
well 1	Top	0.23	0.12
	Middle	0.12	0.12
	Bottom	0.27	0.12
well 4	Top	0.32	0.50
	Middle	0.22	0.40
	Bottom	0.68	0.47
well 7	Top	Not swept	0.94
	Middle	0.46	0.83
	Bottom	Not swept	0.94

Figure 4.22 shows a comparison of breakthrough curves at the pumping well for water injection (1.0 Vp of tracer followed by 8.0 Vp of water without tracer) and the injection of two first xanthan solutions at 250 mg/L (with chloride tracer) and 500 mg/L (without chloride tracer) (for a total of 2.72 Vp).
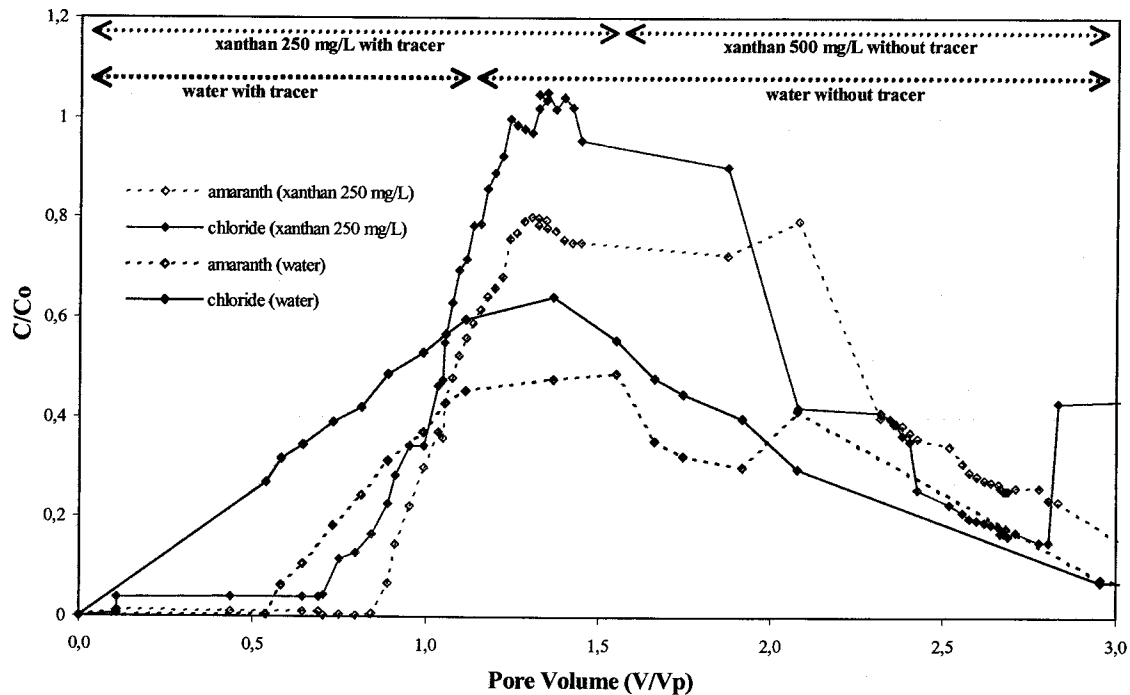
Figure 4.22: Comparison of tracers breakthrough at the pumping well between water injection and the two first xanthan solutions at 250 mg/L and 500 mg/L

The sweep with xanthan solutions is more effective compared to water injection as showed previously, due to the sweep of the three layers and a straighter displacement front. The tracers concentration reaches also a maximum value with the xanthan compared to water and so, there is not mass loss with the xanthan solutions. At the opposite, with water injection, a dilution of solutions with tracers can occurs. During the injection of 250 mg/L xanthan solution, the width of the non-diluted front is equal to 0.3 pore volume compared to 1.6 pore volumes injected. Therefore, a dilution effect is created by the different arrival times of the xanthan solution in the three sand layers. The displacement front of 250 mg/L xanthan solution is straight compared to a water injection, indicating a stable front. The results confirm the efficiency of the xanthan gum on the sweep of porous media.

Figure 4.23 shows the tracers breakthrough (bromides and chlorides) at the pumping well during the injection of xanthan solutions of 250 mg/L (chlorides), 500 mg/L (bromides), the second xanthan solution at 250 mg/L (chlorides) and finally water without tracer.
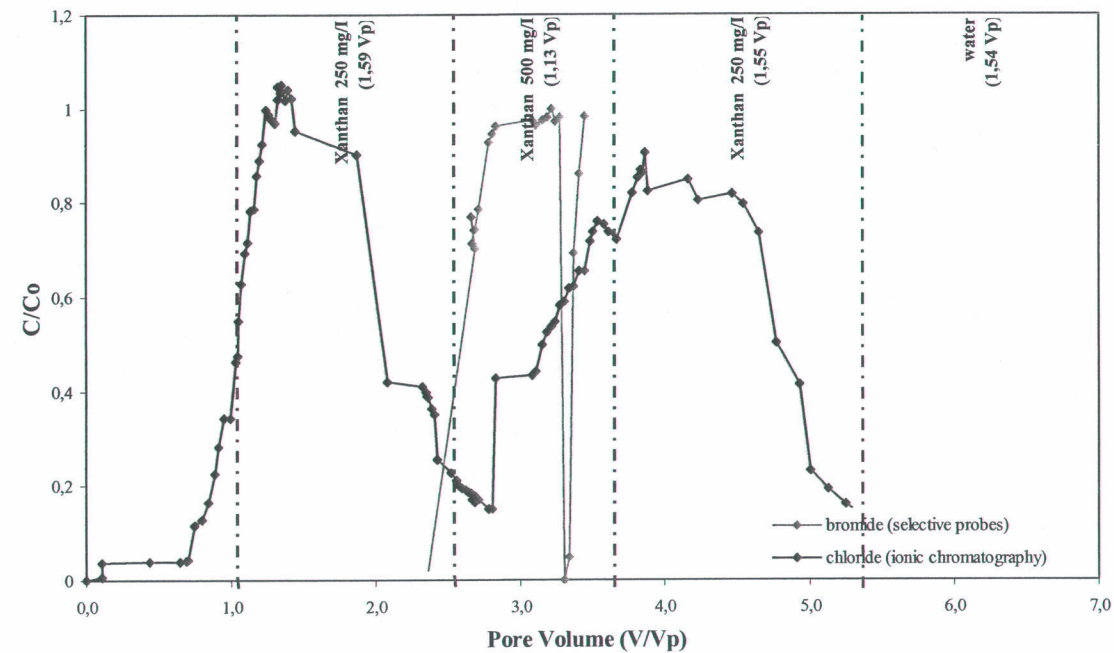
Figure 4.23: Tracers breakthrough at pumping well for the three xanthan injections and water

During the first xanthan injection at 250 mg/L (1.59 Vp), the chloride concentration increases at the pumping well with a sharp displacement front. With the xanthan solution injection at 500 mg/L (1.13 Vp) including the bromide tracer, the xanthan solution at 250 mg/L is pushed to the outlet tank and so, the chloride concentration tends to decrease. In parallel, the bromide concentration increases. During the second xanthan solution at 250 mg/L (1.55 Vp), the sweep is also present but with a broader displacement front showing more dispersion. As the xanthan solution of 250 mg/L is less viscous than the xanthan solution at 500 mg/L, viscous fingering is expected between the two fluids due to viscosity contrasts. The xanthan solution at 250 mg/L tends to flow through the tank by preferential ways without sweeping the entire sand tank. This is also indicated by the early arrival of the second 250 mg/L xanthan bank on the 500 mg/L xanthan solution containing the bromide tracers. Finally, after the water injection, almost all the tracers are absent.

Displacement front advancement

Figures 4.24 represents the displacement front advancement for the chloride tracer through the sand tank for the three sand layers during water injection compared to the different xanthan solutions.
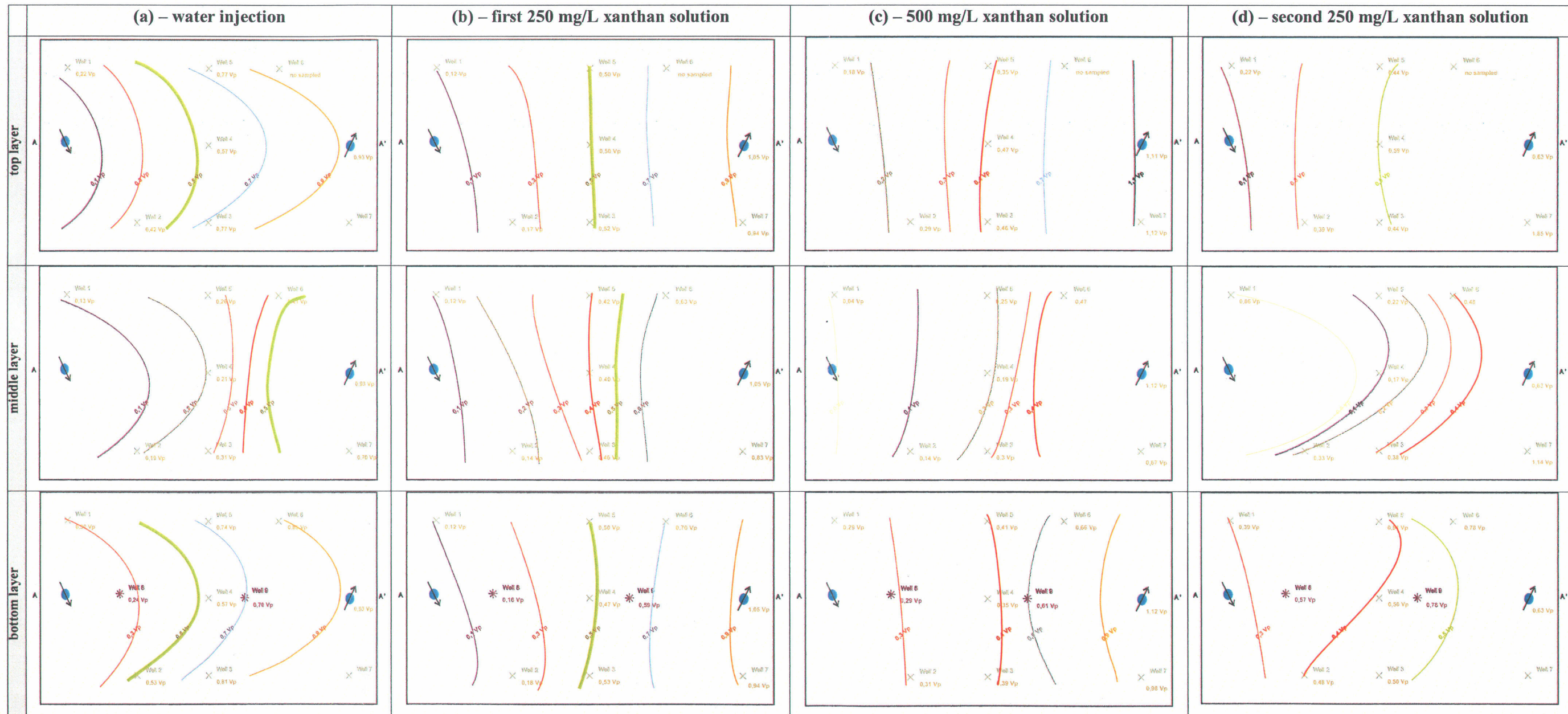
Figure 4.24: Comparison of front advancement in view areal in the three sand layers between (a) water injection, (b) the first xanthan injection at 250 mg/L, (c) the xanthan injection at 500 mg/L and (d) the second xanthan injection at 250 mg/L

The sweep of porous medium with the first xanthan solution at 250 mg/L is more effective through the three sand layers than with water, due to a displacement front more stable, straighter and more uniform (Figure 4.24a and Figure 4.24b). The xanthan solution allows a better circulation through the fine layers (in the top and bottom layers) and slows down the circulation in the coarse layer (in the middle layer) as shown in Figure 4.25.
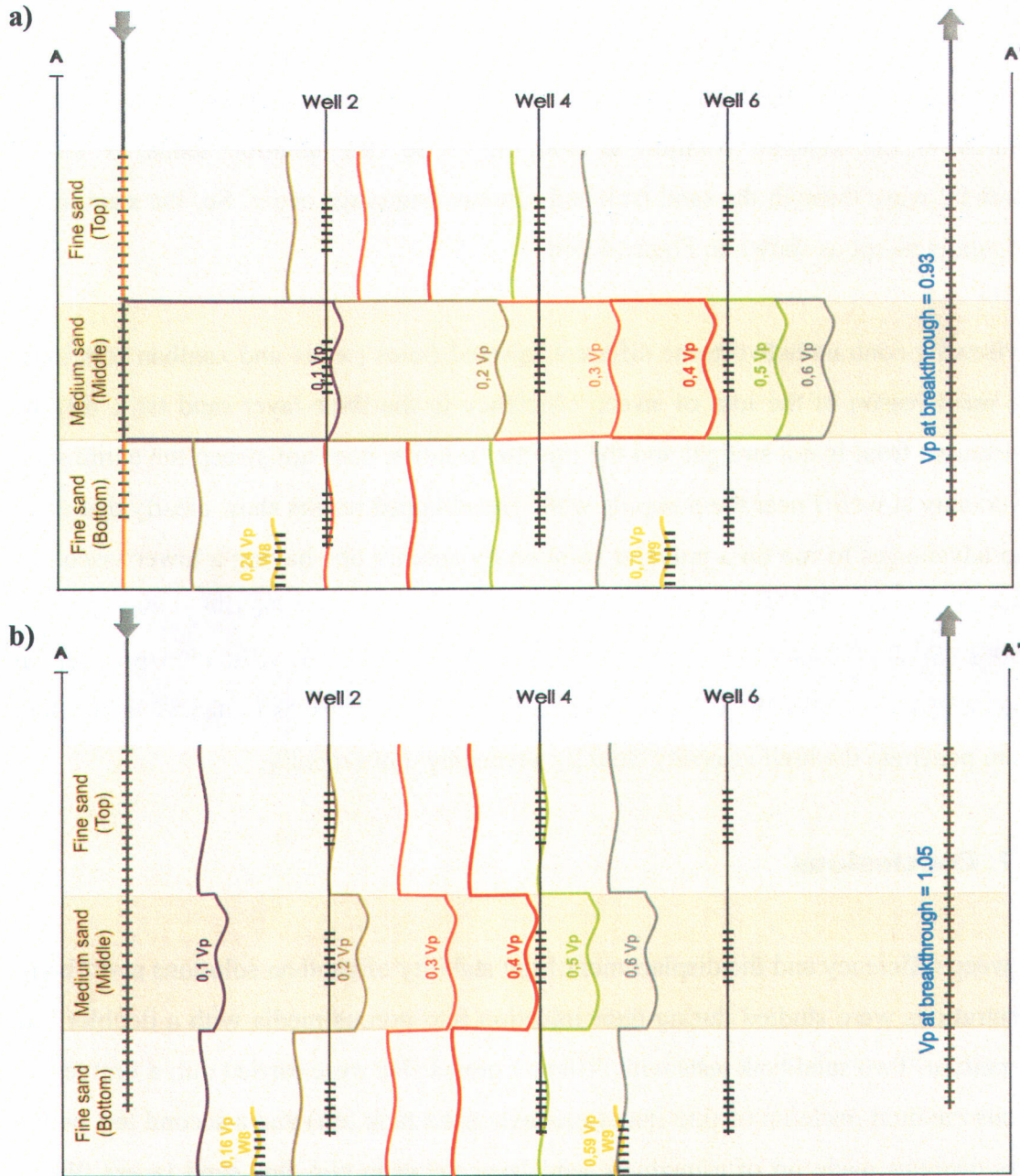
Figure 4.25: Comparison of front advancement in the three-sand layers between (a) water injection and (b) the first xanthan injection at 250 mg/L

The xanthan solution at 500 mg/L ensures also an effective sweep of the porous medium through the three sand layers, due to a higher viscosity as shown in Figure 4.24c. The displacement front through each layer is very straight and so effective, even for the well 7 near the pumping well. Nevertheless, the front arriving to the pumping well is slightly curved, due to the effect of pumping.

Finally, with the second xanthan injection at 250 mg/L, the displacement front is much less vertical than the two others xanthan injections because the solution is less viscous compared to the xanthan solution at 500 mg/L. So, the solution tends to follow preferential ways through the sand tank and viscous fingerings occur. So, the sand thank is not totally swept as shown in Figure 4.24d.

The viscosity contrast between the different injected fluids (water and xanthan solutions) is the main reason of the loss of sweep efficiency in the three-layer sand tank. So, the displacement front is not straight and the injected solution does not sweep the entire sand tank, notably at well 7 near the pumping well. The obtained results show clearly that there are no advantages to run on a polymer solution by another one having a lower viscosity. Displacement front instabilities due to viscosity contrasts between the two injected solutions (500 mg/L and the second 250 mg/L) bring problems related to preferential viscous fingering. Under these instability conditions, the low viscosity displacement fluid tends to penetrate the high viscosity fluid by advancing more rapidly.

4.2.7. Conclusions

The sweep efficiency and the displacement front stability of xanthan solutions at different concentrations were studied during their injection into porous media with a doublet line drive pattern. Two sand tank tests with different grains size were carried out: a first test in a porous medium made up of fine sand (one-layer sand tank test) and a second test with a porous medium made up of a medium sand layer between two fine sand layers (three-layer sand tank test). In the one-layer sand tank, two tests were realized: i) one first test with water injection at different flow rates and ii) one second test with a xanthan solution

at 100 mg/L, followed by two xanthan solutions at 250 mg/L. Chloride and bromide tracers added in the different injected solutions were used to evaluate their breakthrough and so, their sweep efficiency through a homogeneous porous medium. For the three-layer sand tank, two tests were made: i) one first test with water injection and ii) one second test with a xanthan solution at 250 mg/L, followed by a xanthan solution at 500 mg/L, followed by a second xanthan solution of 250 mg/L and finally, a water injection to complete the experiment. Many tracers were also used and added to injection solutions (chlorides, bromides and amaranth). The amaranth was more employed to facilitate the visual follow up of front advancement. Many observation wells were installed at different positions in the sand tank to evaluate the sweep efficiency and the displacement front stability on the entire tank surface as a function of grain sizes and depth. All the tests were done at constant head.

The sand tank tests confirmed the role of xanthan gum on the sweep. In fact, the geological formation is better swept with a xanthan solution than with water, due to a stable, uniform and vertical displacement front. Nevertheless, the realization of these sand tank tests showed that the configuration of porous medium (heterogeneity, etc.) and the injection/pumping strategy used influence hardly the sweep, leading to a incomplete sweep. The injection/pumping strategy with one injection well and one pumping well aligned at each end of the sand tank showed the limits of the set up, avoiding to obtain a complete sweep. However, the sweep is still more difficult being given that the injection and the pumping wells do not reach the base of the sand tank.

In the one-layer sand tank test, the sweep efficiency of water varies between 64 and 75 % even though the sweep with xanthan solution is of 84 %, meaning that xanthan gum is more effective. Nevertheless, the sweep is not complete and some zones, notably at ends of sand tank, are not swept (estimated between 10 % and 20 %), due to a wall effect. This incomplete sweep is confirmed by the fact that the tracers breakthrough (at $C/C_0 = 0.5$) is observed before the injection of one pore volume.

For the three-layer sand tank test, the sweep is more effective with xanthan solutions than with water injection, confirming the results in the one-layer sand tank. The breakthrough of tracers at each sampling well occurs practically at the same time through the three sand layers compared to water injection. The benefic effect of the xanthan gum on the sweep is so confirmed. With water injection, some zones, principally in the fine layers, are poorly swept, notably for a well near the pumping well (well 7). That can be explained by the fine sand texture where the flow rate is lower than in the coarse sand layer. A wall effect can also be the reason. The water solution is pumped before that it has reached really the observation well. However, the sweep efficiency at the pumping well (at $C/C_0 = 0.5$) reaches almost 100 %, due notably to the fact that the pumping well is aligned with the injection well and that the majority of the injected solution flows through the middle layer of the sand tank. With xanthan injection, all sampling wells are swept, even the wells situated deeper than the injection and the pumping wells (wells 8 and 9).

During the injection of different xanthan solutions at various concentrations, the sweep of porous medium with the first xanthan solution at 250 mg/L is more effective through the three sand layers than with water. That is explained by the formation of a displacement front more stable, straighter and more uniform. The xanthan solution allows a better circulation through the fine layers (in the top and bottom layers) and slows down the circulation in the coarse layer (in the middle layer). The xanthan solution at 500 mg/L ensures also an effective sweep of the geological formation through the three sand layers, due to a higher viscosity. The displacement front through each sand layer is very straight even for the well 7 near the pumping well. Finally, with the second xanthan injection at 250 mg/L, the displacement front is much less vertical than with the 500 mg/L xanthan solution because the solution is less viscous. So, the second 250 mg/L xanthan solution tends to follow preferential ways through the sand tank and preferential viscous fingerings occur, leading a incomplete sweep of the tank. Under these instability conditions, the low viscosity of displacement fluid tends to penetrate the fluid of high viscosity by advancing more rapidly. These viscosity contrasts between the different injected fluids is the main reason of the loss of sweep efficiency in the sand tank.

Consequently, there are no advantages to flush a polymer solution by another one having a lower viscosity.

Concerning the different tracers used to evaluate the front advancement and the sweep efficiency, the chlorides and bromides are more suitable than amaranth. In fact, the advancement of the displacement front between the chlorides tracer and amaranth is slightly different. The samples containing chlorides tracer are collected before the samples containing amaranth (the delay factor for amaranth varies between 1.1 and 1.3 compared to chlorides tracer). That can be explained by the fact that the amaranth has a organic chemical structure which tends to form hydrogen links between these oxygen atoms and the water molecules present in the pores of porous medium. This leads to a decrease of amaranth concentration during its injection and consequently, it undergoes a mass loss. However, in each test, notably in the pumping well, the maximum concentration of tracers is not reached because the pumped solution comes directly from the three layers and as the front advancement is different according to the grains size (faster in the coarse medium sand), a dilution of injected solutions can occur during their way through the sand tank.

For the future, all the results indicated that xanthan gum could be injected at larger scale in non consolidated sandy media by keeping the low temperature, similar at field conditions. The xanthan gum could also be added to washing solutions during the flushing process of the porous media for the remediation of contaminated aquifers. However, triangular sand tank tests could be carried out to study the radial effect of an injection well for different solutions (water and xanthan gum). Other tests in sand tank could also be performed by varying the injection/pumping strategy and/or by playing on the distance between the injection and the pumping wells. As the xanthan is biodegradable and no toxic, no environmental problems can occur.

4.2.8. References

AATDF 1997. Technology practices manual for surfactants and cosolvents, AATDF rapport TR-97-2, Rice University (Houston, USA).

Bear J. 1972. Dynamics of fluids in porous media, American Elsevier Pub. Co. (New York, USA), 764 pp.

Chauveteau G. and N. Kohler 1980. Influence of microgels in xanthan polysaccharide solutions on their flow through various porous media, 55th Annual Fall Technical Conference and Exhibition of the SPE of AIME (Dallas, TX, USA), SPE 9295, 1-13.

Chauveteau G. and A. Zaitoun 1981. Basic rheological behavior of xanthan polysaccharide solutions in porous media: Effects of pore size and polymer concentration, European Symposium on Enhanced Oil Recovery (Bournemouth, England), 197-214.

Chen C.S.H. et E.W. Sheppard 1979. Conformation and hydrolytic stability of polysaccharide from *Xanthomonas campestris*, Journal of Macromolecular Science and Chemistry, 2, (13), 239-259.

Fetter C.W. 1988. Applied Hydrogeology, second edition, Merrill Publishing Company, (Ohio, USA).

Freeze R.A. and J.A. Cherry 1979. Groundwater, Prentice Hall Inc., Englewood Cliffs, (New Jersey, USA).

Garcia-Ochoa F., V.E. Santos, J.A. Casas and E. Gomez 2000. Xanthan gum: production, recovery and properties, Biotechnology Advances, 18, 549-579.

Gogarty W.B. 1967. Mobility control with polymer solutions, Society of Petroleum Engineers Journal, 7, (2), 161-173.

Hébert A. 1998. Etude du comportement des fluides lors d'un essai de décontamination in situ à l'aide d'une solution tensioactive à l'Assomption, Québec, Mémoire pour l'obtention du grade de maître ès sciences, Août, Département de géologie et génie géologique, Université de Laval, (Québec, Canada).

Hornof V. and N.R. Morrow 1987. Gravity effects in the displacement of oil by surfactant solutions, Reservoir Engineering Society of Petroleum Engineers, 2, (4), 627-633.

Jeanes A.R., J.E. Pittsley and F.R. Senti 1961. Polysaccharide B-1459: A new hydrocolloid polyelectrolyte produced from glucose by bacterial fermentation, Journal of Applied Polymer Science, **5**, 519-26.

Lake L.W. 1989. Enhanced oil recovery, Prentice-Hall Inc, (New Jersey, USA), 550 pp.

Mackay D.M. and J.A. Cherry 1989. Groundwater contamination: pump-and-treat remediation, Environment Science Technology, **23**, (6), 630-636.

Laliberté D. et P. Aubé 2002. Les sols contaminés, Centre de santé publique de la région de Québec, Ministère de l'Environnement et de la Faune du Québec (http://ecoroute.uqcn.qc.ca/envir/sante/1_m7.htm).

Lide D.R 2000. CRC Handbook of Chemistry and Physics, 81st Edition 2000-2001, CRC Press LLC (Florida, USA).

Martel K.E. 1995. Utilisation de solutions de polymères pour améliorer l'efficacité de balayage des solutions tensioactives développées pour la restauration d'aquifères contaminés aux hydrocarbures immiscibles lourds, Mémoire pour l'obtention du grade de maître ès sciences, Décembre, Département de géologie et génie géologique, Université de Laval, (Québec, Canada).

Martel K.E., R. Martel, R. Lefebvre and P.J. Gélinas 1998. Laboratory study of polymer solutions used for mobility control during in situ NAPL recovery, Groundwater Monitoring and Remediation, **18**, (3), 103-113.

Martel R. and P.J. Gélinas 1996. Surfactant solutions developed for NAPL recovery in contaminated aquifers, Groundwater, **34**, 143-154.

Martel R., A. Hébert, R. Lefebvre, P.J. Gélinas and U. Gabriel 2004. Displacement and sweep efficiencies in a DNAPL recovery test using micellar and polymer solutions injected in a five-spot pattern, Journal of Contaminant Hydrology, **75**, 1-29.

Pankow J.F. and J.A. Cherry 1996. Dense chlorinated solvents and other DNAPL in groundwater, Waterloo Press, (Portland, USA), 522 pp.

Robert T., R. Martel, S.H. Conrad, R. Lefebvre and U. Gabriel 2006. Visualization of TCE recovery mechanisms using surfactant polymer solutions in a two-dimensional heterogeneous sand model, Journal of Contaminant Hydrogeology, **86**, 3-31.

Roubroeks J.P., R. Andersson, D.I. Mastromauro, B.E. Christensen and P. Aman 2001. Molecular weight, structure and shape of oat (1→3), (1→4)-β-d-glucan fractions

obtained by enzymatic degradation with $(1\rightarrow4)$-β-d-glucan 4-glucanohydrolase from Trichoderma reesei, Carbohydrate Polymers, **46**, (3), 275-285.

Sandiford B.B. 1977. flow of polymers through porous media in relation to oil displacement. in: improved oil recovery by surfactant and polymer flooding. Shah, D.O. and Schechter R.S. (eds.). Academic Press inc., New-York, USA, 487-509.

Szabo M.T. 1975b. Laboratory investigation of factors influencing polymer flood performance, Society of Petroleum Engineers Journal, **15**, (4), 338-346.

CHAPITRE 5
Conclusions et recommandations

$\mathcal{Ce}$e projet de recherche visait à étudier le comportement de la gomme de xanthane lors de son injection en milieux poreux. La caractérisation physique du polymère en solution aqueuse a été réalisée à l'aide de tests en colonne de sable (de granulométrie variable) pour en évaluer son comportement rhéofluidifiant. Des mesures de viscosité *in situ* en fonction du taux de cisaillement ont permis de confirmer son comportement rhéologique spécifique. D'autres tests à l'échelle intermédiaire en bac de sable rectangulaire ont permis d'évaluer l'efficacité de balayage de solutions de xanthane à différentes concentrations ainsi que la stabilité de front de déplacement.

Les tests en colonne de sable ont confirmé le comportement rhéofluidifiant de la gomme de xanthane: la viscosité tend à diminuer avec le taux de cisaillement. Pourtant, ce comportement rhéologique n'est plus respecté pour des taux de cisaillement plus importants. La viscosité a tendance dès lors à augmenter progressivement, causée par un colmatage du milieu poreux. Une accumulation de polymère au sein de la colonne est la principale cause de ce colmatage. Un autre essai en colonne de sable mettant en œuvre une solution de xanthane préalablement cisaillée par passage à travers un bac de sable et

une solution de xanthane intacte a démontré que le pré-cisaillement avait une influence négative sur les propriétés du polymère. En effet, le xanthane perd en partie ses propriétés rhéologiques particulières, due possiblement à une modification de la structure chimique de la gomme de xanthane par une rupture des chaînes, une adsorption du polymère à la surface des grains de sable du bac, un piégeage mécanique dans le bac ou encore une dilution par l'eau présent initialement au niveau des pores du bac. Un dernier essai en colonne de sable a consisté à injecter une solution de xanthane durant trois cycles à débits variables (augmentation – diminution – augmentation). Ce test a permis de mettre en évidence l'effet d'hystérésis ou de "mémoire" de la gomme de xanthane pendant les trois cycles d'injection.

Les essais en bac de sable rectangulaire ont permis d'évaluer l'efficacité de balayage de la gomme de xanthane et la stabilité du front de déplacement lors de son injection en milieu poreux. Un premier essai en bac de sable composé d'une seule couche de sable fin a permis de confirmer que la gomme de xanthane assurait un meilleur balayage de la formation géologique par rapport à une injection d'eau. Ceci est dû notamment à un front de déplacement plus stable et vertical. Aucun phénomène de colmatage n'est d'ailleurs observé. Un second essai en bac de sable dans lequel trois couches de sable (une couche de sable grossier entre deux couches de sable fin) ont été déposées, a permis d'évaluer l'effet du balayage à travers les trois couches de perméabilité différente. Le suivi du front de déplacement a été possible à l'aide de traceurs (chlorures, bromures et amarante). La gomme de xanthane assure un meilleur balayage à travers tout le milieu poreux par rapport à l'eau en réduisant dans un premier temps l'écoulement dans les couches plus grossières (plus perméables) et en augmentant de façon relative l'écoulement dans les couches plus fines (moins perméables). Dans le bac de sable à trois couches, certaines zones sont très peu balayées lors de l'injection d'eau, principalement dans les couches moins perméables, dues notamment à un effet de paroi ou encore à un débit plus faible. Néanmoins, ces problèmes de balayage peuvent être corrigés lors de l'injection de solutions de xanthane. Tous les puits d'échantillonnage sont balayés, notamment ceux à proximité du puits de pompage et ceux situés dans la zone inférieure du bac en profondeur. Dans chaque cas, un balayage plus rapide à travers la couche grossière est

observé, du à un débit plus important, notamment grâce à une perméabilité plus élevée. Enfin, pour les différents traceurs utilisés, les traceurs à chlorures et bromures s'est avéré être les meilleurs par rapport à l'amarante qui subit un certain retard (facteur de retard de 1.1 à 1.3). Ceci peut être expliqué par la structure chimique organique de l'amarante. Ce traceur a été davantage utilisé pour sa coloration rouge assurant un suivi visuel de l'essai et du front de déplacement.

Dans le futur, la gomme de xanthane pourra être ajouté aux solutions de lavage pour la réhabilitation des aquifères contaminés. Néanmoins, d'autres essais à l'échelle intermédiaire seraient fortement recommandés, notamment des tests en bac de sable triangulaire permettant d'évaluer l'effet radial des solutions injectées. Un système "line drive" composé de trois puits d'injection alignés pourrait également permettre d'augmenter le balayage du milieu poreux. Tout en connaissant les limites rencontrés lors des essais en colonne de sable (colmatage et dégradation des propriétés rhéologiques du polymère), il est possible de minimiser ces problèmes pour les travaux à plus grande échelle en jouant notamment sur le débit d'injection, la distance entre les puits d'injection et de pompage, le diamètres des puits mis en place ou encore le temps de séjour de la solution de polymère dans le milieu poreux.

BIBLIOGRAPHIE

Abdul A.A. et T.L. Gibson 1991. Laboratory studies of surfactant-enhanced washing of biphenyl from sandy material, Environnement Science Technology, **25**, (4), 665-671.

AATDF 1997. Technology practices manual for surfactants and cosolvents, AATDF rapport TR-97-2, Rice University (Houston, USA).

Bai G., M. L. Brusseau et R. M. Miller 1997. Biosurfactant - enhanced removal of residual hydrocarbon from soil, Journal of Contaminant Hydrology, **25**, 157-170.

Bear J. 1972. Dynamics of fluids in porous media, American Elsevier Pub. Co. (New York, USA), 764 pp.

Bettahar M., G. Schafer et M. Baviere 1999. An optimized surfactant formulation for the remediation of diesel oil polluted sandy aquifers, Environnement Science Technology, **33**, (8), 1269-1273.

Blais B. 2001. 3000 sites urbains à décontaminer au Canada, La science au Québec, (http://www.sciencepresse.qc.ca).

Boon J.A. 1984. Chemistry in enhanced oil recovery - an overview, Journal of Canadian Petroleum, Technology January-February, (Montreal, Canada), 59-65.

Boving T.B. et M.L. Brusseau 2000. Solubilization and removal of residual trichloroethene from porous media: Comparison of several solubilization agents, Journal of Contaminant Hydrology, **42**, 51-67.

Boyd G.R. et K.J. Farley 1990. NAPL removal from groundwater by alcohol flooding: Laboratory studies and application, Environmental Systems Engineering, Clemson University, (South Carolina, USA), **26**, 437-460.

Brandes D. et K.J. Farley 1993. Importance of phase behavior on the removal of residual DNAPLs from porous media by alcohol flooding, Water Environment Research, **65**, (7), 869-878.

Casas J.A. et F. Garcia-Ochoa 1999. Viscosity of solutions of xanthan/locust bean gum mixtures, Journal of Scientific Food Agriculture, **79**, 25–31.

Chapelle F.H. 1993. Groundwater microbiology and geochemistry, John Wiley and Sons Inc., (New York, USA), 424 pp.

Chauveteau G. et N. Kohler 1980. Influence of microgels in xanthan polysaccharide solutions on their flow through various porous media, 55th Annual Fall Technical Conference and Exhibition of the SPE of AIME (Dallas, USA), **SPE 9295**, 1-13.

Chauveteau G. et A. Zaitoun 1981. Basic rheological behavior of xanthan polysaccharide solutions in porous media: Effects of pore size and polymer concentration, European Symposium on Enhanced Oil Recovery (Bournemouth, England), 197-214.

Chen C.S.H. et E.W. Sheppard 1979. Conformation and hydrolytic stability of polysaccharide from *Xanthomonas* campestris, Journal of Macromolecular Science and Chemistry, **2**, (A13), 239-259.

Chen C.S.H. et E.W. Sheppard 1980. Conformation and shear stability of xanthan gum in solution, Polymer Engineering and Science, **20**, (7), 512-516.

Cloutier F.D. 2003. Caractérisation en colonne de sable de polymères pour une utilisation dans le traitement des sols contaminés et analyse de leur stabilité à long terme, Travail de fin d'étude, Avril, Département de géologie et génie géologique, Université de Laval, (Québec, Canada).

Cohen R.M. et J.W. Mercer 1993. DNAPL site evaluation, C.K. Smoley, CRC Press, (Florida, USA).

Cullimore D.R. 1993. Practical manual of groundwater microbiology, Lewis Publishers, Regina Water Research Institute, University of Regina, (Regina, Canada).

Dreher K.D. et W.B. Gogarty 1979. An overview of mobility control in micellar/polymer enhanced oil recovery processes, Journal of Rheology, **23**, (2), 209-229.

Dwarakanath V., K. Kostarelos, G.A. Pope, D. Shotts et H. William 1999. Wade anionic surfactant remediation of soil columns contaminated by non aqueous phase liquids, Journal of Contaminant Hydrology, **38**, (4), 465-488.

Falta R.W. 1998. Using phase diagrams to predict the performance of co-solvent floods for NAPL remediation, **GWMR**, 1-9.

Fetter C.W. 1988. Applied Hydrogeology, second edition, Merrill Publishing Company, (Ohio, USA).

118

Fetter C.W. 1993. Contaminant Hydrogeology, Macmillan Publishing Company, (New York, USA)

Fletcher A.J.P., S.P. Lamb et P.J. Clifford 1992. Formation damage from polymer solutions: Factors governing injectivity, Reservoir Engineering Society of Petroleum Engineers, **7**, (2), 237-246.

Fountain J.C. 1998. Technologies for dense non-aqueous phase liquid source zone remediation, Technology Evaluation Report, **GWRTAC**, E Series: TE-98-02.

Fountain J.C., A. Klimek, M.G. Beikirch et T.M. Middleton 1991. The use of surfactants for in situ extraction of organic pollutants from a contaminated aquifer, Journal of Hazardous Materials, **28**, 295-311.

Freeze R.A. and J.A. Cherry 1979. Groundwater, Prentice Hall Inc., Englewood Cliffs, (New Jersey, USA).

Garcia-Ochoa F., V.E. Santos, J.A. Casas et E. Gomez 2000. Xanthan gum: production, recovery, properties, Biotechnology Advances, **18**, 549–579.

Gregoire F. 1993. Biodégradabilité comparée des butan-1-ol, penta-1-ol, toluène, xylène, éthylbenzène et des trois agents tensioactifs Hostapur SAS 60, Genapol LRO et Phenylsulphonate HRS, Rapport du Ministère de l'Environnement du Québec, Direction de l'Expertise Scientifique, 15 pp.

Gogarty W.B. 1967. Mobility control with polymer solutions, Society of Petroleum Engineers Journal, **7**, (2), 161-173.

Gupta A.D., G.A. Pope, K. Sepehrnoori et M. Shook 1988. Effects of reservoir heterogeneity on chemical enhanced oil recovery, Reservoir Engineering Society of Petroleum Engineers, **3**, (2), 479-488.

Haberman M. 2002. Utilisation d'écailles de cacao pour la récupération du plomb solubilisé lors de la lixiviation chimique de sol contaminé, Travail de fin d'étude pour l'obtention du diplôme d'ingénieur, Juin, Institut supérieur industriel de Bruxelles – Institut national de la recherche scientifique, (Québec, Canada).

Hébert A. 1998. Etude du comportement des fluides lors d'un essai de décontamination in situ à l'aide d'une solution tensioactive à l'Assomption, Québec, Mémoire pour l'obtention du grade de maître ès sciences, Août, Département de géologie et génie géologique, Université de Laval, (Québec, Canada).

Hirasaki G.J et G.A. Pope 1974. Analysis of factors influencing mobility and adsorption in the flow of polymer solutions through porous media, Society of Petroleum Engineers Journal, **14**, (4), 337-346.

Hornof V. et N.R. Morrow 1987. Gravity effects in the displacement of oil by surfactant solutions, Reservoir Engineering Society of Petroleum Engineers, **2**, (4), 627-633.

Huang Y. et K.S. Sorbie 1992. The Adsorption and in-situ rheological behavior of xanthan solution flowing through porous media, SPE/DOE Eight Symposium on Enhanced Oil Recovery (Oklahoma, USA), **SPE/DOE 24153**, 507-520.

Jackson R.E., J.C. Fountain et R.W. Wunderlich 1992. Chemically-enhanced solubilization of DNAPL: Advancing the state of pump-and-treat remediation by injection and withdrawal of biodegradable surfactants, Conférence présentée à the Conference of the Canadian Chapter of the International Association of Hydrogeology "Modern Trends in Hydrogeology", (Ontario, Canada).

Jin M., M. Delshad, V. Dwarakanath, D.C. McKinney, G. Pope, K. Sepehrnoori, C.E. Tilburg et C.E. Jackson 1995. Partitioning tracer test for detection, estimation and remediation performance assessment of subsurface non-aqueous phase liquids, Water Resources Research, **31**, (5), 1201-1211.

King R.B., G.M. Long et J.K. Sheldon 1992. Practical environmental bioremediation, Lewis Publishers, (Florida, USA), 149 pp.

Lake L.W. 1989. Enhanced oil recovery, Prentice-Hall Inc, (New Jersey, USA), 550 pp.

Laliberté D. et P. Aubé 2002. Les sols contaminés, Centre de santé publique de la région de Québec, Ministère de l'Environnement et de la Faune du Québec (http://ecoroute.uqcn.qc.ca/envir/sante/1_m7.htm).

Larson R.G. 1979. The Influence of phase behavior on surfactant flooding, Society of Petroleum Engineers Journal, 411-422.

Larson R.G., H.T. Davids et L.E. Scriven 1981. Displacement of residual non-wetting fluid from porous media, Chemical Engineering Science, **36**, 75-85.

Larson R.G., H.T. Davids et L.E. Scriven 1981. Elementary mechanisms of oil recovery by chemical methods, Society of Petroleum Engineers, **24**, 26-41.

Larson R.G. et G.J. Hirasaki 1978. Analysis of the physical mechanisms in surfactant flooding, Society of Petroleum Engineers Journal, 42-58.

Lecourtier J. et G. Chauveteau 1984. Propagation of polymer slugs through porous media, 59th Annual Technical Conference and Exhibition (Houston, USA), **SPE 13034**, 1-22.

Lefebvre R. 2003. Écoulement multiphase en milieux poreux. Notes de cours. INRS-ETE., (Québec, Canada), 5ème édition.

Lide D.R 2000. CRC Handbook of Chemistry and Physics, 81st Edition 2000-2001, CRC Press LLC (Florida, USA).

Lowe D.F., C.L. Oubre et C.H. Ward 1999. Surfactants and co-solvents for NAPL remediation, A Technology Practices Manual, Lewis Publishers, Rice University, (Texas, USA), 412 pp.

Mccray J.E., G. Bai, R.M. Maier et M.L. Brusseau 2001. Biosurfactant - enhanced solubilization of NAPL mixtures, Journal of Contaminant Hydrology, **48**, 45-68.

Mackay D.M. et J.A. Cherry 1989. Groundwater contamination: Pump-and-treat remediation, Environment Science Technology, **23**, (6), 630-636.

Martel K.E. 1995. Utilisation de solutions de polymères pour améliorer l'efficacité de balayage des solutions tensioactives développées pour la restauration d'aquifères contaminés aux hydrocarbures immiscibles lourds, Mémoire pour l'obtention du grade de maître ès sciences, Décembre, Département de géologie et génie géologique, Université de Laval, (Québec, Canada).

Martel K.E., R. Martel, R. Lefebvre et J.P. Gélinas 1998. Laboratory Study of Polymer Solutions used for Mobility Control during in situ NAPL Recovery, Groundwater Monitoring and Remediation, **18**, (3), 103-113.

Martel R. 1996. Développement de solutions tensioactives pour la récupération de phases liquides non aqueuses à saturation résiduelle dans les aquifères, Thèse pour l'obtention du grade de Philosophiae Doctor, Septembre, Département de géologie et de génie géologique, Université de Laval, (Québec, Canada).

Martel R. et P.J. Gélinas 1993. Phase diagrams to optimize surfactants solutions for oil and DNAPL recovery in aquifers, Groundwater, **31**, (5), 789-800.

Martel R. et P.J. Gélinas 1996. Residual diesel measurement in sand columns after surfactant/alcohol washing, Groundwater, **34**, (1), 162-167.

Martel R. et P.J. Gélinas 1996. Surfactant solutions developed for NAPL recovery in contaminated aquifers, Groundwater, **34**, 143-154.

Martel R., P.J. Gélinas et J.E. Desnoyers 1998a. Aquifer washing by micellar solutions: 1 -Optimization of alcohol/surfactant/solvent solutions, Journal of Contaminant Hydrology, **29**, 319-346.

Martel R., P.J. Gélinas et L. Saumure 1998c. Aquifer washing by micellar solutions: 3 - Field test at the Thouin Sand Pit (Québec, Canada), Journal of Contaminant Hydrology, **30**, 33-48.

Martel R., A. Hébert, R. Lefebvre, P.J. Gélinas et U. Gabriel 2004. Displacement and sweep efficiencies in a DNAPL recovery test using micellar and polymer solutions injected in a five-spot pattern, Journal of Contaminant Hydrology, (Sous Presse).

Martel R., R. Lefebvre et P.J. Gélinas 1998b. Aquifer washing by micellar solutions: 2 -DNAPL recovery mechanisms for an optimized alcohol/surfactant/solvent solution, Journal of Contaminant Hydrology, **30**, 1-30.

Morrow N.R. 1979. Interplay of capillary, viscous and buoyancy forces in the mobilization of residual oil, Journal of Canadian Petroleum Technology, **18**, 35-46.

Mungan N. 1969. Rheology and adsorption of aqueous polymer solutions, Journal of Canadian Petroleum Technology, April-June, 45-50.

NATO/CCMS. 1998. Evaluation of demonstrated and emerging technologies for the treatment and clean up of contaminated land and groundwater: Phase II, final report, Report Number 219, North Atlantic Treaty Organization, EPA/542/R/98/001a, (Washington, USA).

Pennell K.D., L.M. Abriola et W.J. Weber 1993, Surfactant-enhancement solubilization of residual dodecane in soil columns: 1 - Experimental Investigation, Environnement Science Technology, **27**, (12), 2332-2340.

Pennell K.D., M. Jin, L.M. Abriola et G.A. Pope 1994. Surfactant enhanced remediation of soil columns contaminated by residual tetrachloroethylene, Journal of Contaminant Hydrology, **16**, 35-53.

Peters R.W., E.J. Saint-Martin, R.K. Rothmel et M.F. DeFlaun 1998. Surfactant foam/biaugmentation technology for in situ treatment of TCE-DNAPLs, Environment Science Technology, **32**, (11), 1667-1675.

Phelps T.J., C.B. Fliermans, T.R. Garland, S.M. Pfiffner et D.C. White 1989. Methods for recovery of deep terrestrial subsurface sediments for microbiological studies, Journal of Microbiological Methods, **9**, 267-279.

Quirion F. et J.E. Desnoyers 1984. Effect of alcohols and surfactants on the lowering of the interfacial tension between water and benzene: A correlation with phase diagrams, AOSTRA Journal of Research, **1**, (2), 121-126.

Robert T., R. Martel, S.H. Conrad, R. Lefebvre and U. Gabriel 2006. Visualization of TCE recovery mechanisms using surfactant polymer solutions in a two-dimensional heterogeneous sand model, Journal of Contaminant Hydrogeology, **86**, 3-31.

Roubroeks J.P., R. Andersson, D.I. Mastromauro, B.E. Christensen and P. Aman 2001. Molecular weight, structure and shape of oat (1→3), (1→4)-β-d-glucan fractions obtained by enzymatic degradation with (1→4)-β-d-glucan 4-glucanohydrolase from Trichoderma reesei, Carbohydrate Polymers, **46**, (3), 275-285.

Roy N. 1996. Biodégradation des ingrédients des solutions tensioactives développées pour la restauration d'aquifères contaminés aux hydrocarbures immiscibles lourds, Mémoire pour l'obtention du grade de maître ès sciences, Département de géologie et génie géologique, Université de Laval, (Québec, Canada).

Sabatini D.A., R.C. Knox, J.H. Harwell, T. Soerens, L. Chen, R.E. Brown et C.C. West 1997. Design of a surfactant remediation field demonstration based on laboratory and modeling studies, Groundwater, **35**, (6), 954-963.

Saint-Pierre C. 2001. Etude en laboratoire des mécanismes de récupération du trichloroéthène (TCE) en phase résiduelle lors de l'injection de solutions micellaires dans des sables, Mémoire pour l'obtention du grade de maître ès sciences, Mars, Département INRS-Géoressources, Université de Québec, (Québec, Canada).

Saint-Pierre C., R. Martel, U. Gabriel, R. Lefebvre, T. Robert et J. Hawari 2003. TCE recovery mechanisms using micellar and alcohol solutions: Phase diagrams and sand column experiments, Journal of Contaminant Hydrology, (Sous Presse).

Salter S.J. 1977. The Influence of type and amount of alcohol on surfactant-oil-brine phase behavior and properties, **SPE 6843,** 52ème Annual Fall Technical Conference of the SPE, Octobre, (Denver, USA), CO, 9-12.

Sandiford B.B. 1977. Flow of polymers through porous media in relation to oil displacement: Improved oil recovery by surfactant and polymer flooding. Shah, D.O. and Schechter R.S. (eds.). Academic Press inc., (New-York, USA), 487-509.

Savins. 1969. Non-Newtonian flow through porous media, Industrial and Engineering Chemistry, **61**, (10), 18-47.

Shah D.O. 1979. Surface phenomena in enhanced oil recovery, Plenum Press, (New York, USA and London, England), 874 pp.

Swisher R.D. 1987. Surfactant biodegradation, 2nd ed., Marcel Dekker. Inc., (New York, USA), 1-147.

Szabo M.T. 1975a. Some aspects of polymer retention in porous media using a C^{14} - tagged hydrolyzed polyacrylamide, Society of Petroleum Engineers Journal, **15**, (4), 323-337.

Szabo M.T. 1975b. Laboratory investigation of factors influencing polymer flood performance, Society of Petroleum Engineers Journal, **15**, (4), 338-346.

Tomich J.F., R.L. Dalton, H.A. Deans et L.K. Shallenberger 1973. Single-well tracer method to measure residual oil saturation, Journal of Petroleum Technology, 211-218.

Truchon-Poliard J.G. 2004. Étude sur la Détérioration du polyacrylamide FA 920 SH ST lors d'essais en colonne de sable, Rapport final, Avril, Département de géologie et génie géologique, Université de Laval, (Québec, Canada).

Tuin B.J.W. et M. Tels 1991. Continuous treatment of heavy metal contaminated clay soils by extraction in stirred tanks and in a countercurrent column, Environmental Technology, **12**, 178-190.

USEPA. 1998. Clean up the nation's waste sites: Markets and technology trends, U.S. Environmental Protection Agency, EPA/542/R/96/005, (Washington, USA).

Wagner O.R. et R.O. Leach 1966. Effect of interfacial tension on displacement efficiency, Society of Petroleum Engineers Journal, Conférence présentée à SPE 41st Annual Fall Meeting held in Dallas, (Texas, USA), 335-344.

Wardlaw N.C. 1982. A review of mechanisms of trapping and mobilization of oil in physical models and porous media, unpublished manuscript, University of Calgary, (Alberta, Canada), 40 pp.

West C.C. et J.H. Harwell 1992. Surfactants and subsurface remediation, Environnement Science Technology, **36**, (12), 2324-2330.

Wheat M.R. et R.A. Dawe 1988. Transverse dispersion in slug - mode chemical EOR processes in stratified porous media, Reservoir Engineering Society of Petroleum Engineers, **3**, (2), 466-478.

Wright R.J. et R.A. Dawe 1983. Fluid displacement efficiency in layered porous media mobility ratio influence, Revue de l'Institut français du pétrole, **38**, (4), 455-474.

Wright R.J., M.R. Wheat et R.A. Dawe 1987. Slug size and mobility requirements for chemically EOR within heterogeneous reservoirs, Reservoir Enginnering Society of Petroleum Engineers, **2**, (1), 92-102.

ANNEXES

Annexe A

Mesures de viscosité *in situ* en fonction du taux de cisaillement à 20°C pour différentes concentrations de xanthane (à l'aide d'un rhéomètre Brookfield)

	200 mg/L			250 mg/L	
rpm	Taux de cisaillement (s⁻¹)	Viscosité (cP)	rpm	Taux de cisaillement (s⁻¹)	Viscosité (cP)
0.5	0.612	9.6	0.3	0.3672	14
1	1.224	8.4	0.6	0.7344	11
2	2.448	7.5	1.5	1.836	8
2.5	3.06	7.08	3	3.672	6
4	4.896	6.6	6	7.344	5.1
5	6.12	6.3	12	14.688	4.575
10	12.24	5.43	30	36.72	3.67
20	24.48	4.605	60	73.44	3.145
50	61.2	3.645	-	-	-

	400 mg/L			500 mg/L			1 000 mg/L	
rpm	Taux de cisaillement (s⁻¹)	Viscosité (cP)	rpm	Taux de cisaillement (s⁻¹)	Viscosité (cP)	rpm	Taux de cisaillement (s⁻¹)	Viscosité (cP)
0.5	0.612	19.8		0.612	18.6		0.066	249.95
1	1.224	17.7	1	1.224	17.4	0.5	0.11	180
2	2.448	12.75	2	2.448	16.05	1	0.22	254.9
2.5	3.06	11.9	2.5	3.06	15.25	2	0.44	217.5
4	4.896	10.1	4	4.896	13.85	2.5	0.55	198
5	6.12	9.78	5	6.12	12.75	4	0.88	165
10	12.24	7.77	10	12.24	10.1	5	1.1	159
20	24.48	6.015	20	24.48	7.875	10	2.2	114
50	61.2	4.555	50	61.2	5.585	20	4.4	80.25
100	122.4	3.7	100	122.4	4.385	50	11	50.1
-	-	-	-	-	-	100	22	33.3

Annexe B

Mesures de viscosité *in situ* en fonction du taux de cisaillement à 8°C pour différentes concentrations de xanthane (à l'aide d'un rhéomètre Brookfield)

100 mg/L			200 mg/L			250 mg/L		
rpm	Taux de cisaillement (s^{-1})	Viscosité (cP)	rpm	Taux de cisaillement (s^{-1})	Viscosité (cP)	rpm	Taux de cisaillement (s^{-1})	Viscosité (cP)
0,5	0,612	6	0,5	0,612	12,6	0,5	0,612	15,6
1	1,224	4,9	1	1,224	8,1	1	1,224	11,7
2	2,448	3,8	2	2,448	7,35	2	2,448	9,2
2,5	3,06	3,7	2,5	3,06	6,6	2,5	3,06	8,8
4	4,896	3,3	4	4,896	5,775	4	4,896	7,9
5	6,12	2,9	5	6,12	5,82	5	6,12	7,3
10	12,24	2,6	10	12,24	4,83	10	12,24	6,1
20	24,48	2,5	20	24,48	4,125	20	24,48	5,2
50	61,2	1,95	50	61,2	3,35	50	61,2	4,3
100	122,4	1,8	100	122,4	2,89	100	122,4	3,5

400 mg/L			500 mg/L			1 000 mg/L		
rpm	Taux de cisaillement (s^{-1})	Viscosité (cP)	rpm	Taux de cisaillement (s^{-1})	Viscosité (cP)	rpm	Taux de cisaillement (s^{-1})	Viscosité (cP)
0,5	0,612	23,4	0,5	0,612	33,6	0,5	0,11	569,9
1	1,224	21,6	1	1,224	32,1	1	0,22	554,9
2	2,448	16,95	2	2,448	25,05	2	0,44	427,4
2,5	3,06	16,2	2,5	3,06	23,4	2,5	0,55	377,9
4	4,896	14,15	4	4,896	20	4	0,88	299,9
5	6,12	13,25	5	6,12	18,5	5	1,1	260,9
10	12,24	10,4	10	12,24	13,9	10	2,2	181,5
20	24,48	8,115	20	24,48	10,4	20	4,4	122,25
50	61,2	5,775	50	61,2	7,165	50	11	69,9
100	122,4	4,57	100	122,4	5,51	100	22	45,15

Annexe C

**Courbe granulométrique des différents sables utilisés lors des
essais en colonne de sable et en bac de sable (méthode ASTM
D422-63)**

Sable fin (d$_{50}$ = 0,45 mm)

Maille du filtre (ASTM D422-63)	Maille du filtre (mm)	% de sable retenu	% de sable retenu cumulatif
25	0.71	0.1	0.1
30	0.59	1.9	2
35	0.5	31.5	33.5
40	0.42	36	69.5
50	0.3	26.7	96.2
70	0.21	3	99.2

Sable grossier (d$_{50}$ = 0,87 mm)

Maille du filtre (ASTM D422-63)	Maille du filtre (mm)	% de sable retenu	% de sable retenu cumulatif
14	1.41	0.1	0.1
16	1.19	1.9	2
18	1	16	18
20	0.84	22.8	40.8
25	0.71	32.7	73.5
30	0.59	19.4	92.9
35	0.5	5.7	98.6
40	0.42	0.9	99.5

Annexe D

**Influence de la présence de microgels sur la viscosité d'une
solution de gomme de xanthane à 400 mg/L (d'après Chauveteau
et Kholer, 1980)**

Présence de microgels		Absence de microgels	
Taux de cisaillement (s^{-1})	Viscosité $(Pa.s)$	Taux de cisaillement (s^{-1})	Viscosité $(Pa.s)$
0.5	13	0.6	10
1.2	13	1.3	10
2.6	12	2.7	9.7
5.1	10.5	3.5	9.6
20	7.4	6	9
53	5.7	7.2	8.7
85	5	22	6.8
250	3.4	58	5.2
500	2.7	88	4.6
730	2.3	260	3.2
1 500	1.8	510	2.6
-	-	800	2.2
-	-	910	2.12
-	-	1 510	1.8

Annexe E

Données des essais en colonne de sable et bac de sable

(voir CD-ROM)

L'annexe E présentée sur le CD-ROM regroupe toutes les données se référant aux essais en colonne de sable et en bac de sable. Le CD-ROM est subdivisé en deux grands fichiers: i) essais en colonne de sable et; ii) essais en bac de sable.

Le fichier se rapportant aux **essais en colonne de sable** comporte cinq fichiers Excel, chacun d'entre eux correspondant à un test en colonne différent (Table 3.2). Le chiffrier contenu dans ces feuilles Excel reprend en détail toutes les données nécessaires pour le calcul du débit, des différences de charge hydraulique, de la conductivité hydraulique, du taux de cisaillement et de la viscosité des solutions injectées. Les charges hydrauliques à l'extérieur de la colonne ($\Delta h4$) et dans le sable ($\Delta h2$), la durée de l'essai et les caractéristiques des colonnes de sable (diamètre, longueur, aire, masse de sable, porosité, etc.) sont les paramètres mesurés lors des différents tests en colonne afin de déterminer la viscosité de la gomme de xanthane et évaluer ainsi son comportement rhéofluidifiant.

Le fichier se rapportant aux **essais en bac de sable** se subdivise en deux fichiers: i) le bac de sable à une couche (one-layer sand tank test) et; le bac de sable à trois couches (three-layer sand tank test). Les essais en bac de sable à une couche, comportant trois fichiers Excel, reprennent toutes les données sur l'évolution de la différence de charges hydrauliques et de l'avancement du front de déplacement pour les différentes injections d'eau (à débit variable) et pour l'injection des solutions de xanthane (Table 4.3). Les essais en bac de sable à trois couches comprennent trois fichiers différents: un premier fichier pour le test avec injection d'eau, un second fichier pour le test avec injection des solutions de xanthane à différentes concentrations (ces deux tests sont mentionnés dans le Table 4.4) et enfin un troisième fichier sur la simulation numérique réalisée avec le logiciel UTCHEM. Pour l'essai avec injection d'eau, neuf réservoirs d'eau ont été injectés dans le bac de sable. Le volume injecté pour chacun d'entre eux ainsi que l'évolution de la différence de charge hydraulique entre les puits d'observation OBS 2 et OBS 3 sont notés dans les chiffrier Excel. Le fichier "données traitées" traite de l'efficacité de balayage et de la stabilité du front de déplacement par le dosage des concentrations en traceurs. L'évolution de la conductivité hydraulique durant tout l'essai est également contrôlée. Pour les solutions de xanthane, quatre réservoirs ont été injectés (trois solutions de xanthane et

une injection d'eau pour le rinçage final). Chaque fichier reprend en détail le volume injecté dans le bac, le contrôle du débit durant l'essai et l'évolution de la conductivité hydraulique et de la différence de charge hydraulique entre les puits d'observation OBS 2 et OBS 3. Le dosage des traceurs pour l'évaluation de l'efficacité de balayage et de la stabilité du front de déplacement sont également repris dans le fichier "données traitées". Enfin le fichier de modélisation reprend un mode d'emploi du logiciel ainsi que les données brutes de la simulation (volumes de pore et concentrations du traceur) facilitant la mise en place de la stratégie d'échantillonnage.

Annexe F

Matériel expérimental (colonnes de sable)

Tubes verticaux pour les mesures de charges hydrauliques

Colonne de sable

$\Delta h4$

$\Delta h1$

$\Delta h2$

$\Delta h3$

Pompe péristaltique

Solution de polymère

Laser pour niveau de référence

Colonne de sable
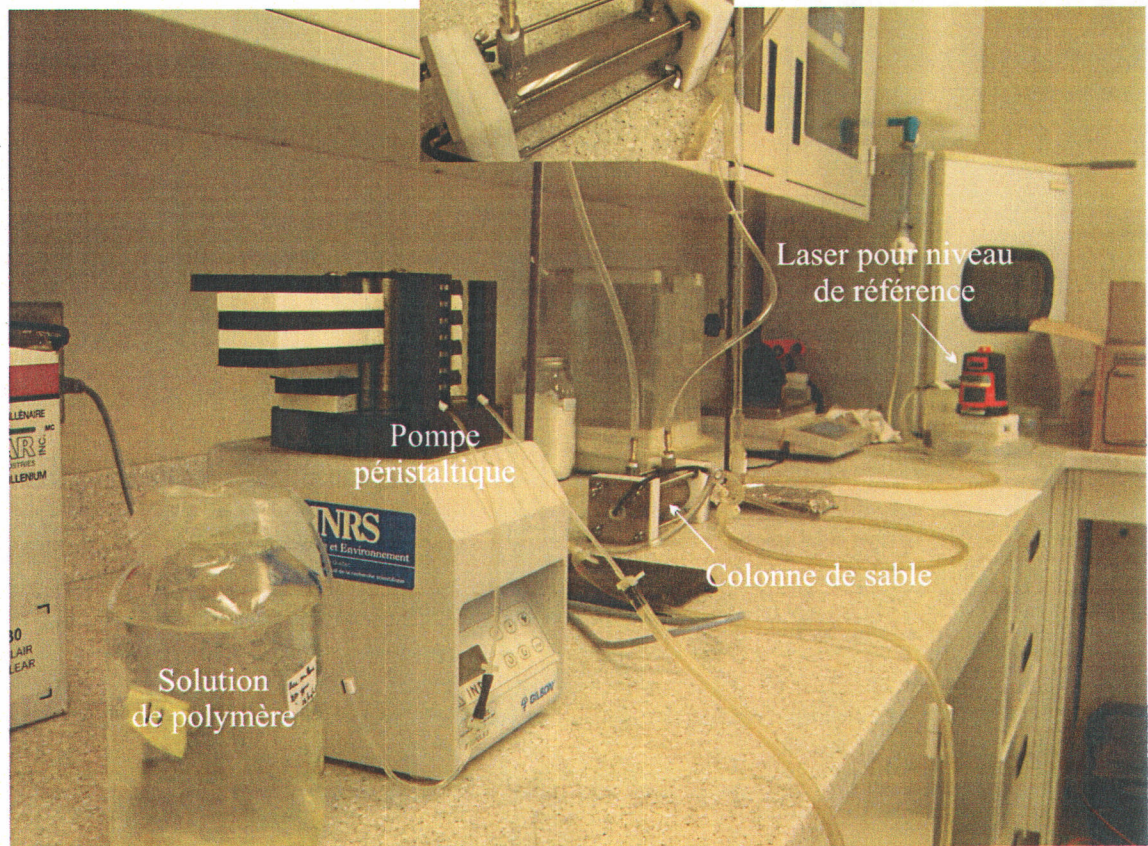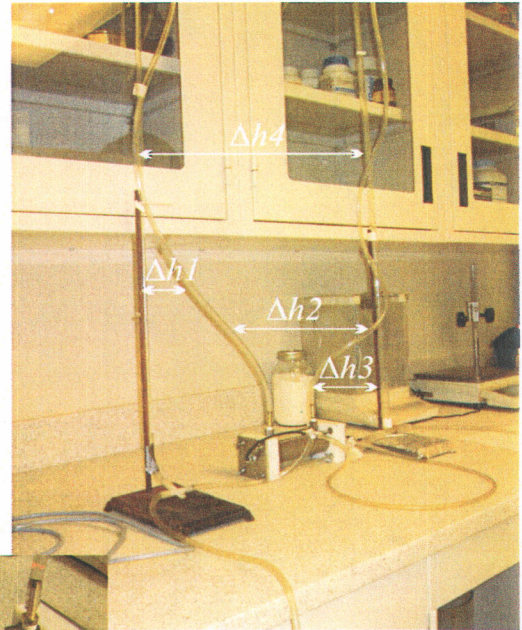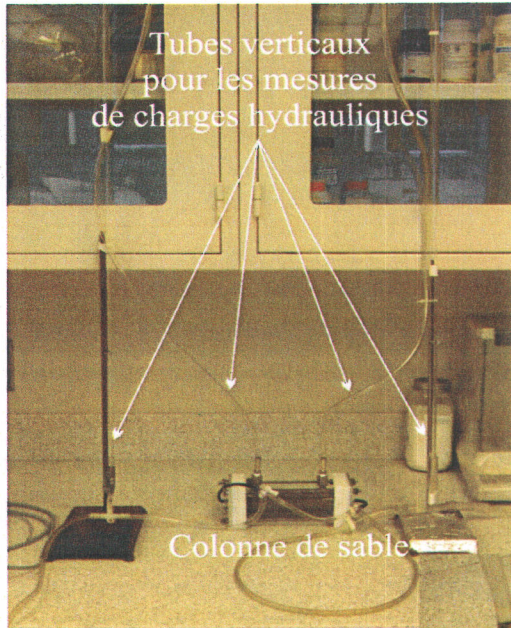
Annexe G

Matériel expérimental (bac de sable)

Tube de pompage

Puits de pompage

Well 7

Well 6

Well 5

OBS 4

Well 4

OBS 3

Well 3

Well 9

OBS 2

Well 2

Well 1

OBS 1

Well 8

Puits d'injection

Bac de sable

Front de déplacement d'une solution de xanthane avec traceur (amarante)

Front de déplacement d'une solution de xanthane avec traceur

Front de déplacement de l'eau sans traceur
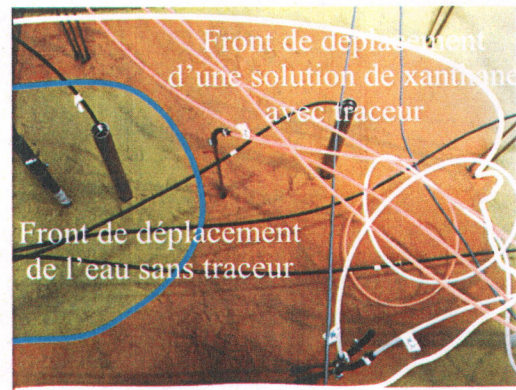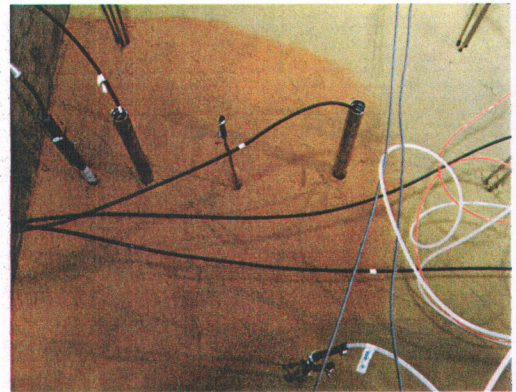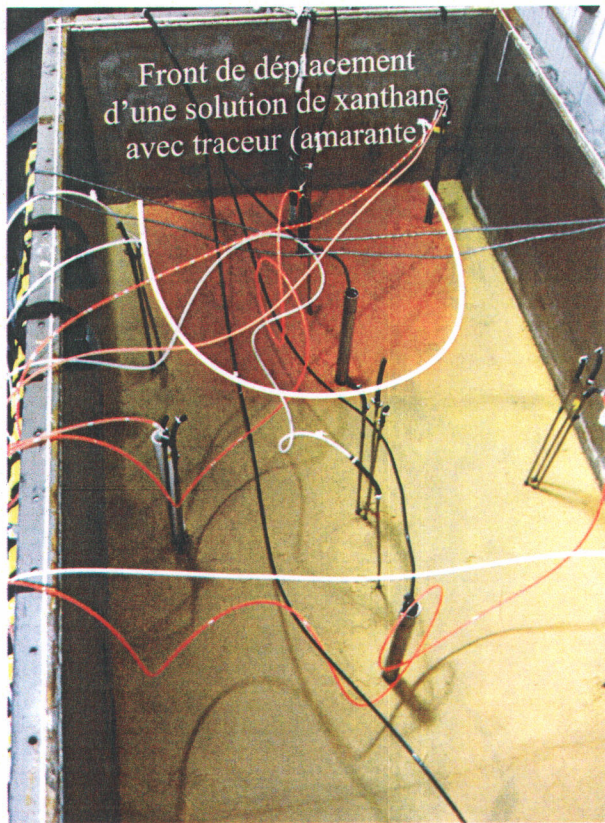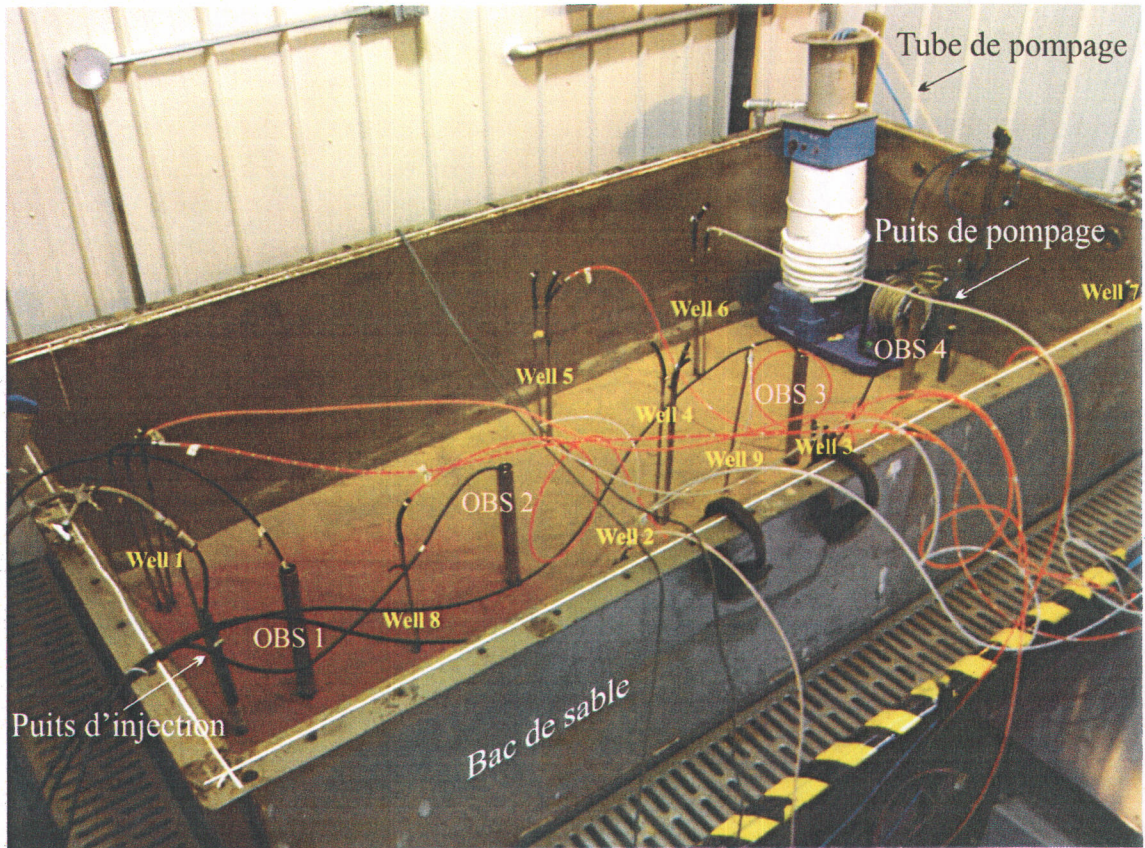
Annexe H

Simulation numérique réalisée à l'aide du logiciel UTCHEM lors de l'injection d'eau pour le test en bac de sable à trois couches comme outil pour la stratégie d'échantillonnage

| Caractéristiques du logiciel	Données utilisées pour le modèle		
3D, Différence finie	Nombre d'éléments: 10 (x) x 40 (y) x 9 (z) (= 3 600 éléments)	Taille des éléments	dx = 0.150 m
			dy = 0.075 m
			dz = 0.166 m
	Nœuds par élément: 8	dt = 86.4 s	
Propriétés du milieu poreux: porosité, perméabilité, dispersivité	Débit	0.83×10^{-5} m³/s	
	Porosité	0.374	
	Conductivité hydraulique du sable grossier	21×10^{-4} m/s	
	Conductivité hydraulique du sable fin	7×10^{-4} m/s	
	Dispersivité	Considéré nulle	
Propriétés des fluides (à 8°C): densité, viscosité, tension interfaciale	Densité de l'eau	999.91 kg/m³	
	Viscosité de l'eau	1.386×10^{-3} kg/m.s	
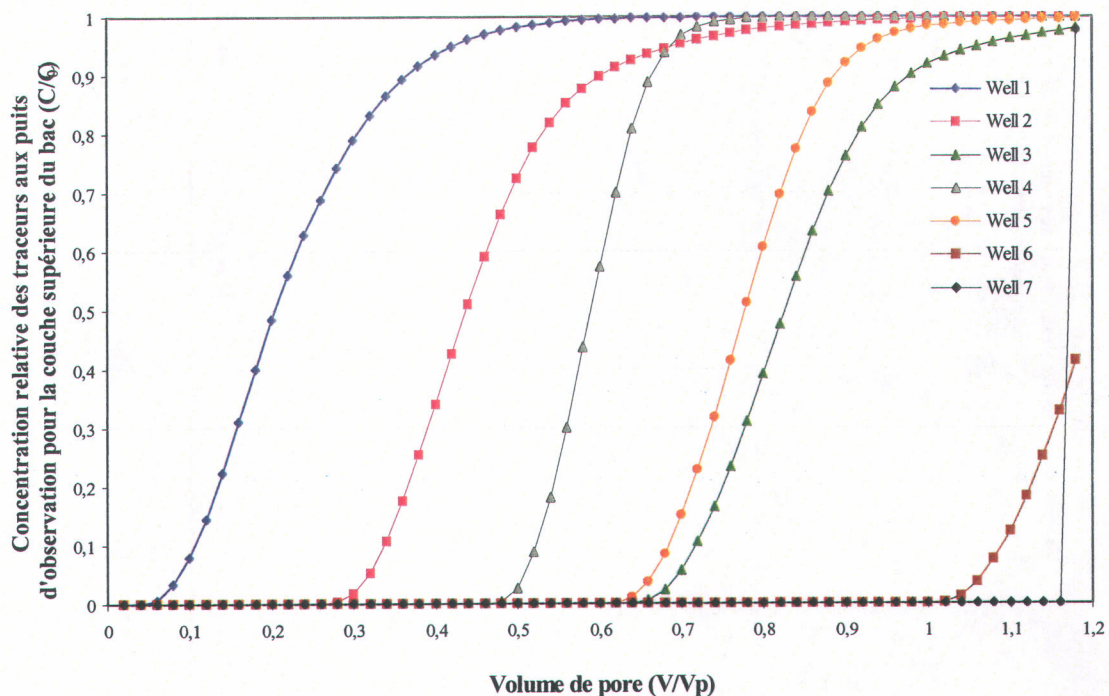
Simulation de l'avancement du front de déplacement des traceurs pour les puits situés dans la couche supérieure du bac (sable fin)
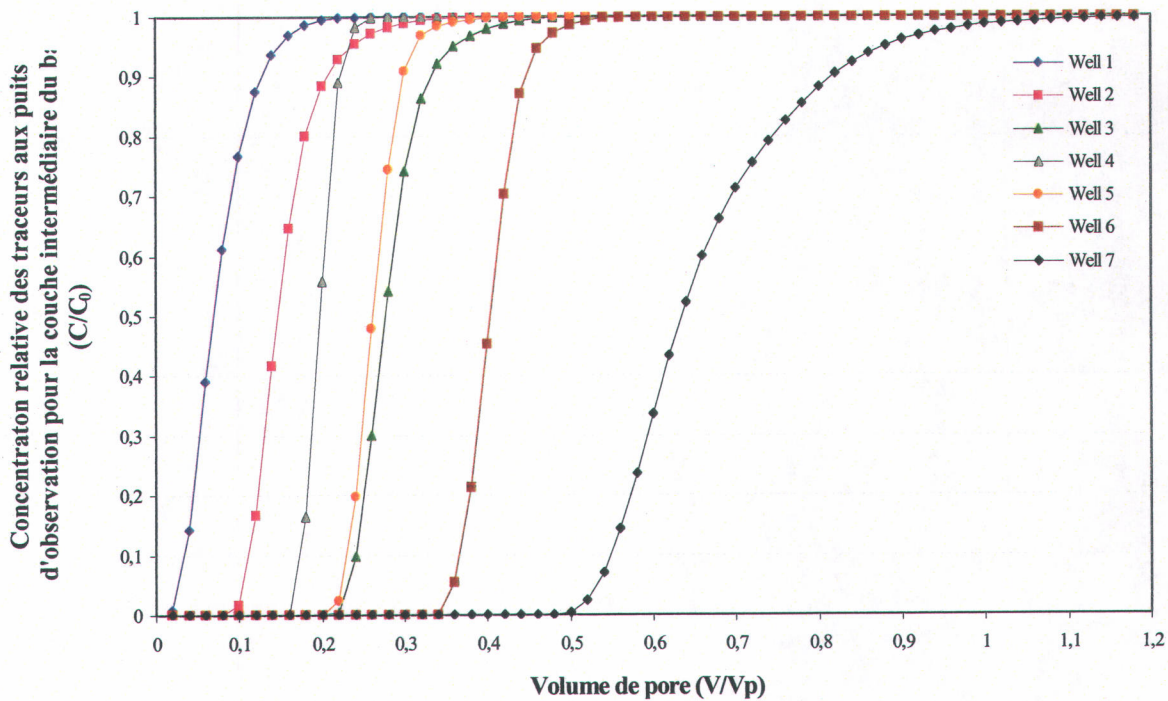
Simulation de l'avancement du front de déplacement des traceurs pour les puits situés dans la couche intermédiaire du bac (sable grossier)
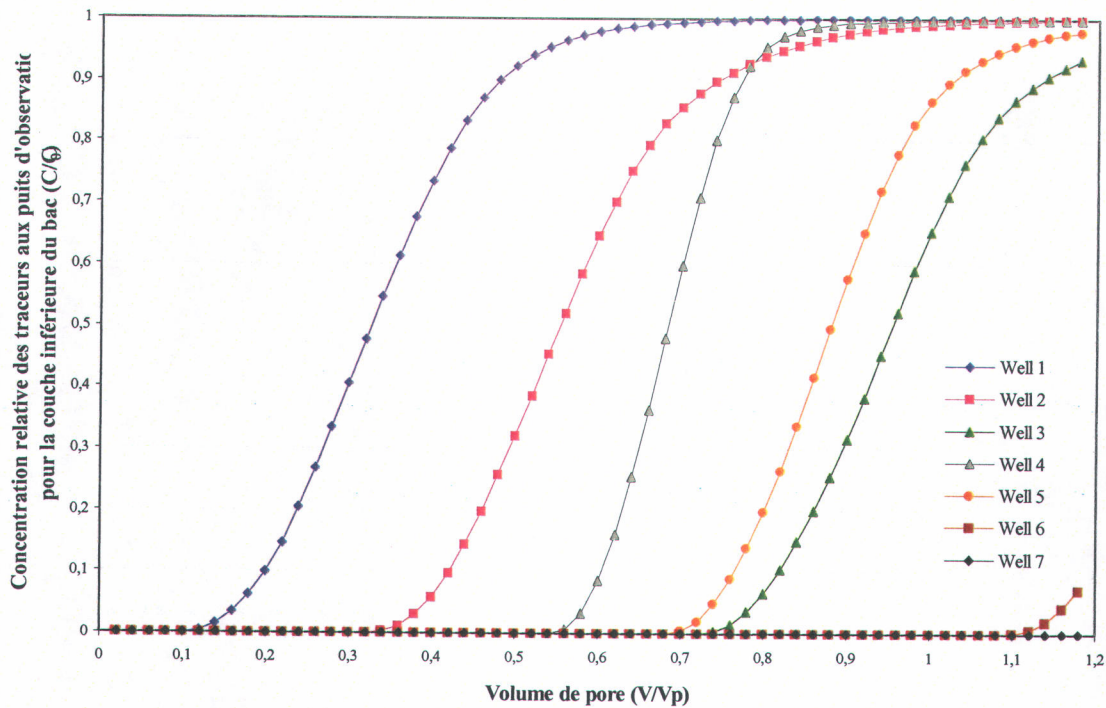
Simulation de l'avancement du front de déplacement des traceurs pour les puits situés dans la couche inférieure du bac (sable fin)
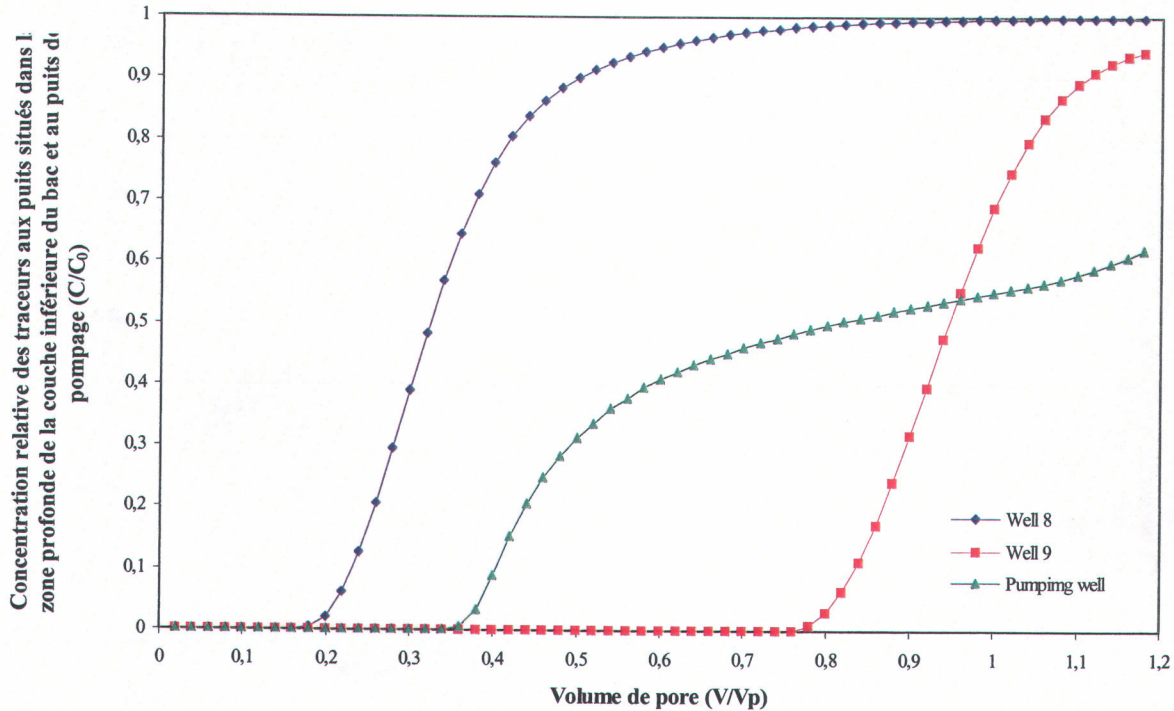
Simulation de l'avancement du front de déplacement des traceurs dans la zone profonde de la couche inférieure du bac (sable fin) et au puits de pompage (dans les trois couches de sable combinées)

Annexe I

Article présenté à la conférence conjointe de l'AIH et SCG à

Saskatoon, Septembre 2005

STUDY OF THE BEHAVIOR OF SHEAR THINNING POLYMERS DURING THEIR INJECTION IN HOMOGENEOUS POROUS MEDIA

Michael Haberman, Institut national de la recherche scientifique-Eau, Terre et Environnement
Richard Martel, Institut national de la recherche scientifique-Eau, Terre et Environnement
Uta Gabriel, Institut national de la recherche scientifique-Eau, Terre et Environnement
René Lefebvre, Institut national de la recherche scientifique-Eau, Terre et Environnement
Luc Trepanier, Institut national de la recherche scientifique-Eau, Terre et Environnement

ABSTRACT

Tests in sand columns confirmed the shear thinning behavior of xanthan gum: the viscosity of this polymer decreases gradually with the shear rate (and thus the flow rate). However, at a fixed shear rate, the viscosity increases due to the clogging of the porous medium. This clogging is mainly caused by an accumulation of polymer inside the column. Other tests showed that the intrinsic rheological properties of xanthan gum are modified when it has undergone a first shearing through a porous medium. The polymer then loses its properties, probably due to a modification of the chemical structure of xanthan gum, notably by chain break off.

RÉSUMÉ

Des essais en colonnes de sable ont confirmé le comportement rhéofluidifiant de la gomme de xanthane: la viscosité de ce polymère diminue progressivement avec le taux de cisaillement (et donc la vitesse d'écoulement). Cependant, à partir d'un certain taux de cisaillement, la viscosité augmente à cause du colmatage du milieu poreux. Ce colmatage est principalement dû à une accumulation de polymère au sein de la colonne. Les essais ont également montré que les propriétés rhéologiques intrinsèques de la gomme de xanthane sont modifiées lorsque celle-ci a subi un premier cisaillement à travers le milieu poreux. Le polymère perd alors ses propriétés, probablement dû à une modification de la structure chimique de la gomme de xanthane, notamment par une rupture des chaînes.

1. INTRODUCTION

Non Aqueous Phase Liquids (NAPL) causes many difficulties for the remediation of contaminated aquifers. NAPL present in an aquifer at residual saturation are characterized by a low solubility in water, forming a distinct phase. NAPL can be found at the surface of a contaminated aquifer (Light Non Aqueous Phase Liquids, LNAPL) or at its base (Dense Non Aqueous Phase Liquids, DNAPL) on an impermeable layer. Due to their low aqueous solubility, high toxicity and low biodegradation, NAPL-forming substances can be the source of long-term groundwater contamination.

Many processes for the remediation of NAPL source zones have already been studied (such as thermal, biological, physico-chemical treatments, etc.) but one limitation to their use is the depth of the contamination. *In situ* treatment by soil washing can remediate NAPL-contaminated sites (Gogarty, 1967; Szabo, 1975b; Sandifore, 1977; Martel, 1998; Martel et al., 2004). In soil washing, the use of polymers injected in pre or post treatment allows a better distribution of contaminants, a better sweep of the geological formation with more contact between the cleaning solution and the medium and in this manner, ensures a better recovery of contaminants, avoiding the problems related to displacement front instabilities and preferential viscous fingerings (Hornof and Morrow, 1987; Robert et al., 2005).

The objective of this study is to better understand the behavior of polymers dissolved in water in porous media. Laboratory tests with sand columns (of various grain sizes) and sand tank tests allowed the characterization of the physical behavior of xanthan gum aqueous solutions.

2. LITERATURE REVIEW

Previous studies showed that the use of these polymers dissolved in water and injected in pre or post treatment contribute to a better sweep of the contaminated aquifer (Gogarty, 1967; Sandiford, 1977; Martel, 1996). The effectiveness is explained by the formation of stable fronts between the different fluids, because of an increase of the water viscosity containing polymer and a reduction of the mobility ratio M (Lake, 1989):

$$M = \frac{\lambda_{water+polymer}}{\lambda_{NAPL}} = \frac{k_{water+polymer}}{\mu_{water+polymer}} \times \frac{\mu_{NAPL}}{k_{NAPL}} \quad [1]$$

where k (m^2) is the relative permeability to fluids, μ (Pa·s) is the viscosity of fluids and λ is the mobility (k/μ).

The particularity of polymer solutions is their shear thinning behavior, i.e. they can thicken the aqueous solution with very low concentrations, thus increasing the fluid relative viscosity when the shear

rate is low (in a coarse porous medium). Relative viscosity is also reduced when the shear rates are important in order to support the circulation of polymer through the fine porous medium (Figure 1). Another advantage of the use of xanthan gum is that it is non toxic and easily biodegradable (Garcia-Ochoa et al., 2000).
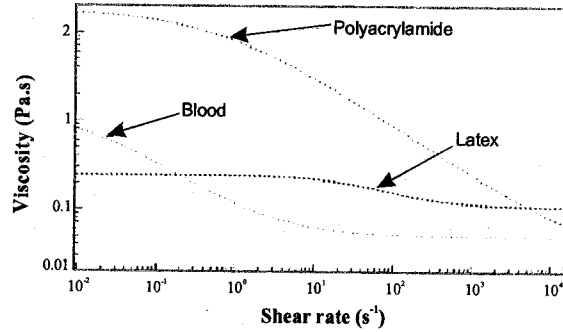

Figure 1: Viscosity as a function of shear rate for three shear thinning polymers (Bico, 2004)

3. METHODOLOGY

The physical properties of xanthan gum were studied with laboratory tests in sand columns to better understand their intrinsic behavior. This section presents characteristics of sands and polymer used and the equipment description.

3.1. Sand Column Tests

3.1.1. Porous media selection

For the column tests, a medium and a fine sand were used (Filpro Well Gravels sands U.S. Silica, New Jersey). These sands are relatively uniform industrial rounded to sub-angular quartz (Table 1).

Table 1: Characteristics of sands used for tests

Sand	ρ (g/cm^3)	K (m/s)	k (m^2)	d_{50} (mm)	d_{pore} (μm)
Fine	2.65	4×10^{-4}	3.6×10^{-11}	0.45	59
Medium		11×10^{-4}	10×10^{-11}	0.87	98

where ρ is mineral density, K hydraulic conductivity, k permeability, d_{50} mean size diameter of sand grains and d_{pore} pore size diameter.

Pore size was calculated as follows (Chauveteau and Zaitoun, 1981):

$$d_{pores} = 2\sqrt{8\frac{k}{n}} \qquad [2]$$

where k (m^2) is intrinsic permeability and n porosity (dim.).

The grain size distribution was characterized according to ASTM D422-63 method (Figure 2).
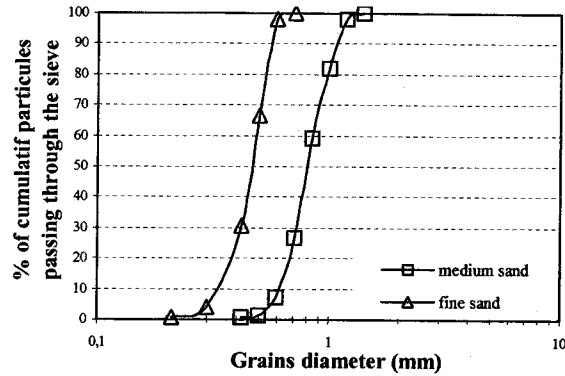

Figure 2: Grain size distribution of the selected sands

3.1.2. Polymer selection

Xanthan gum was chosen for its rheological behavior, its long-term chemical stability, low toxicity and low cost. This polymer is characterized by a high aqueous solubility at 20 °C (lab temperature) and its shear thinning behavior.

Xanthan gum is a polysaccharides biopolymer. Its molecular weight is between 1×10^6 and 50×10^6 g/mol depending on the presence of microgels. It is made by extra cellular fermentation of glucose with the bacterium *Xanthomonas campestris*.

3.1.3. Preparation of the polymer solutions

A xanthan solution of 1000 mg/L was prepared by gradually adding the polymer under the form of white powder to degassed distilled water. A slight agitation is necessary to avoid degradation of rheological properties of the polymer. Because xanthan is an easily degradable polysaccharide, a bactericide (400 mg/L of sodium azide NaN$_3$) was added to the solution. The xanthan solution was diluted to 250 ppm, the concentration used in all the tests.

3.1.4. Experimental equipment

Figure 3 schematically represents the set up used for polymer characterization in sand column.
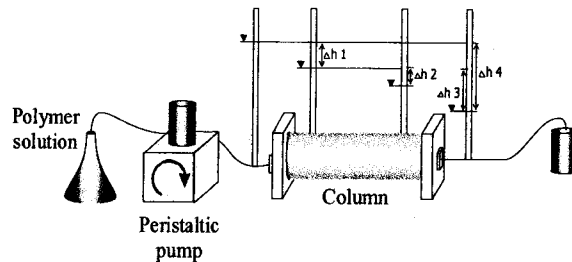
Figure 3: Set up for polymer characterization

The column is made of a 14.3 cm long and 3.6 cm diameter Plexiglas cylinder (Figure 3). Each extremity consists of two stacked Teflon plates with holes of 1 mm diameter covered with a filter of 160 □m in stainless steel to avoid the sand particles exiting from the column.

Column filling is done with 5 g sand layers introduced into the column and compacted 12 times with a sliding weight of 204 g attached to a vertical stem and dropped from a 13 cm height. The surface of the layer is scarified to ensure a link with the next layer. This process is repeated until complete filling of the column. The column is flushed with carbon dioxide (CO_2) to eliminate ambient air trapped before the saturation of the column with degassed water.

The polymer solution is injected into the sand column using a peristaltic pump. Two vertical tubes connected to the Plexiglas cylinder allow the measurement of hydraulic heads in the sand ($\Delta h2$). Two other tubes are put outside the column to measure the external heads ($\Delta h4$) (Figure 3). A laser beam (Black & Decker) is used to provide a reference level. By measuring the height of fluid in each tube, it is possible to witness by difference the hydraulic head between the different tubes. Knowing the mass of sand and water, it is possible to evaluate the viscosity of the polymer solution by measuring the flow, the hydraulic heads and the sand properties (porosity and hydraulic conductivity).

Four sand column tests were carried out to determine the different physical properties of xanthan gum: three columns with fine sand and one column with medium sand. Among these tests, one column used an already sheared polymer that had undergone shearing by passing through a sand tank (sheared polymer). Another column test consisted in injecting a xanthan solution continually with variable flow rate (increasing-decreasing-increasing shear rate) (cycled polymer).

3.2. Sand Tank Tests

Sand tank tests were carried out to evaluate and understand the sweep effectiveness of the xanthan solution.

3.2.1. Experimental equipment

The sand tank (3 m x 1.5 m x 2 m) made of stainless steel contained quartz sand (Temisca 30) of 1.5 m height. This tank was placed in a controlled temperature chamber (8 °C). The sand was introduced using barrels (300 kg of sand and 4 L of water per barrel). Each barrel can make a layer of about 4 cm. The sand was compacted between layers using 7.2 kN compactor (Mikasa MVC-40G) and scarified before introducing the following layer. This operation was repeated 37 times. The mobile water fraction was drained using openings of 10 mm

at the bottom of the container, two on each side. The sand tank was covered and a slight vacuum was applied. The sand tank was saturated with carbon dioxide (CO_2) before applying vacuum again. Five co-vacuum cycles were done. Finally, the sand tank was saturated with degassed tap water from the bottom-up to minimize air invasion. Table 2 shows the physical characteristics of the sand in the tank after compaction.

Table 2: Sand tank conditions after compaction

Sand mass (kg)	10 980
Sand volume (m^3)	6.75
Porosity	0.39
Pore volume (m^3)	2.6
Bulk density (kg/m^3)	1 630

Three wells were placed and aligned in the middle of the sand tank (injection, monitoring and pumping wells) and equipped with pressure transducers (KPSI Pressure Systems inc.). The injection well also contained a water level detector, which served as additional shut down criteria.

The experimental set up was controlled by two softwares: NETSOLVER (Cutler-Hammer, 1999) for collecting data, computing and piloting components; NETPOINT (Cutler-Hammer and PC Soft International, Version 7.51) as the interface with the user to visualize components and results and to modify parameters during the experiment.

3.2.2. Preparation of injected solutions

Injected fluids were prepared in three different stainless steel 2.23 m^3 reservoirs (0.87 pore volume V_p), provided with a stirrer. The temperature of the liquid was measured with a probe. Each reservoir had an automated valve. Four water level detectors and pressure transducers allowed flow rate measurements at the tank outlet. Manual flow rate measurements were also made in a large bucket at the tank outlet. The three reservoirs were interconnected and pumped with a compressed air membrane pump (Marathon Pump, IDEX Corporation) to the injection well. The pumping well was also equipped with a similar membrane pump. A constant head was kept in the wells by positioning a tube in the pumping well.

3.2.3. Tracer experiments

Two different tracers were used for the sand tank tests: chloride with a concentration of 1 g/L and bromide with a concentration of 0.1 g/L. Six solutions with different flow rates were injected: five tests with water and one test with a xanthan solution at 100 mg/L (0.87 V_p) followed by a second xanthan solution of 250 mg/L (1.3 V_p). No bactericide was added to these solutions.

All tests were done at constant head based on the pressure transducer in the injection well and the position of the extracting tube in the pumping well. Resulting hydraulic heads were measured in the monitoring well and the pumping well. Liquids were pumped from the pumping well in a 1 L stirred overflowing beaker in which ion selective probes (TempHion2, Instrumentation Northwest, Chloride - Bromide) and a peristaltic pump allowed automatic 250 ml sampling controlled by the software NETSOLVER at selected time or according to chloride and bromide concentration.

Water levels were measured in the reservoirs and used for the calculation of flow rates. Hydraulic head was continuously controlled in the monitoring and pumping wells. Temperatures in wells, tracer concentrations and the position of reservoirs valves were also recorded.

4. RESULTS

4.1. Sand Column Tests

Four tests in sand column determined the physical properties of xanthan gum and identified the intrinsic characteristics of tested sands:

Table 3: Characteristics of sands used and hydraulic conductivity according to hydraulic heads ($\Delta h2$)

Column	Characteristics	Hydraulic conductivity associated to $\Delta h2$ K (m/s)
1	Fine sand [Xanthan] = 250 ppm	7.50×10^{-4}
2	Medium sand [Xanthan] = 250 ppm	2.11×10^{-3}
3	Fine sand [Xanthan] = 250 ppm sheared	5.35×10^{-4}
4	Fine sand [Xanthan] = 250 ppm cycled	5.89×10^{-4}

4.1.1. Characterization of the sand columns with water

Sand column tests were characterized by injecting water. Flow rate and water heights inside each vertical tube were used to calculate the head difference $\Delta h2$ and $\Delta h4$ (Figure 3) and to determine the corresponding hydraulic conductivity (Table 3) according to Darcy's law:

$$K = \frac{Q}{\Delta h} \times \frac{L}{A}$$ [3]

where K (m/s) is hydraulic conductivity, Q (m³/s) flow rate, $\Delta h2$ or $\Delta h4$ difference in hydraulic heads (m), L (m) length of the porous medium and A (m²) column surface area.

The relative viscosity μ_r of the polymer solutions is calculated from the following equation:

$$\mu_r = \frac{K_{water}}{K_{xanthane}}$$ [4]

where K_{water} is hydraulic conductivity to water and $K_{xanthan}$ is hydraulic conductivity to xanthan solution in the column.

4.1.2. Shear thinning behavior of polymer

For shear rate from 0.1 to ~ 3 - 10 s⁻¹, the decrease in viscosity is function of the increase in shear rate (increase in injection rate), which confirms the shear thinning behavior of xanthan gum (Figure 4). For shear rate higher than 10 s⁻¹, the shear thinning behavior is lost and viscosity increases with shear rate.
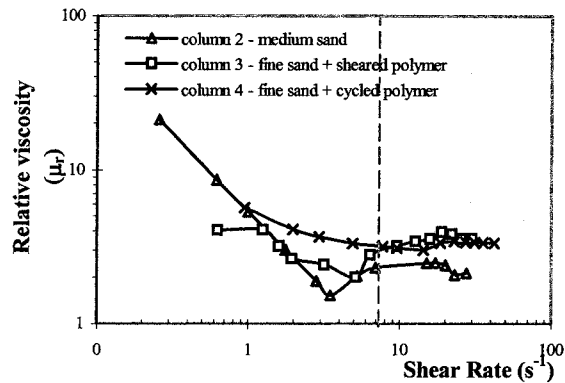

Figure 4: Shear thinning of behavior xanthan gum
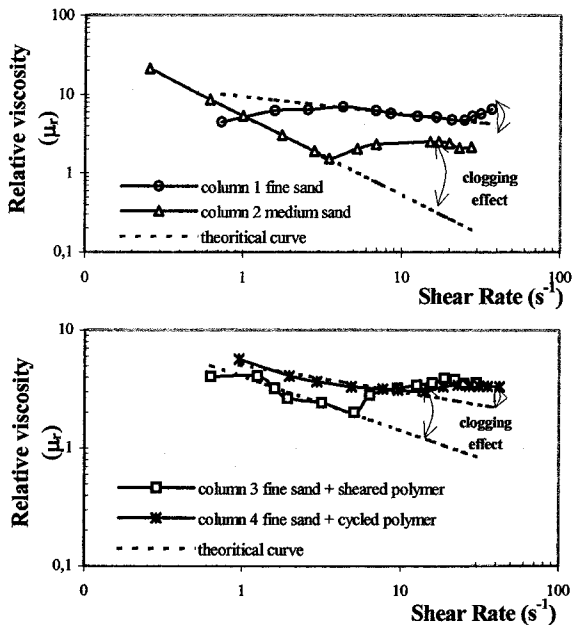
Figure 5: Experimental data and theoretical curve

Measured viscosities are compared with a theoretical curve in Figure 5. There was clogging in the column by the polymer. For the same shear rate, μ_r is higher in the fine sand than in the medium sand, which is the opposite of what was expected. For column 1, the equilibrium of the system needed some time to be reached (shear rates between 0.7 s^{-1} and 3 s^{-1}) because the polymer solution was warmer than the sand laboratory temperature. For column 2, shear thinning follows theoretical data.
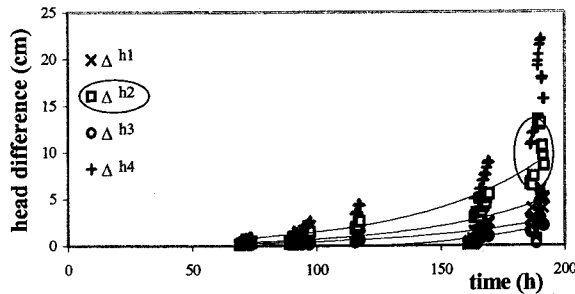
Figure 6: Head difference in column 1 (fine sand test)
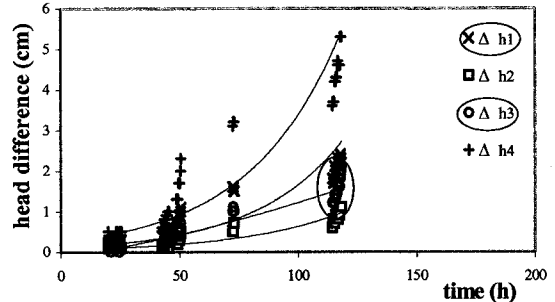
Figure 7: Head difference in column 2 (medium sand test)
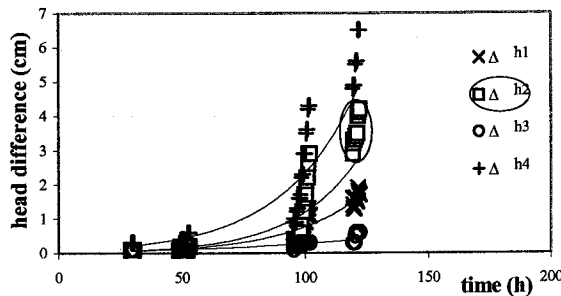
Figure 8: Head difference in column 3 (fine sand + sheared polymer test)
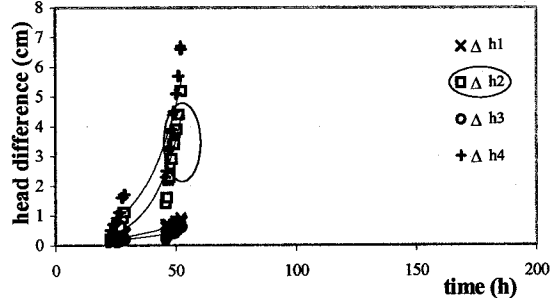
Figure 9: Head difference in column 4 (fine sand + cycled polymer test)

4.1.3. Clogging process

In all column tests, clogging cannot be explained by the presence of microgels because of their small dimension (6 µm) in comparison with pore size (respectively of 59 µm and 98 µm for fine and medium sand) and the mesh size of the metallic screen at the inlet and the outlet of columns (160 µm) (Chauveteau et al., 1980). Two hypotheses are considered for the clogging process: i) polymer accumulation inside columns or ii) obstruction of pores in the screen at the inlet and outlet of columns due to a bad homogenization of the polymer solution.

Figures 6 through 9 show the hydraulic head observed inside and outside of the columns. For the fine sand column tests (Figure 7, 9 and 10), the contribution of Δh2 to the global clogging of the column (Δh4) is more important than Δh1 and Δh3. This observation confirms that the clogging is essentially caused by an accumulation of polymer in the column and not by an obstruction of the screen pores. At the opposite, for column 2 test (Figure 8), the contribution of Δh1 and Δh3 is more noticed than Δh2, showing that the screen's pores are clogged. A

bad preparation of the xanthan solution or a bad homogenization could also be the main reason.

To better illustrate the clogging effect, we traced down the viscosity ratio curve (ratio of measured to calculated viscosity) as a function of time (Figure 10). We noticed in all cases that the viscosity ratio is relatively stable during the shear thinning behavior part of the curve (flat curve). When the viscosity ratio is superior to 1, the clogging occurs. We observed for column 1 a ratio inferior to 1 at the beginning of the test created by the warm temperature of the polymer solution at the beginning of the test. Clogging is observed in all column tests.
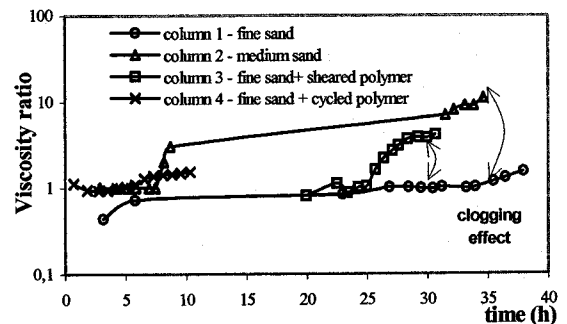

Figure 10: Viscosity ratio as a function of time
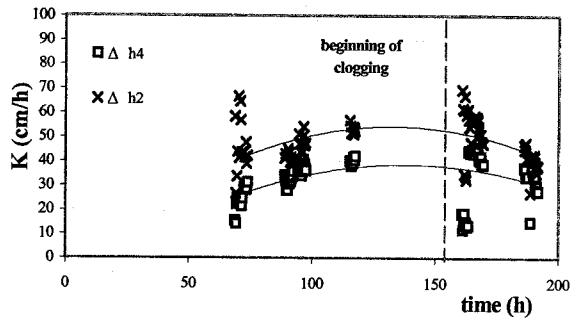
Figure 11a: Behavior of K with time for column 1 (fine sand test)
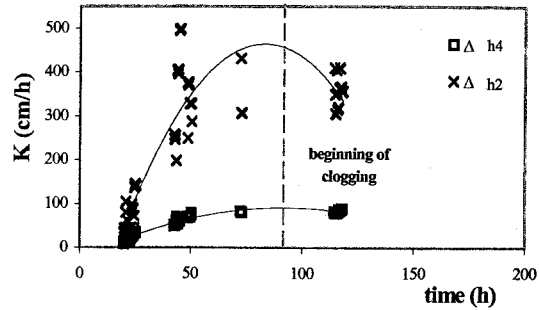
Figure 11b: Behavior of K with time for column 2 (medium sand test)
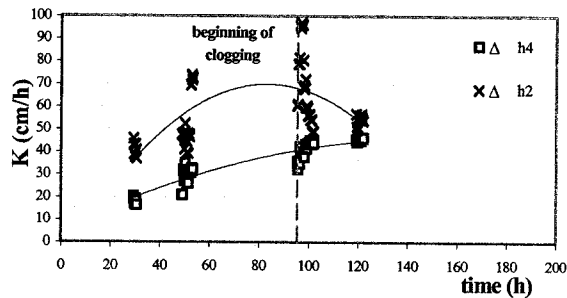

Figure 11c: Behavior of K with time for column 3 (fine sand + sheared polymer test)
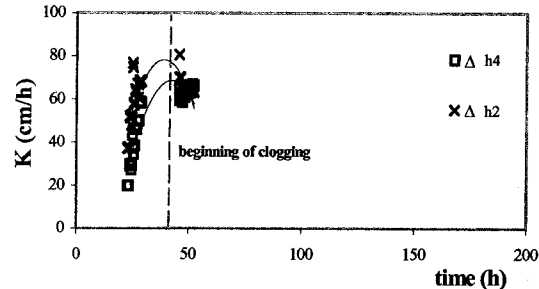
Figure 11d: Behavior of K with time for column 4 (fine sand + cycled polymer test)

4.1.4. Evolution of the hydraulic conductivity

The clogging phenomenon can also be illustrated by the evolution of the hydraulic conductivity (Figure 11a to 11d). Each figure shows a progressive increase in hydraulic conductivity with time as calculated as follows:

$$K = k\frac{\rho \cdot g}{\mu} \qquad [5]$$

where K (m/s) is hydraulic conductivity, k (m^2) intrinsic permeability of the medium, ρ (kg/m^3) fluid density, g (9.81 m/s^2) gravitational acceleration and μ (Pa·s) viscosity. Hydraulic conductivity is inversely proportional to the viscosity of the injected solution. A viscosity reduction (by shear thinning of xanthan gum) led to an increase in hydraulic conductivity. Hydraulic conductivity decrease is observed when the column begins to clog as showed by the vertical line in figures 11a to 11d.

4.1.5 Influence of the shearing on the rheological properties of polymer

To understand the effect of shearing on the physical and chemical properties of xanthan gum, an intact polymer solution (column 4) and sheared polymer (column 3) were injected through two different sand columns (Figure 12).
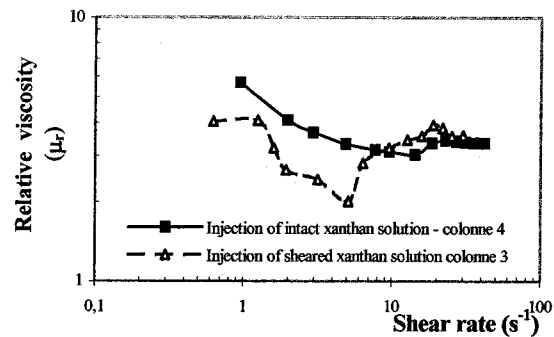

Figure 12: Influence of the shearing on the polymer properties

The sheared xanthan solution has a slightly lower viscosity than the intact one. That can be explained by a loss of the intrinsic polymer properties. The shear thinning behavior is nevertheless present. Furthermore, because the polymer solution flowed already through the sand, it is possible that the solution has not the initially injected xanthan concentration. It is also possible that the sand adsorbed some polymer (adsorption of xanthan on sand varies from 3 to 16 µg/g of dry sand as of K-E. Martel, 1995) or that the polymer is trapped mechanically, considering the adsorption of xanthan and the dilution from pore water in the sand tank. So, the initial concentration of xanthan in the

column 3 test is modified of 182 ppm to 237 ppm according to the adsorbed xanthan mass.

4.1.6. Influence of Shear Rate

The hysteretic effect of the polymer solution is showed by applying three successive cycles: i) increase of the shear rate (1st cycle), ii) reduction of the shear rate (2nd cycle) and finally iii) again increase of the shear rate (3rd cycle) obtained by increasing and decreasing the injection flow rate (Figure 13).
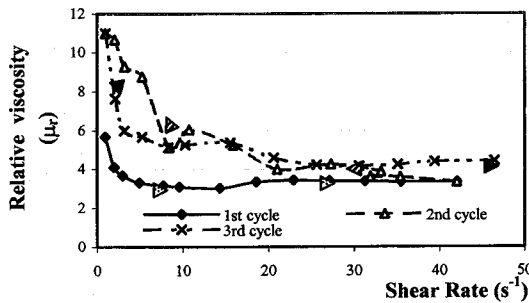

Figure 13: Hysteresis effect on relative viscosity for a xanthan solution sheared in fine sand (arrows indicate the increasing or decreasing shear rate on the solution)

The shear thinning behavior of xanthan gum is observed during the 1st cycle. By decreasing the shear rate (2nd cycle), the clogging is noticed. This is explained by an accumulation of polymers in the column. When the shear rate is increased again (3rd cycle), the shear thinning behavior is again observed but with a higher viscosity than in the first cycle. We can consequently describe this phenomenon as "memory" or hysteresis.

4.2. Sand Tank Tests

Five tests with water were carried out to characterize the homogeneous sand medium and one test with xanthan gum to test whether pore clogging would occur. Table 4 shows different characteristics of each test.

Table 4: Characteristics of tests in the sand tank

Tests	Fluid	Flow rate (m^3/day)	V_p/day	Δh (cm)	K $(10^{-4} m/s)$
A	Water	1.2	0.47	4.5	3.6
B	Water	3.3	1.28	8.9	4.9
C	Water	0.74	0.29	3.0	3.3
D	Water	1.5	0.59	6.3	3.2
E	Water	2.0	0.78	8.5	5.2
F	Xanthan	1.35	0.53	10.7	1.7

where Vp is pore volume (dim.), Δh (m) difference of hydraulic heads between the injection well and the pumping well and K (m/s) hydraulic conductivity.

4.2.1. Evolution of hydraulic head

Figure 14 shows the evolution of hydraulic heads for three tests with water injection. In each test, the hydraulic head was kept constant. However, in some cases, the hydraulic head reaches a zero value, corresponding to the shut down of the experiments.
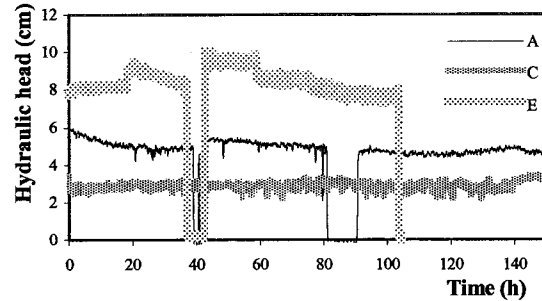

Figure 14: Evolution of the hydraulic head for tracer tests

For the injection of xanthan solutions, even though the hydraulic head between the injection well and the pumping well was kept constant, the hydraulic head between the monitoring well and the pumping well increased continuously with the time (Figure 15). The hydraulic conductivity decreased steadily during the injection of xanthan solutions. After the injection of the 100 ppm xanthan solution, the decrease continued for the first reservoir of the 250 ppm xanthan solution. For the second reservoir of 250 ppm xanthan solution, the hydraulic conductivity became constant, indicating that neither pore clogging nor polymer accumulation occurred in the sand tank. This steady effect indicated an effective pore volume less important than the total porosity calculated from sand mass and tank volume.
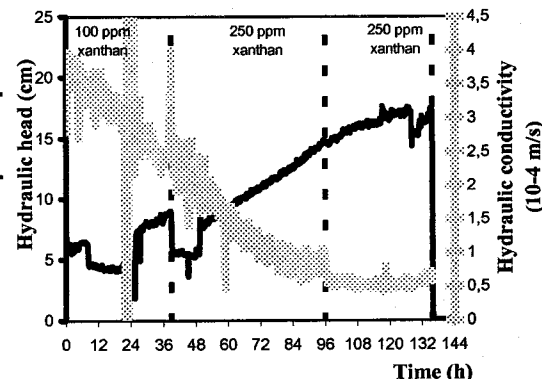

Figure 15: Evolution of hydraulic head and hydraulic conductivity with time

At the changing of each reservoir (indicated by dotted lines in Figure 15), we also noticed three slight increases due to the rounded shape of the bottom of the reservoir.

5. CONCLUSIONS

The shear thinning behavior of xanthan gum was studied with experiments in sand columns and a sand tank. These experiments showed that viscosity decreases with an increase in shear rate. However, after a certain time a partial pores clogging started to occur, leading to a general viscosity increase, independent of the shear rate. The clogging was probably not due to bacterial growth as a bactericide has been added to all xanthan solutions. This clogging is caused by an accumulation of polymer inside the column or by the obstruction of the screen at the inlet and outlet of the column.

The comparison between a sheared polymer and an intact polymer showed a loss of the rheological properties of the sheared polymer. This can probably be explained by a loss of polymer in solution by adsorption on the porous medium or mechanical trapping.

A hysteretic behavior in the sand was observed when xanthan solutions were injected continuously with a cycle of increasing-decreasing-increasing flow rate (shear rate).

Finally, for the sank tank tests, the results indicated that xanthan gum can be injected at larger scale in non consolidated sandy media without adding bactericides. The temperature was kept low and the bacterial contamination has been avoided as much as possible to represent natural porous medium as soils or sediments. The good results in the sand tank are probably also due to the absence of close-meshed screens as at column extremities.

For the future, the different xanthan solutions could be added to washing solutions without worrying about pore blocking during the flushing of porous media. It is also interesting to notice that the presence of active matter might in some cases decrease the effectiveness of the xanthan gum, leading to the necessity of a higher concentration for the same viscosity (Robert et al., 2005).

6. REFERENCES

Bico J., Fermigier M. and Kurowski P. 2004, Fluides non newtoniens, note de cours, Centre National de la Recherche Scientifique et École supérieure de Physique et de Chimie Industrielle de la ville de Paris, Paris, France.

Chauveteau G. and Kohler N. 1980, Influence of microgels in xanthan polysaccharide solutions on their flow through various porous media, 55th Annual Fall Technical Conference and Exhibition of the SPE of AIME (Dallas, TX, USA), SPE 9295, 1-13.

Chauveteau G. and Zaitoun A. 1981, Basic rheological behavior of xanthan polysaccharide solutions in porous media: effects of pore size and polymer concentration, European Symposium on Enhanced Oil Recovery (Bournemouth, England), 197-214.

Garcia-Ochoa F., Santos V.E., Casas J.A. and Gomez E. 2000, Xanthan gum: production, recovery and properties, Biotechnology Advances, 18, 549-579.

Gogarty W.B. 1967. Mobility control with polymer solutions, Society of Petroleum Engineers Journal, 7, (2), 161-173.

Hornof V. and Morrow N.R. 1987, Gravity effects in the displacement of oil by surfactant solutions, Reservoir Engineering Society of Petroleum Engineers, 2, (4), 627-633.

Lake L.W. 1989, Enhanced oil recovery, Prentice-Hall Inc, New Jersey, 550 pp.

Martel K.E. 1995. Utilisation de solutions de polymères pour améliorer l'efficacité de balayage des solutions tensioactives développées pour la restauration d'aquifères contaminés aux hydrocarbures immiscibles lourds, Mémoire pour l'obtention du grade de maître ès sciences, Décembre, Département de géologie et génie géologique, Université de Laval, Québec, Québec, Canada.

Martel K.E., Martel R., Lefebvre R. and Gelinas J.P. 1998. Laboratory Study of Polymer Solutions used for Mobility Control during in situ NAPL Recovery, Groundwater Monitoring and Remediation, 18, (3), 103-113.

Martel R. and Gelinas J.P. 1996. Surfactant Solutions developed for NAPL Recovery in Contaminated Aquifers, Groundwater, 34, 143-154.

Martel R., Hebert A., Lefebvre R., Gelinas J.P. and Gabriel U. 2004, Displacement and sweep efficiencies in a DNAPL recovery test using micellar and polymer solutions injected in a five-spot pattern, Journal of Contaminant Hydrology, 75, 1-29.

Robert T., Martel R., Conrad S.H., Lefebvre R. and Gabriel U., 2005, Visualization of TCE recovery mechanisms using surfactant polymer solutions in a two-dimensional heterogeneous sand model, Journal of Contaminant Hydrogeology (in press).

Sandiford B.B. 1977, flow of polymers through porous media in relation to oil displacement. in: improved oil recovery by surfactant and polymer flooding. Shah, D.O. and Schechter R.S. (eds.). Academic Press inc., New-York, USA, 487-509.

Szabo M.T. 1975b, Laboratory investigation of factors influencing polymer flood performance, Society of Petroleum Engineers Journal, 15, (4), 338-34